In presenting this thesis in partial fulfillment of the requirements for an advanced degree at Idaho State University, I agree that the Library shall make it freely available for inspection. I further state that permission for extensive copying of my thesis for scholarly purposes may be granted by the Dean of the Graduate School, Dean of my academic division, or by the University Librarian. It is understood that any copying or publication of this thesis for financial gain shall not be allowed without my written permission.

Signature ___________________________________

Date _______________________________________

High-Speed Velocity Measurement Instrumentation of Air-Driven Water Jet

for a Wave Impact Simulation Device

by

Soumadipta Jash

A thesis

submitted in partial fulfillment

of the requirements for the degree of

Master of Science in Nuclear Engineering

Idaho State University

Spring 2018

To the Graduate Faculty:

The members of the committee appointed to examine the thesis of Soumadipta Jash find it satisfactory and recommend that it be accepted.

____
Dr. Bruce Savage
Major Advisor

____
Dr. Chad Pope
Committee Member

____
Dr. Hossein Mousavinezhad
Graduate Faculty Representative

To my parents Tushar and Anuradha, for their love and support.

Acknowledgements

I would like to thank both Dr. Chad Pope and Dr. Bruce Savage for giving me the opportunity to be a part of the Component Flooding Evaluation Laboratory team. I would like to express my sincere gratitude to both of them for their continuous support, insight, immense knowledge and guiding me through my thesis. I would also like to thank my team members Rojin Tuladhar and Larinda Nichols.

Vita

Soumadipta Jash was born on July 10, 1991 in Mumbai, India. He moved to United States in 2010 after completing his high school education. In 2014, he received his undergraduate degree in Nuclear Engineering from Idaho State University (ISU). In the same year he enlisted in the US Army and was stationed in Schofield Barracks, Hawaii on active duty. Later in 2016, he was accepted into the Nuclear Engineering master’s program at ISU. Upon completion of his master’s degree, he plans to pursue his career in various government and private sector industries.

Table of Contents

List of Figures

List of Tables

List of Abbreviations

CFEL	Component Flooding Evaluation Laboratory
LDA	Laser Doppler Anemometer
LDR	Light Dependent Resistors
LDV	Laser Doppler Velocimetry
LTA	Laser Transit Anemometer
PET	Portal Evaluation Tank
PIV	Particle Image Velocimetry
PTV	Particle Tracing Velocimetry
WISD	Wave Impact Simulation Device

Abstract

Research work at CFEL at ISU is important. It provides probabilistic data and models for safeguarding non-containment components of nuclear power-plant. WISD team designed a physical model that generates high-velocity water-jet that simulates a tsunami using air-pressure as motive force. Instrumentation for measuring the wave velocity is the topic of this paper.

The team designed a scaled sectional model made of Plexiglass utilizing gate system. The team also successfully designed a small-scale model that validated the use of air-pressure systems and U-shaped design. Water initially was contained in a U-shaped clear PVC pipe section. The water in the U-section was subjected to air-pressure using combination of solenoid valves. Optomax sensors were deemed viable for measuring wave velocity of the wave generated by physical model. 2.75-psi for 0.53 seconds was chosen as ideal data due to close similarity with theoretical kinematics analysis. The measured velocity of the water-jet was 11.57 feet/second.

Key Words: CFEL, WISD, Sensor, High Velocity Water Jet

Introduction

The Component Flooding Evaluation Laboratory (CFEL) at Idaho State University is responsible for generating flooding centric probabilistic data through models and physical testing for safeguarding non-containment components of a nuclear power plant. This is important for risk assessment of flooding scenarios caused by tsunamis and other potential flooding events. One such event occurred on March 11, 2011 at the Fukushima Daiichi nuclear power plant in Japan. A major earthquake triggered a 15-meter tsunami that disabled the power supply and cooling of the reactors [26].

The CFEL focuses on water rise, water spray, and wave impact capabilities, and the data and information collected will be applied to risk modeling studies. Important components of CFEL are the Portal Evaluation Tank (PET), Wave Impact Simulation Device (WISD) design, and pipe leakage research. Topics investigated for this thesis include a brief literature review on artificial wave generation, the proposed WISD design explored by Greg Roberts (a former student in the CFEL project), and various methods of measuring velocity of fluid flow.

The full-scale experiments began with design and construction of the PET in 2016. The PET is a steel semi-cylindrical tank, with a height and diameter of 8 feet. It has an opening to the outside of 8 feet x 8 feet, two 3-inch inlets on the sides, a 2-inch outlet that is used for the draining system at the bottom, a new 12-inch inlet, and four 1.25-inch instrumentation ports at the top. The PET is connected through a 3-inch PVC pipe to a 5-HP submersible pump which is located inside a ~8,000-gallon water reservoir. The new 12-inch inlet is connected to a 50-HP pump. An electromagnetic flow-meter is used to measure the water flow into the tank, while an ultrasonic sensor and a pressure transducer are used to measure the water elevation and calculate the leakage rate. The PET is also equipped with top mounted pressure and air relief valves and a pressure gauge; the purpose of these instruments is to allow safe pressurized experiments in the PET. The original PET piping configuration is shown in Figure 1 [19].

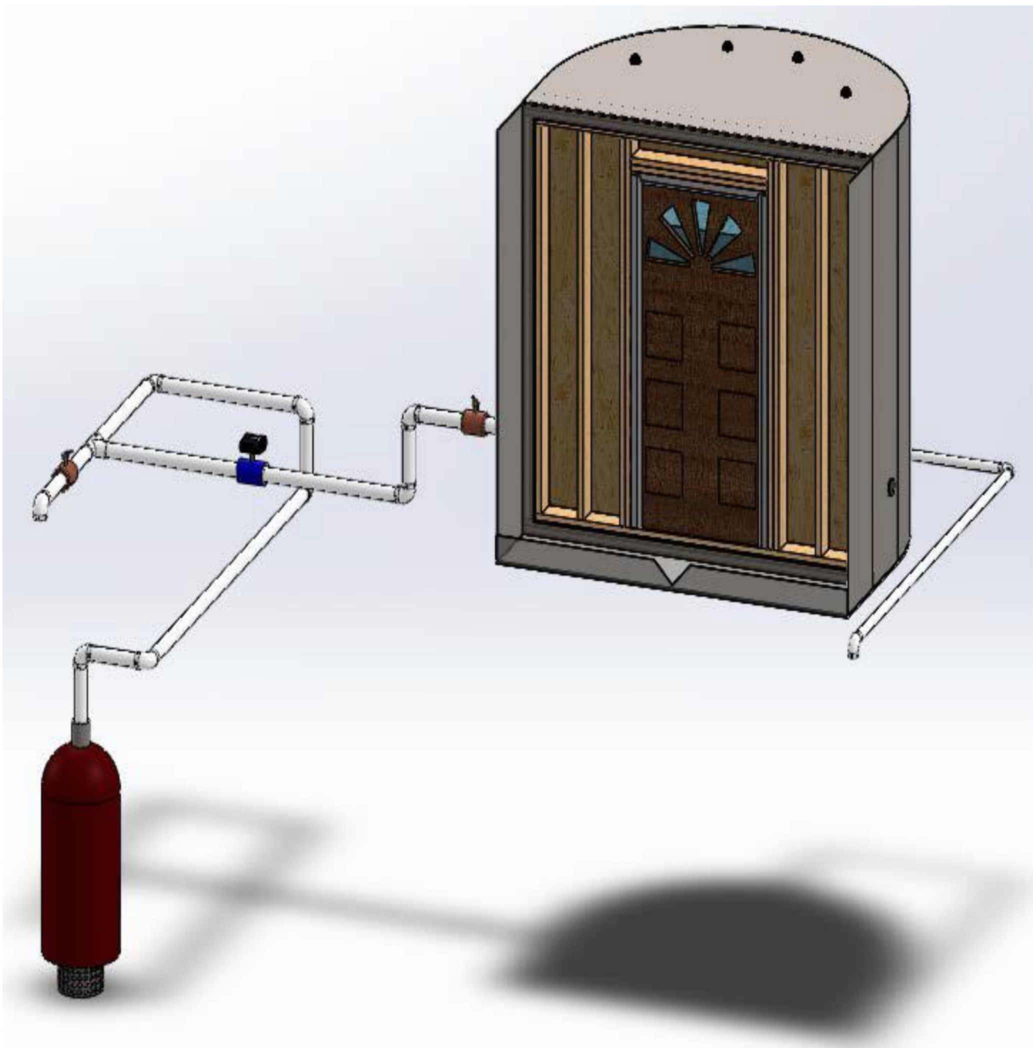

Figure 1: Original PET Piping Configuration

To increase the PET capabilities, design work was pursued following the initial door testing experiments in the PET. In the initial PET door tests, the water flow was limited to a single inlet with a flow rate of ~300 gpm. Additionally, the initial piping configuration was limited in its ability to allow tests where the tank was pressurized to simulate additional hydrostatic head. There were limitations associated with data and video recording that were also identified in the initial tests. Modifications to the PET were designed to support variable inlet flow rates up to ~4500 gpm. The designed modifications support the filling of the PET completely and then relying on the pump to provide additional hydrostatic head to simulate water depths up to 20 feet. Additionally, design work was pursued to improve data and video recording [19]. Figure 2 shows the improved PET piping configuration [19].

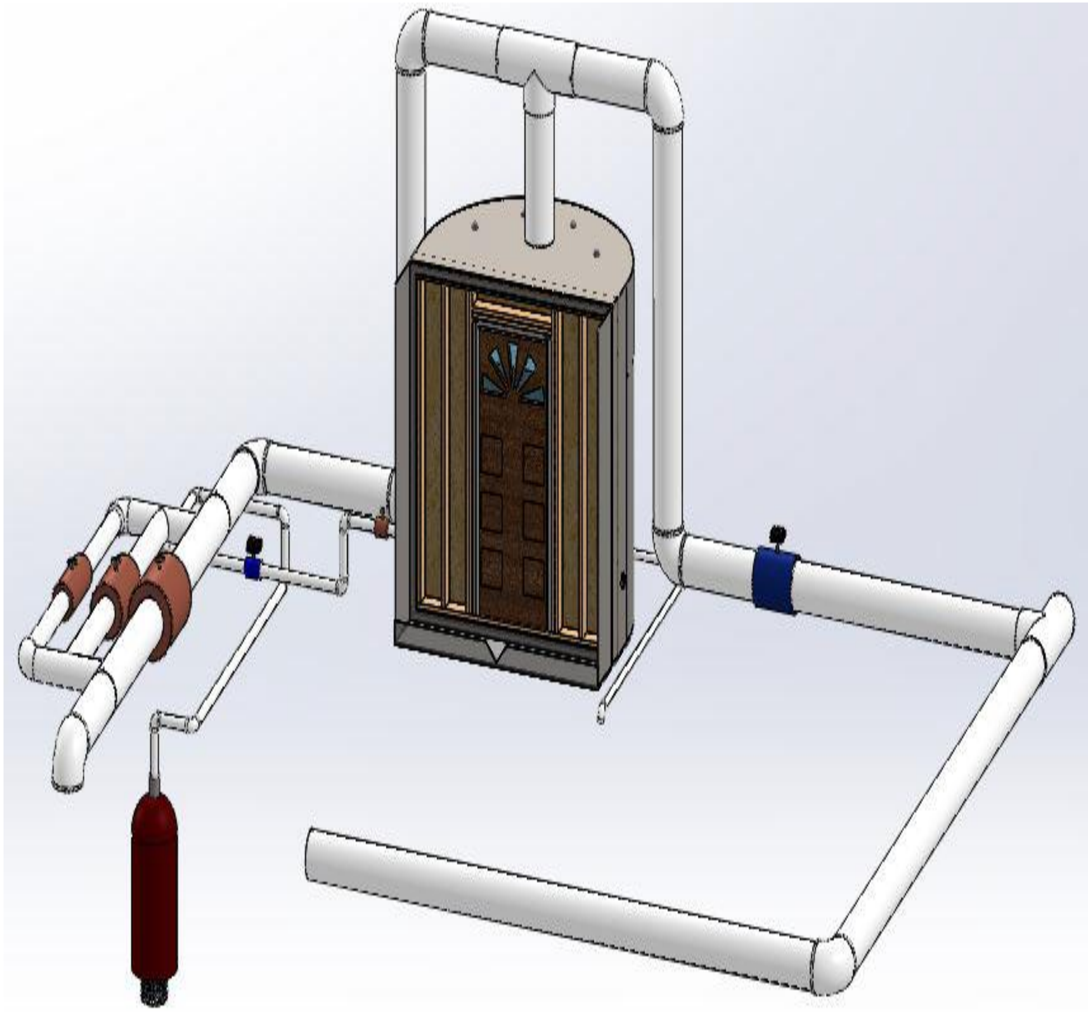

Figure 2: Improved PET Piping Configuration

Another major component of CFEL is the design of a Wave Impact Simulation Device (WISD). Greg Roberts using the computational fluid dynamic code Flow-3D numerically completed the original concept design [21]. The current WISD team consists of Rojin Tuladhar, Larinda Nichols, and Soumadipta Jash. The primary goal of this research team was to further refine the work completed by Roberts and design a sectional physical model of the WISD to validate numerical models. The proposed physical model is a 1:5 reduced scale model of the prototype. The prototype is required to simulate a wave of 20 feet high with a velocity of 25.4 feet/second. Hence the need of instrumentation to measure this high-speed water velocity. The sectional model consists of five components as listed in Table 1. Rojin Tuladhar did the general design of this model. Figure 3 shows the layout of the sectional physical model.

Table 1: Components of the Physical Model

Component. No.	Description	Quantity
1	Inclined Inlet	
	25˚	1
	35˚	1
	45˚	1
2	Gate Channel	1
3	Outlet box	1
4	Additional Length component	
	0.2'	2
	0.4'	4
	1'	2
5	Flanges	22

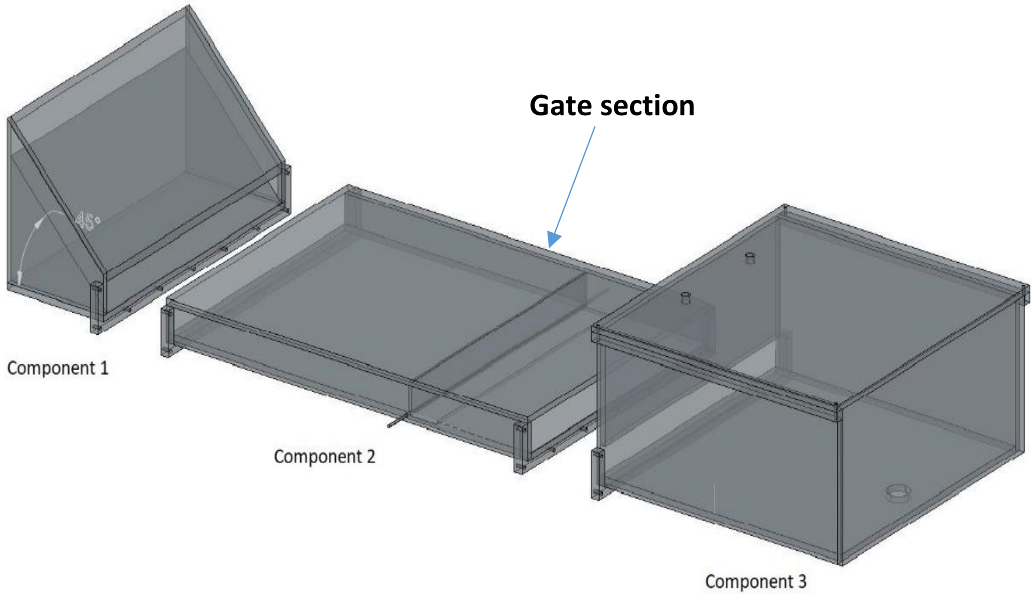

Figure 3: Layout of the Sectional Physical Model (flow moves from left to right)

The entire model is to be built with Plexiglass in order to observe the fluid behavior. The water rests in component 1 and 2 behind the gate section. Air pressure is applied through the angled inlet, which forces the water into motion after the gates open via a bottom hinge. Finally, the fluid is pushed into the outlet box and flushed out through an opening at the bottom. Flanges are attached to each component for the purpose of connecting/disconnecting them as required. Details of the design can be found in Appendix C.

Larinda Nichols developed the gate section. The gate system designed had the following design parameters: the gates were designed to withstand limited water pressure before water is released; it did not interfere with the target flow profile, opened nearly instantaneously, and the leakage from the reservoir parts prior to the gates opening were minimized. Electromagnets were integrated to the final design for opening and closing of the gate system. Figure 4 and Figure 5 show the closing and opening mechanism of the gates using the electromagnets. Details of the gate design can be found in Appendix C as well.

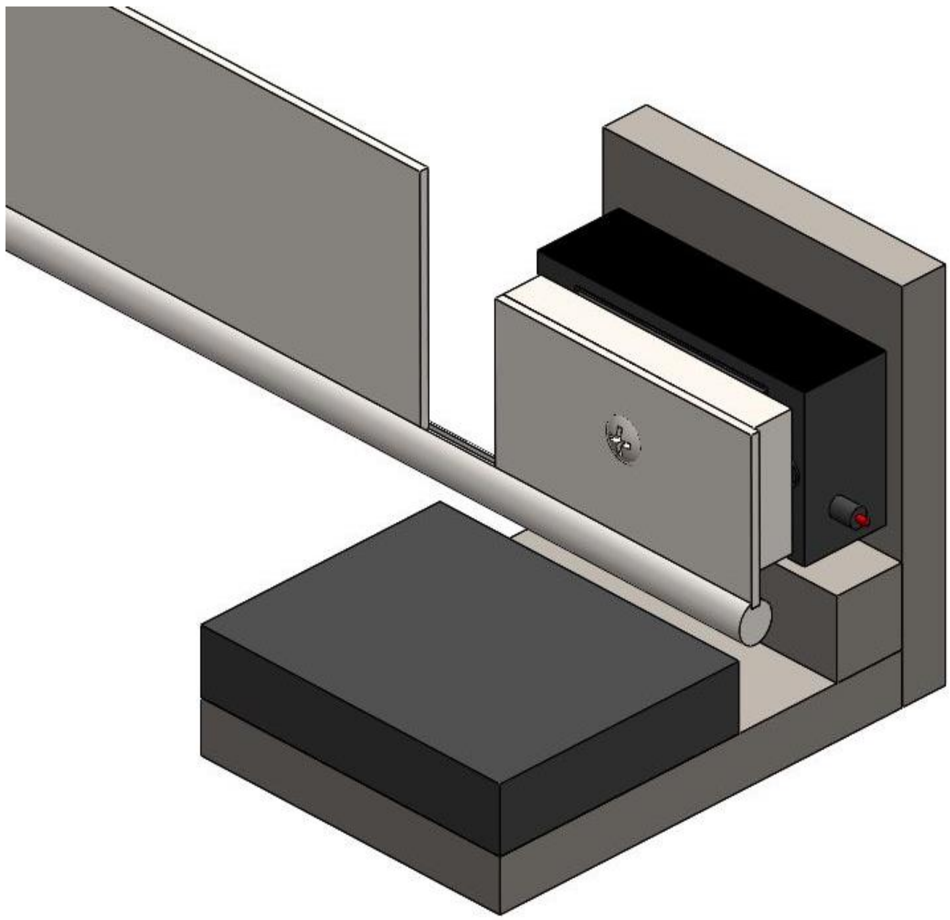

Figure 4: Simulation of the Energized Electromagnet Holding Gate in Closed Position

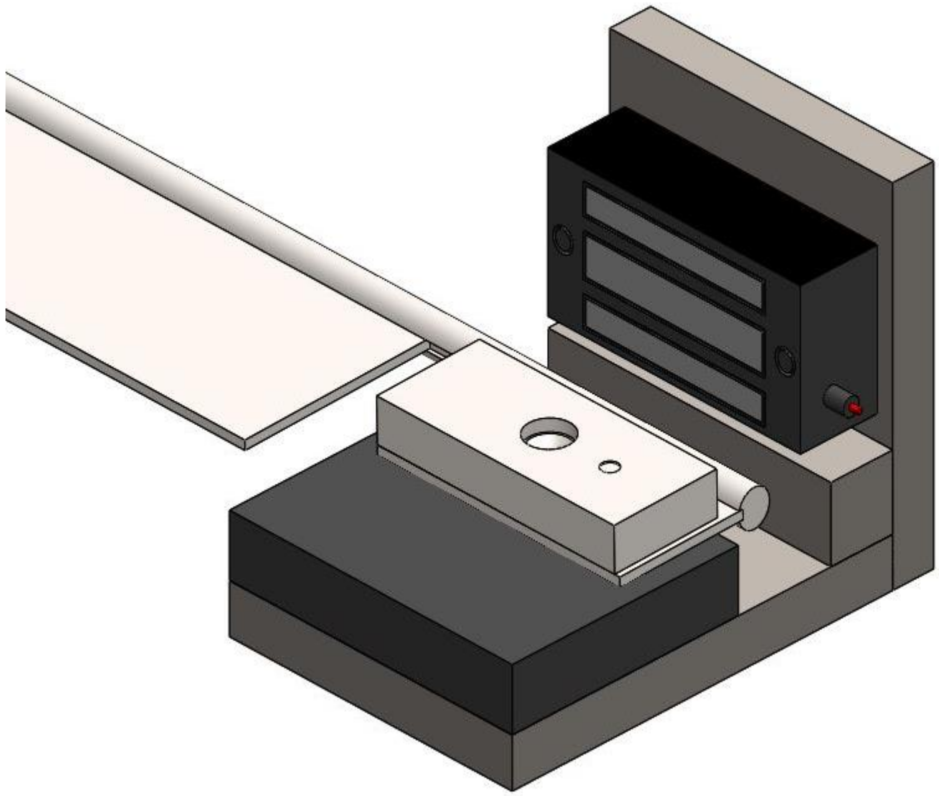

Figure 5: Simulation of the De-energized Electromagnet Releasing Gate to Opening Position

Literature Review

The ability to accurately measure the velocity of a jet that will be used to simulate a wave section is important. Without being able to measure the jet velocities, the simulated force of a wave cannot be matched. For the CFEL research project, this provides impact testing capabilities and the data acquired will be used for risk modelling studies [19]. In the long run, the data and risk modelling studies are hoped to better safeguard non-containment components (such as generators, doors, etc.) in a nuclear power plant or any other facility in the event of flooding or tsunami.

Artificial Wave Generation

The largest artificial wave generation facility in the world is located in Netherlands known as the Deltares Delta Flume. A view of the facility is displayed in Figure 6 [21] and an article with details can be found in Appendix D. Figure 7 displays a wave being generated at the same facility [28]. The facility is capable of producing solitary waves with heights up to 14.8 feet (4.5 meters) [23].

Figure 6: Deltares Delta Flume in Netherlands

Figure 7: Wave Generated at Deltares Delta Flume

In North America, the largest artificial wave generation facility is located at Oregon State University's O. H. Hinsdale Wave Research Laboratory and is known as The Large Wave Flume. It is capable of producing waves with heights up to 5.6 feet (1.7 meters). Figure 8 illustrates the Large Wave Flume [12].

Figure 8: Large Wave Flume at Oregon State University

Another facility at the same laboratory is the Directional Wave Basin. It is primarily used for tsunami research and is capable of producing waves with heights up to 2.5 feet (0.75 meters). Figure 9 illustrates the Directional Wave Basin [6]. A datasheet for both Large Wave Flume and Directional Wave Basin can be found in Appendix D.

Figure 9: Directional Wave Basin at Oregon State University

In these artificial wave generation facilities, channels or basins are used to contain a given depth of water, while paddles, plates or pistons are used for displacement purposes which in turn produce waves of different wavelengths and amplitudes [10] [14] [16]. These waves have a height restriction because wave speed in open channel flow cannot exceed a Froude number of one [21]. For the CFEL project, it is expected that the WISD can simulate wave heights of 20 feet. Clearly, there is currently no facility in the world that can produce waves as high as 20 feet.

WISD Design J (proposed by Greg Roberts)

To simulate a wave impact, the conduit geometry was determined to be a constant rectangular profile. The reservoir initially holding water was divided into ten discrete channels by extending horizontal plates to the back of the reservoir. Gates of 0.25 inch thickness were placed to rotate horizontally. Each channel had an independent gate. Additionally the channels were extended by plates angled at 45 degrees. This allowed air pressure to act on the free surface of water [21]. Figure 10 illustrates the dimensions of this design J [21]

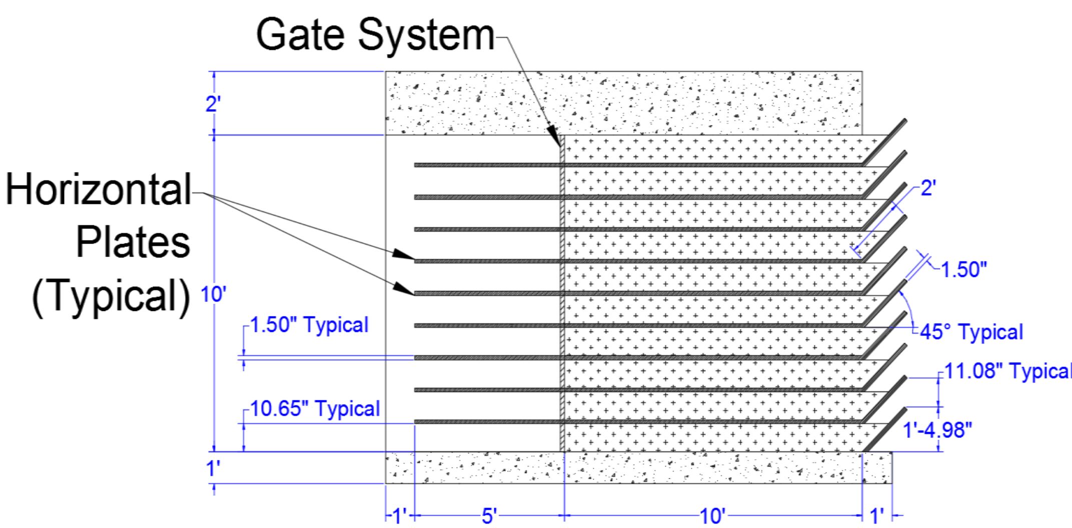

Figure 10: Dimensions of Design J

Figure 11 displays the isometric view of Design J using Flow-3D. Velocity represented is in feet/second [21].

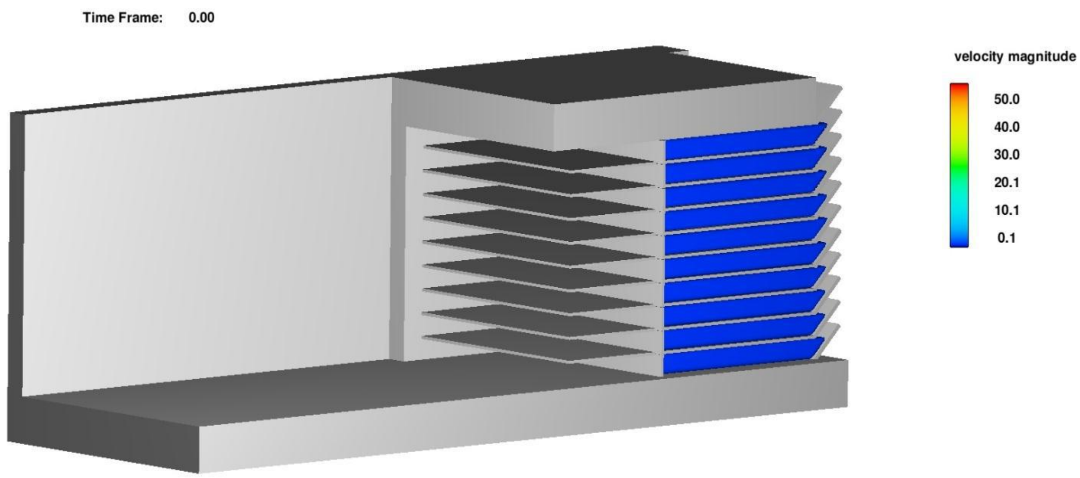

Figure 11: Isometric View of Design J

Figure 12 displays the simulation of the resulting wave using Flow-3D. Velocity represented is in feet/second [21].

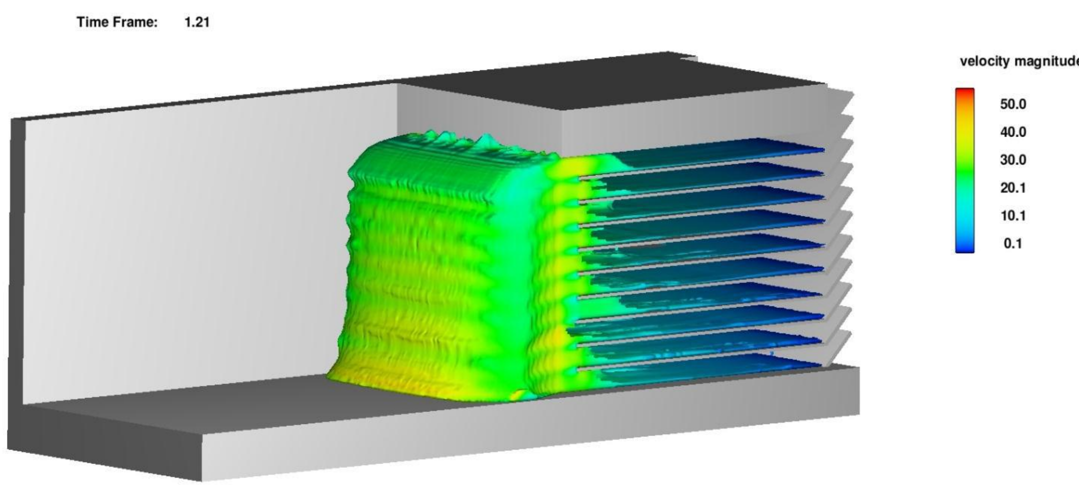

Figure 12: Wave Simulation Using Flow-3D

To test the validity of Design J, a physical model was proposed to be built with a specific scale ratio based on the Froude number. Table 2 presents the various model to prototype scale ratios [19].

Table 2: Modeling Parameters

Model Scale Ratios and Prototype Equivalence		
Scale	**Scale Value**	**Model to Prototype Equivalence**
Length scale	$L_r = 5$	1ft = 5 ft
Time scale	$t_r = 2.24$	1s = 2.24 s
Velocity scale	$V_r = 2.24$	1ft/s = 2.24 ft/s
Pressure Scale	$P_r = 5$	1 psi = 5 psi
Design Parameters (For small scaled Model)		
Scale factor	1:5	
Prototype-Model Similarity	Froude Number	
Velocity	11.36 fps	
Pressure	125 psf (0.868 psi)	
Materials to be used (Model)		
Outer walls	Plexiglass	
Inner plates & gates	Steel	

Methods of Measuring Velocity of Fluid Flow

The basic technique of measuring the velocity of fluid flow consists of acquiring the time of flight of the fluid particles passing through two or more points placed at known distances [8] [15]. Some of the techniques investigated were laser velocimetry, particle image velocimetry, particle tracing velocimetry, and velocity measurement using an infrared break beam sensor.

Laser Velocimetry

Laser velocimetry is based on the principle of either a laser Doppler anemometer [17] or laser transit anemometer (LTA) [3]. The process is also known as laser Doppler velocimetry (LDV). The method consists of creating light fringes by means of some interference between the laser beams that are coherent at the same wavelength [7]. In LTA, also known as two-focus or laser dual-focus anemometer [11], a single laser beam is split in two equal parts creating two focal points. As the fluid particle passes through both these focal points, it generates a scattering light which is detected and converted to a voltage signal. Once the time of flight of the particle is determined between the two spots, the velocity is then calculated with the simple formula of the known distance between the spots over the time of flight [2]. Figure 13 illustrates a single-component dual-beam LDA system [27].

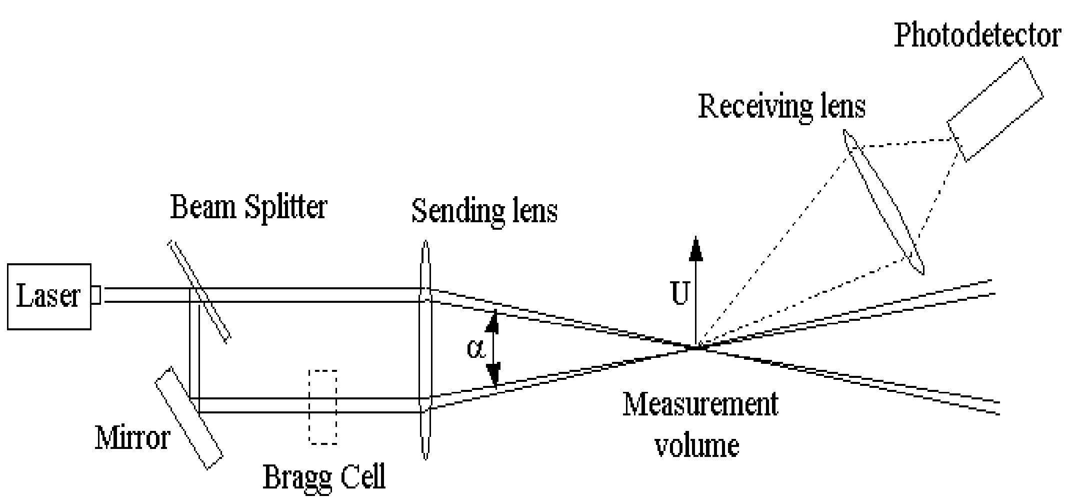

Figure 13: LDA System

This LDA system was used to measure the velocity of water for a high-speed water jet cutting system, measuring high-speed water velocities at the exit of the cutting head nozzles [2]. The high value of the Doppler signal frequency that is generated due to the high-speed of the fluids makes it difficult for the LDV method to be implemented while measuring velocity of high-speed fluid flow. A major limitation is the high-frequency photodetector itself, resulting in reduced sensing area and therefore lowering the sensitivity overall [2]. In addition, the LTA method requires high precision for positioning and alignment of the laser beams [11].

Particle Image Velocimetry

The main principle of particle image velocimetry (PIV) consists of recording two successive time images of particles lighted by a laser. A high-speed photo or video camera is used to capture images. The instantaneous velocity of the fluid is measured by determining the displacement of the particles. The advantage of this method is that it allows a section of the flow field to be mapped [5]. Usually, a high-speed camera is used to take a number of pictures at each section of the flow field. All data is recorded by a computer for further analysis. The computer software associated with the high-speed camera analyzes each frame to determine the time of flight of the particle between two grids separated at a known distance, thereby calculating the velocity of the particle. This process was used to measure the terminal velocity of water for a building's drainage stack network. The goal was to measure the flow rate for drainage systems in order to comply with the standards of the National Plumbing Code of the United States [4]. Again, this process also requires high precision for alignment of the laser, positioning of the camera for optimal resolution [4]. Figure 14 illustrates a flow chart for particle image velocimetry [25]. Figure 15 illustrates a general experimental setup of the particle image velocimetry [5].

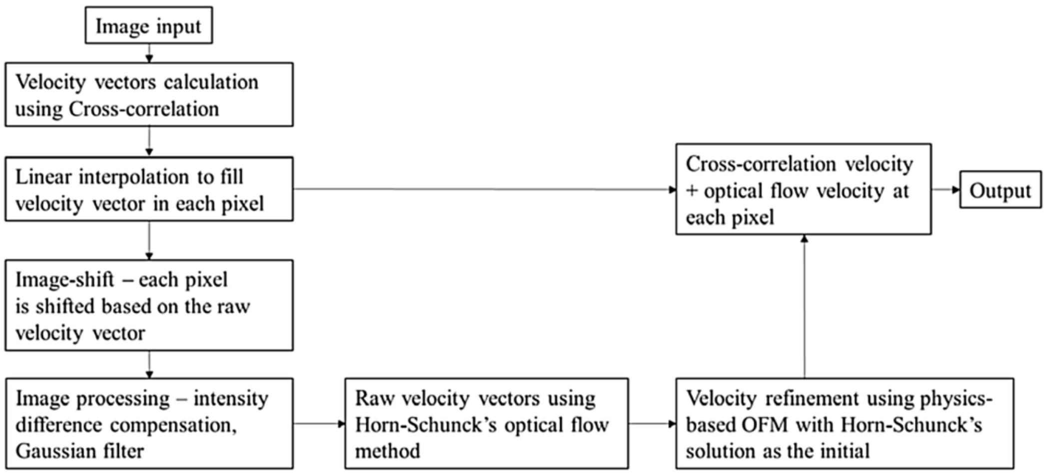

Figure 14: Flow Chart of Particle Image Velocimetry

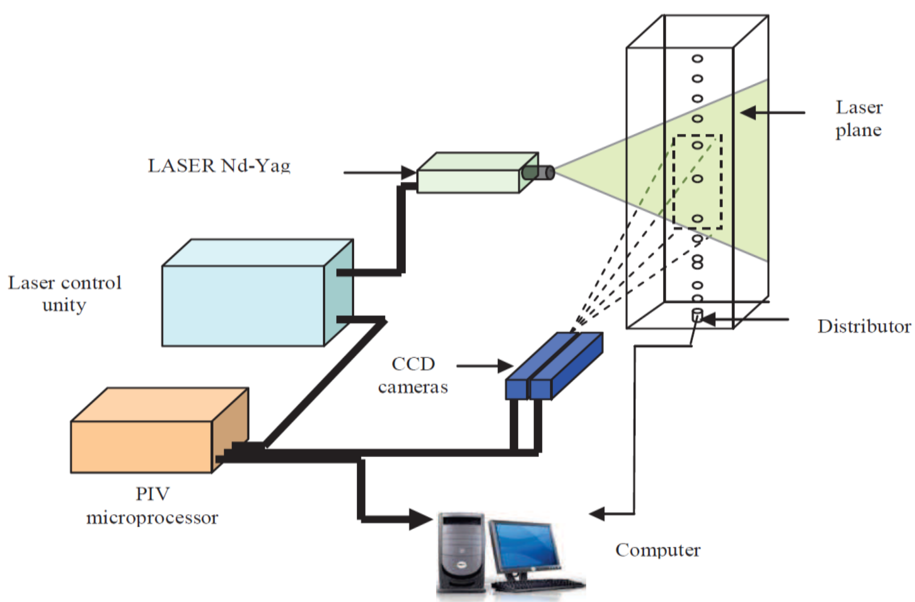

Figure 15: Experimental Setup of Particle Image Velocimetry

Particle Tracing Velocimetry

The particle tracing velocimetry (PTV) method is mainly useful for measuring the flow velocity under a surface, such as water flow within a gravel layer [13]. The measurement of shallow water flow commonly involves the use of tracers such as dyes [1], electrolytes (such as salts) [18] [22], or magnetic materials [24]. Particle tracing velocimetry involves the use of instrumentation to detect the tracer movement [13]. A typical flow velocity measurement system utilizing the particle tracing velocimetry method is illustrated in Figure 16 [13].

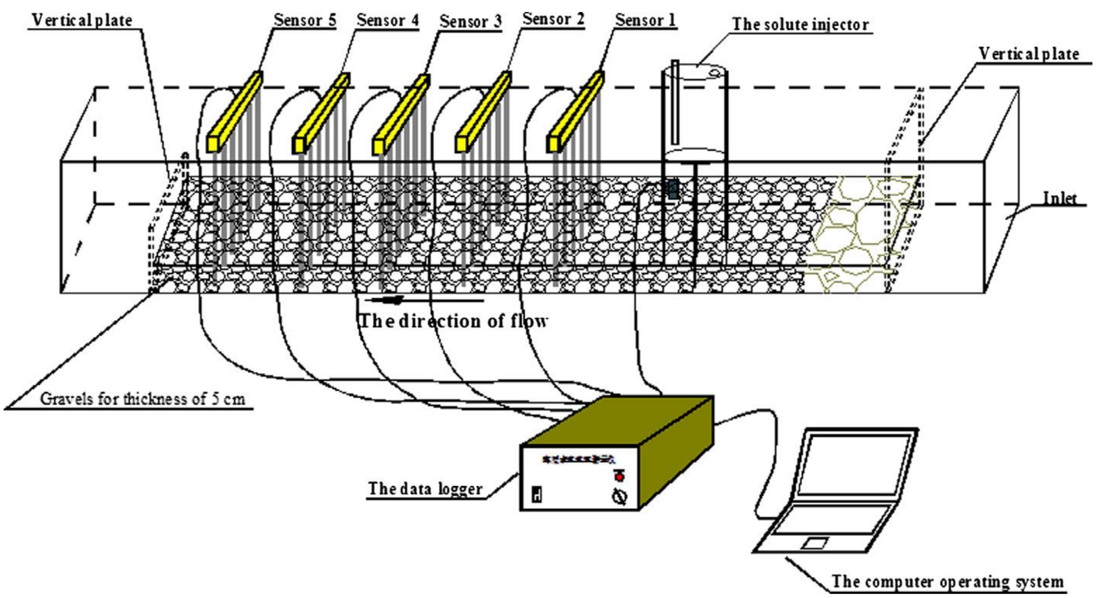

Figure 16: Experimental Setup of Particle Tracing Velocimetry

The PTV system includes a data logger, computer, sensors and solute injector. In this example, the solute was electrolytic solution tracer and the sensors were ion-sensitive electrodes. The concept of measuring velocity is similar to those of the other methods discussed before. The distances between the sensors are known. The time of flight of the tracer between each sensor was determined using the data logger and the computer, thus enabling it to calculate the velocity of the fluid flow [13].

The aim of this research is to measure the velocity of a high-speed jet of water that is not continuous. It is based on an off-on-off concept. Stationary water is subjected to pressurized air for a specific amount of time. The above mentioned processes are either not capable of measuring high-speed flow or are only ideal for continuous flow.

Infrared Break Beam Sensor Method

The basic purpose of a break beam sensor is to detect motion. They are a two-component sensor consisting of an emitter and a receiver. Once setup, the emitter sends out an infrared light (invisible to human eye) and the same light is received by the receiver component. When something passes between the two components and is not transparent to infrared, the beam is broken and is notified by the receiver. Water exhibits strong absorptions from vibrations of its molecule in the infrared spectrum and hence is not transparent to infrared [29]. Figure 17 displays the infrared break beam sensor [30]. The component on the right is the transmitter and the component in the left is the receiver.

Figure 17: Infrared Break Beam Sensor

Connecting the break beam sensor to a microcontroller and placing it in series of known separation distance creates a measurement device similar to a PTV. Placing the sensors along the walls of a transparent pipe where the water will flow, the time of occurrence of beam being broken can be measured and the velocity of water flow can be calculated using the distance over time formula. Efforts were made to implement this technique but problems were encountered. Although water is not transparent to infrared, but during the process of implementing the break beam sensor for this thesis, clear water could not break the infrared beam and hence the detector was unable to detect any motion. A datasheet for the break beam sensor can be found in Appendix E. Figure 18 illustrates the sensors connected to an Arduino micro-controller [30].

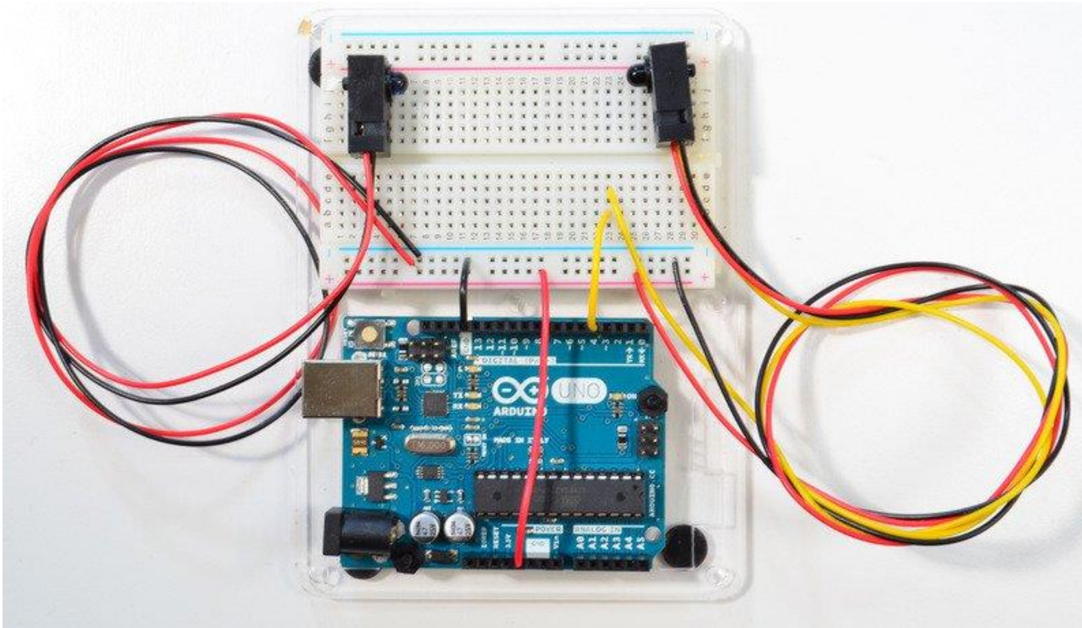

Figure 18: Break Beam Sensor with Arduino Micro-controller

Experiment

Due to the complexity of the sectional model (mainly the gate section) that was supposed to be built with Plexi glass and time constraint, another small scale physical model was proposed to verify the usability of air pressure and functionality of the velocity measurement devices (sensors). The advantages of using this small-scale model was that it mainly allowed us to investigate the possibility of using a PVC pipe with a “U-tube” shape rather than the gate system.

The conduit was a clear 4-inch diameter schedule 40 PVC pipe, with inlet and outlet angles of 45 degrees. The water depth was maintained at one foot from the ground level. The purpose of using clear PVC pipes was to observe the fluid behavior upon application of air pressure. Figure 19 shows a schematic side view of the U-section of the experimental model.

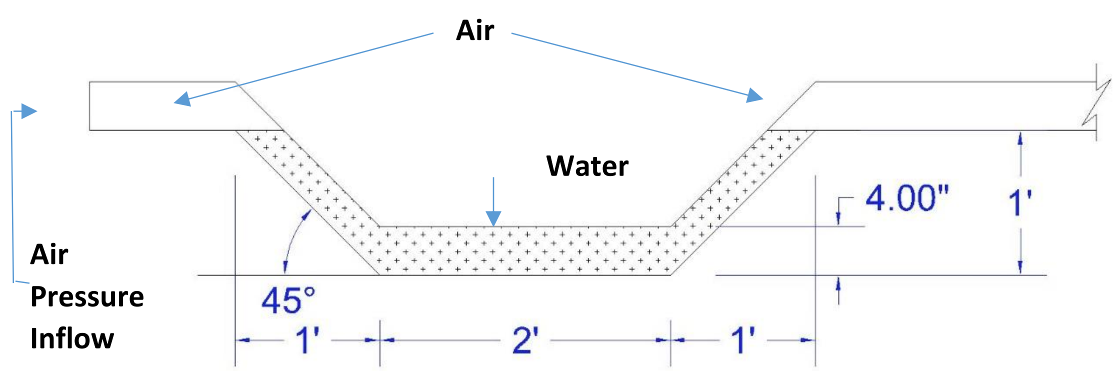

Figure 19: Schematic Side View of the U-section

Figure 20 shows the actual U-section used in the experiment. The left-hand side is the outlet that was connected to a 10 foot clear schedule 40 PVC pipe of 4-inch diameter (wave development section). The right-hand side is the inlet that was connected to the solenoid valves that are discussed later in this section. It also had a tee with threaded fitting in order to attach a pressure transducer to monitor the air pressure upstream of the U-section. An Omega high-speed USB output pressure transducer was used for this purpose. Figure 21 shows the pressure transducer that was used [33]. It came with a digital software application that was simple to use. It allowed us to record 80 pressure readings per second. The transducer has an accuracy of 0.08% (linearity, hysteresis, and repeatability combined). Details of the pressure transducer can be found in Appendix H.

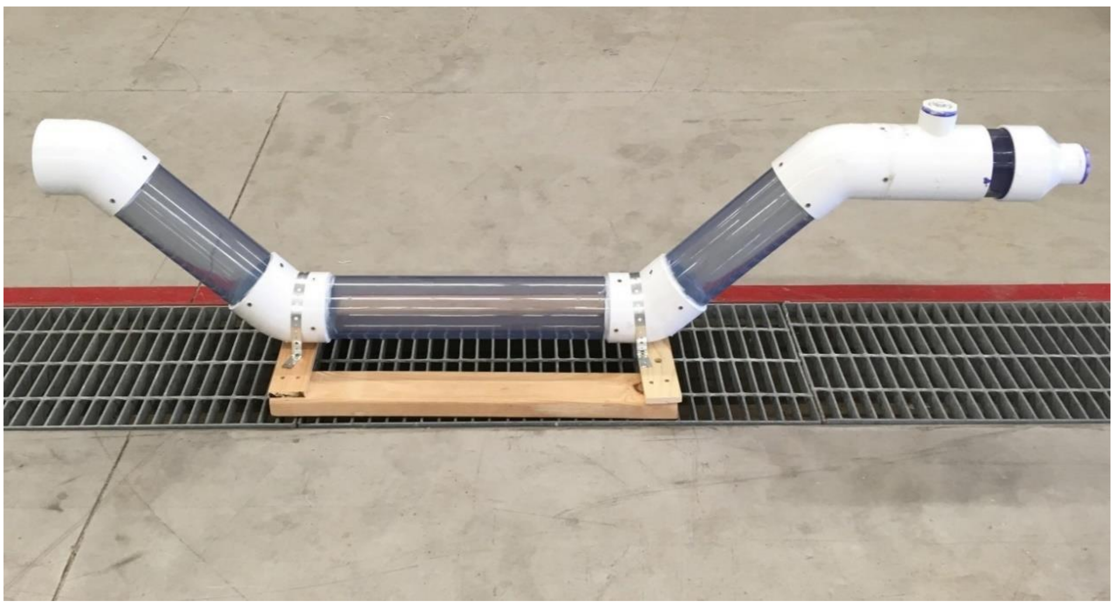

Figure 20: U-section Physical Model

Figure 21: Omega Pressure Transducer

Figure 22 shows the chamber used for building the required air pressure and holding air before being released in a controlled manner to the U-section. The air pressure chamber is constructed from an 8-inch diameter schedule 40 PVC pipe. The left-hand side had two adapter inlets for feeding the two air compressors used to pump air in to the chamber. The right-hand side was reduced to 1-inch diameter (using an 8-inch to 4-inch, 4-inch to 2-inch, and 2-inch to 1-inch reducers consecutively) for connecting to the solenoid valves.

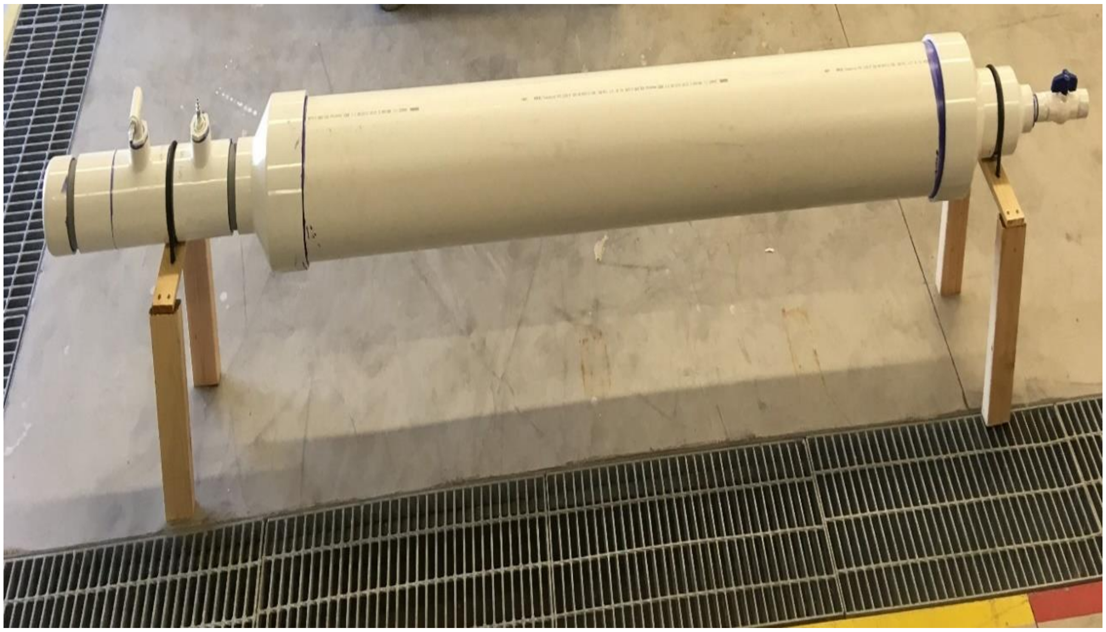

Figure 22: Air Pressure Chamber Physical Model

The reason for using the solenoid valves was to control the time for which the air pressure was applied to the water in the U-section. Figure 23 shows the solenoid valve system being used. Figure 24 shows the solenoid valve section connected to the entire system. The left-hand side connected to the U-section and the right-hand side connected to the air pressure chamber.

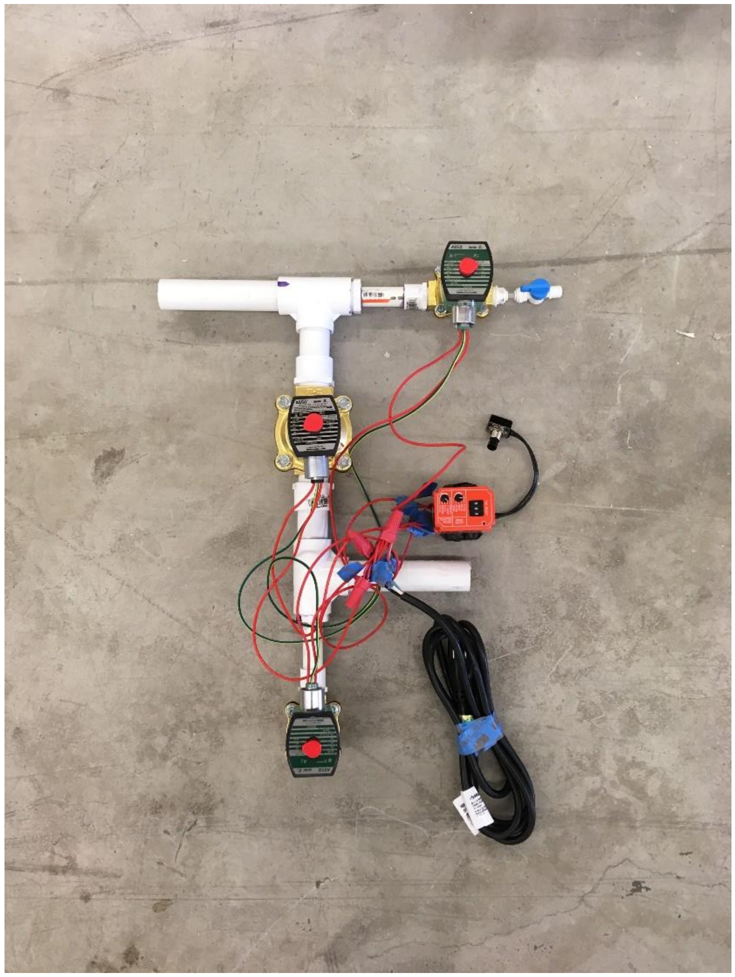

Figure 23: Solenoid Valve Section

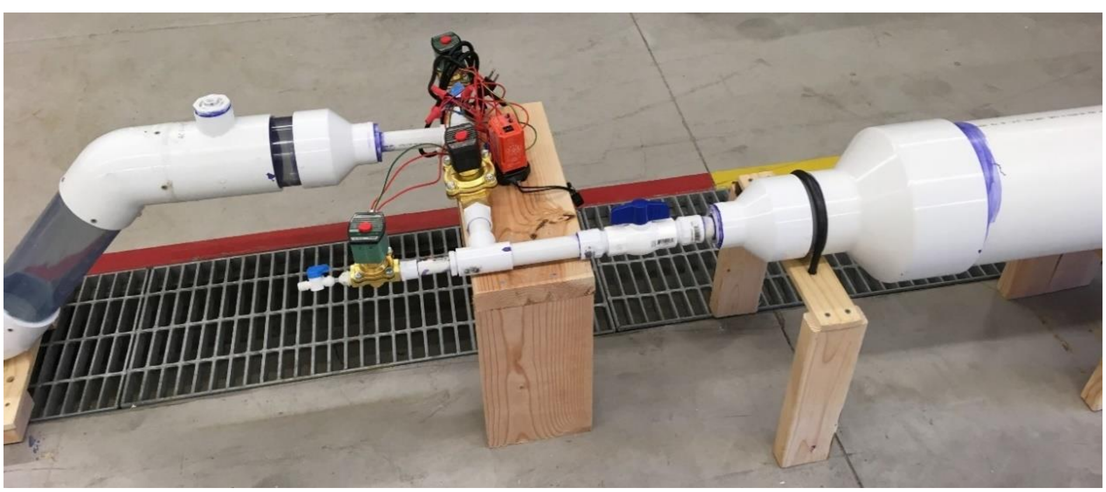

Figure 24: Solenoid Valve Section in Connection

The valves used had to be fast-acting. As manually operating them could not be accomplished in necessary timeframe. Therefore, solenoid valves with less than 50 milliseconds response time were chosen. This was done since the Flow-3D model showed that to generate a steady wave with a velocity of 11.36 feet/second, the air pressure needed to be applied for 0.38 seconds. Figure 25 shows the diagram of pneumatic system for the solenoid valves. Valves 1 and 3 are normally open and closed when energized. Valve 2 is normally closed and opened when energized. These valves were all powered using a multifunction timer relay.

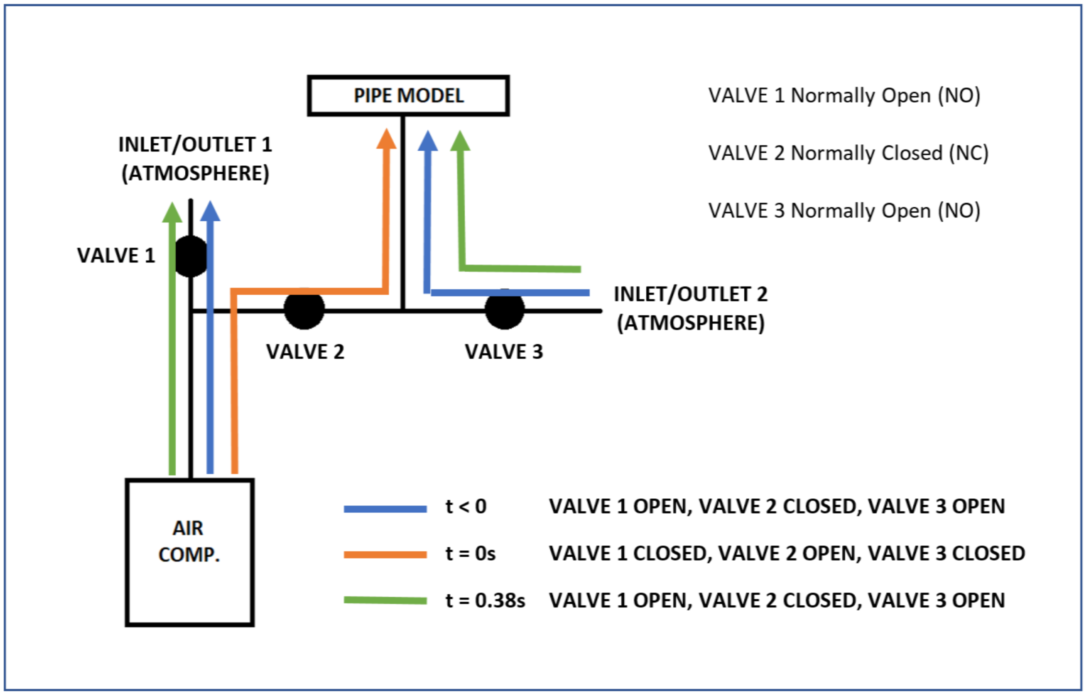

Figure 25: Pneumatic System for Solenoid Valves

Sensors were connected to the 10 foot clear schedule 40 PVC pipe section that was attached to the outlet side of the U-section. Ten type 1 sensors (five pairs) and two type 2 sensors (one pair) were used. This shown in Figure 26. Figure 27 shows the sensor electrical connections.

Figure 28 and Figure 29 shows the overall physical experimental model.

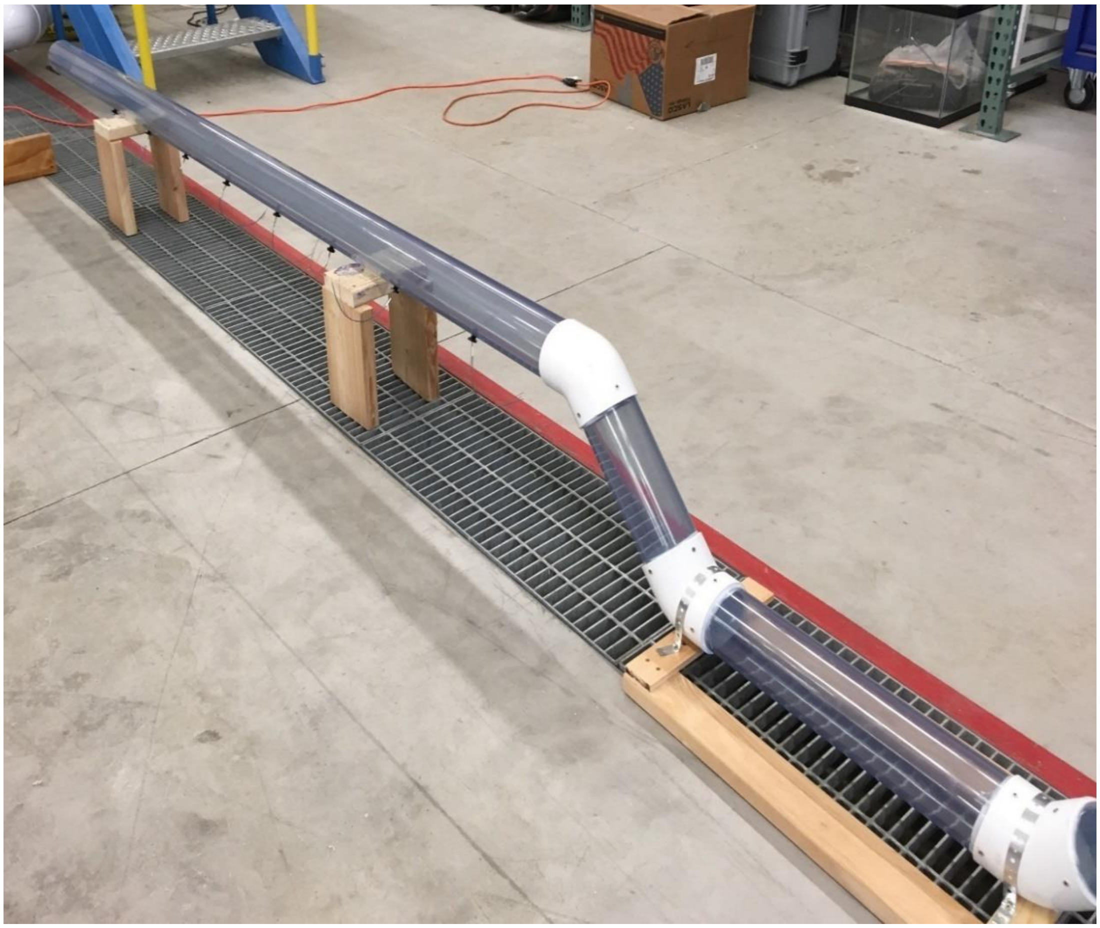

Figure 26: Sensors on Developmental Section

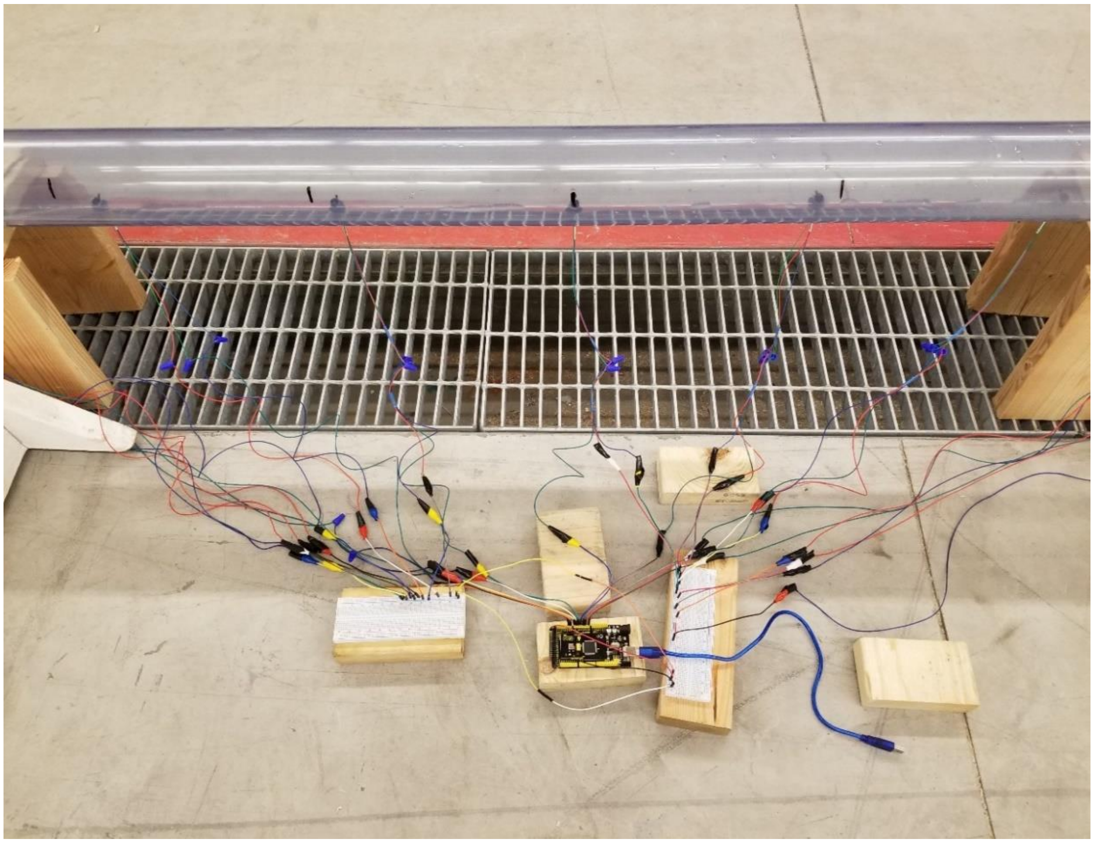

Figure 27: Sensor Electrical Connections

Figure 28: Entire Physical Model (Without Sensors)

Figure 29: Entire Physical Model (Side View)

Methodology

The primary task is to measure the velocity of the wave in the developmental length section of the pipe model. That is the 10 feet clear schedule 40 PVC pipe section that was attached to the outlet side of the U-section.

Two different sensors were tried for comparing accuracy of the measured velocity. Sensor type 1 is a single component sensor from Adafruit Industries called Optomax digital liquid level sensor. Sensor type 2 is a combination that was designed. It uses a photo-resistor connected in series with a 10K resistor. The functioning of these sensors are explained in the following sections. The sensors were configured to work in pairs and were distributed along the whole length. This will enable the wave velocity to be measured at different points. All individual sensors are powered and configured through a single Arduino mega microcontroller board, which in turn is connected to a computer. A code is then written in C in the Arduino platform and can be found in Appendix A. The code directly outputs the computed average velocity between the two sensors in a pair. Same methodology and code is used for both the sensor types. Figure 30 shows a flow chart of the code used. The sensors were placed one feet apart from each other. The code used can be modified to record velocity at each sensor location rather than combining them as pairs. Though, this modified code can be more complex, but it would provide more velocity readings. A flow chart for the modified code can be found in Appendix I.

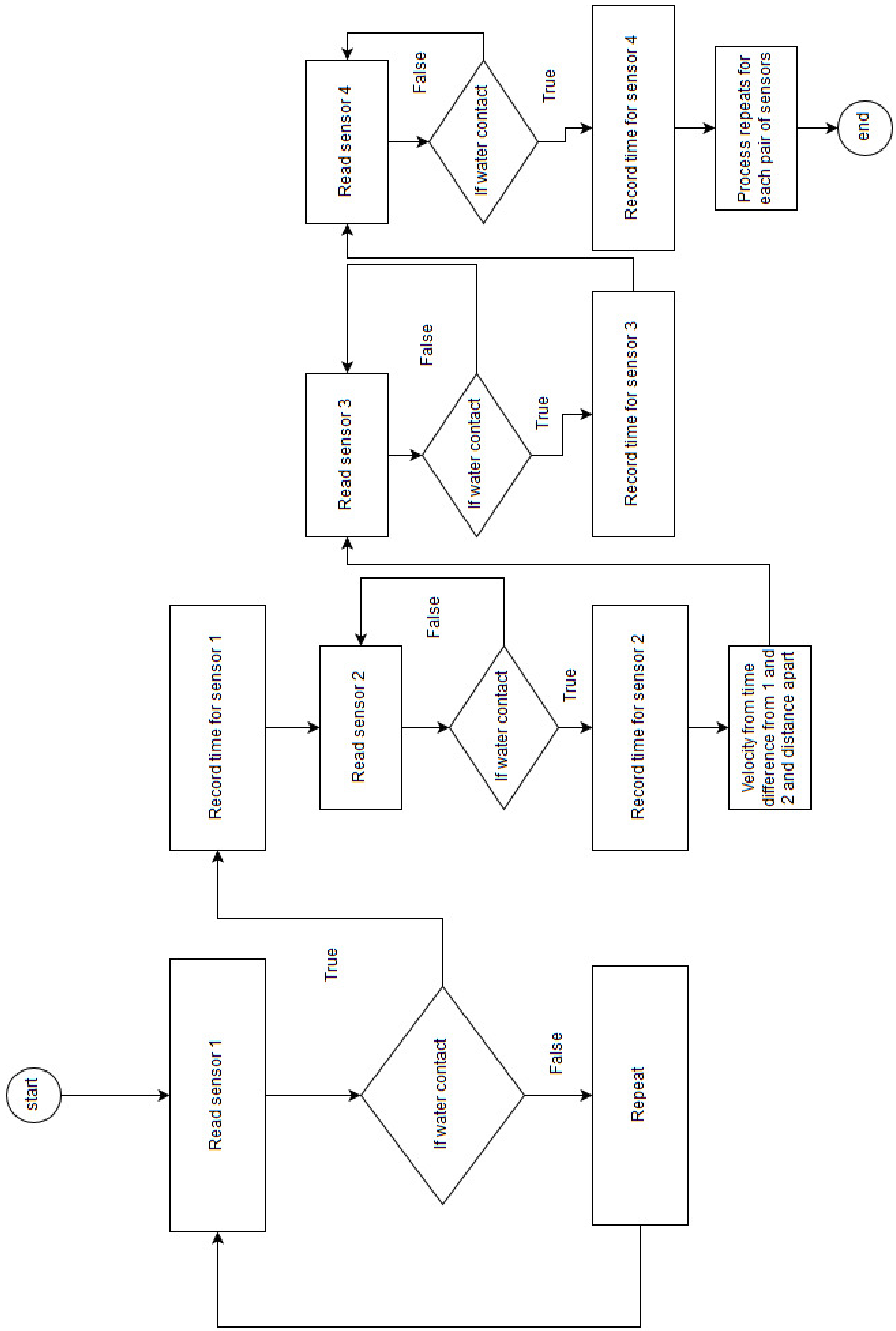

Figure 30: Flow Chart of the Code Used

Figure 31 shows the microcontroller being used in these processes [31]. A datasheet with details on the pin configuration and how to use the micro-controller can be found in Appendix F [31].

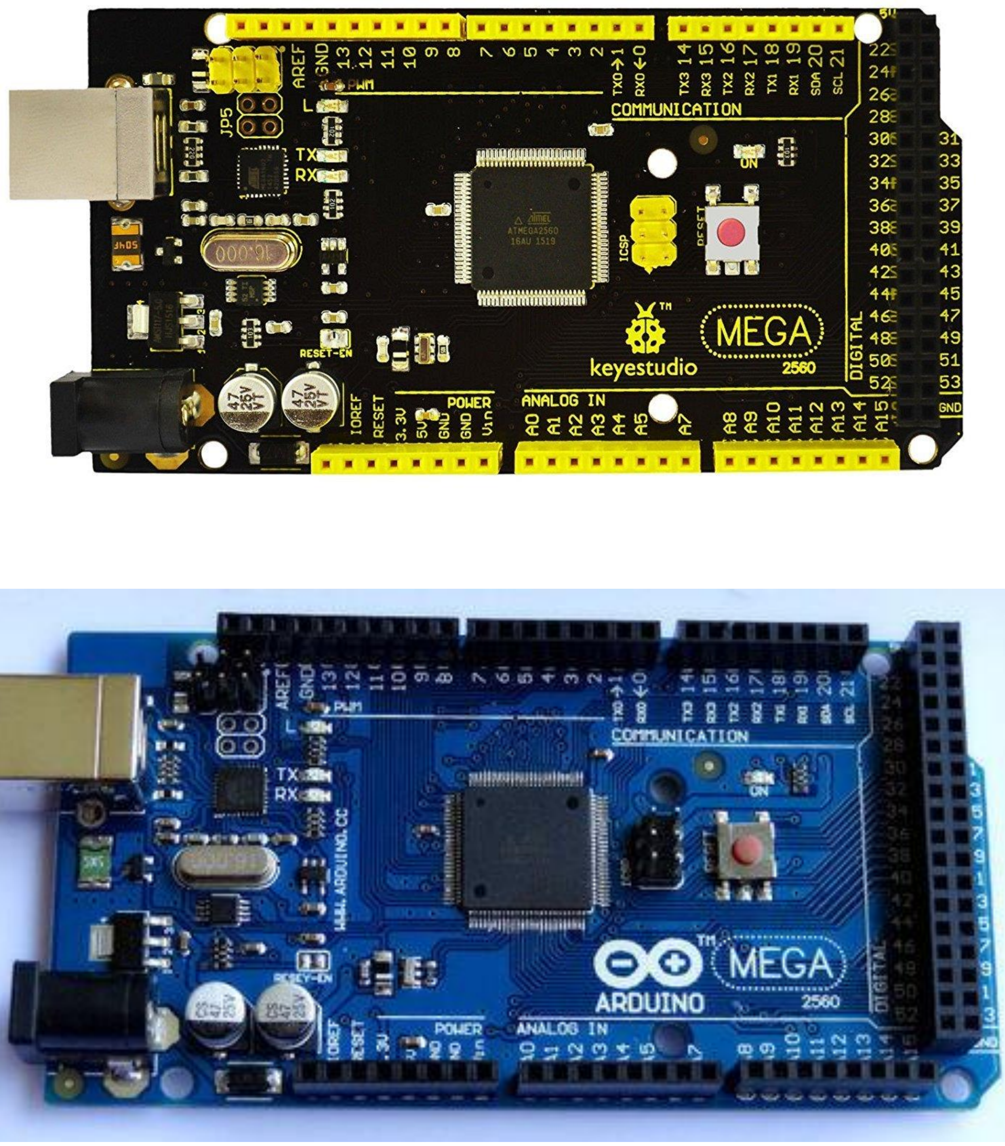

Figure 31: Arduino Mega 2560 Micro-controller

First Sensor Type:

This is a single component sensor from Adafruit Industries called Optomax digital liquid level sensor. Figure 32 is a picture of the Optomax sensor [30].

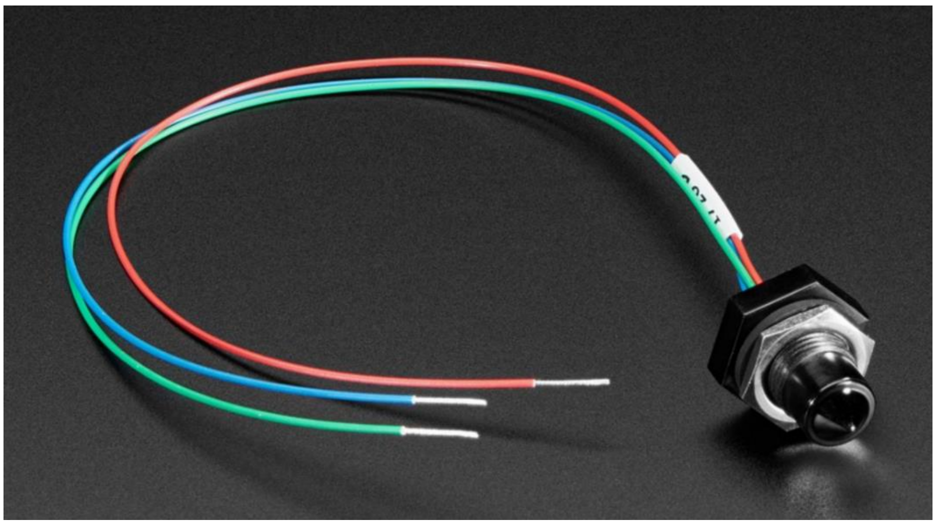

Figure 32: Optomax Digital Liquid Level Sensor

This is expected to measure the velocity with more accuracy since it is pre-built and involves less complexity in positioning it along the developmental length. It simply needs to be screwed in the pipe section. This sensor has an infrared LED and a matching phototransistor inside the plastic casing. When the sensing tip is in open air, the infrared light is bounced back to the sensor because of being dry. When the tip of the sensor is immersed in liquid, it lets the infrared light escape, which causes the transistor to turn off. The sensor is capable of detecting most liquids that are oil or water based. The sensor has three wires. The blue wire is for grounding, red for voltage supply, and the green is the input wire to the microcontroller. When the sensing tip is dry, the output is the same as the red wire. When it is wet, the output is zero volts. This sensor is highly sensitive and any volume of liquid triggers it [30]. Figure 33 displays the sensing tip [30]. Using the code in Appendix A, the time stamps when the sensor detects any liquid were derived. As the distance between a pair of sensors is predetermined, it becomes simple to calculate the velocity with distance over time equation. Details of the Optomax sensor can be found in Appendix G [30].

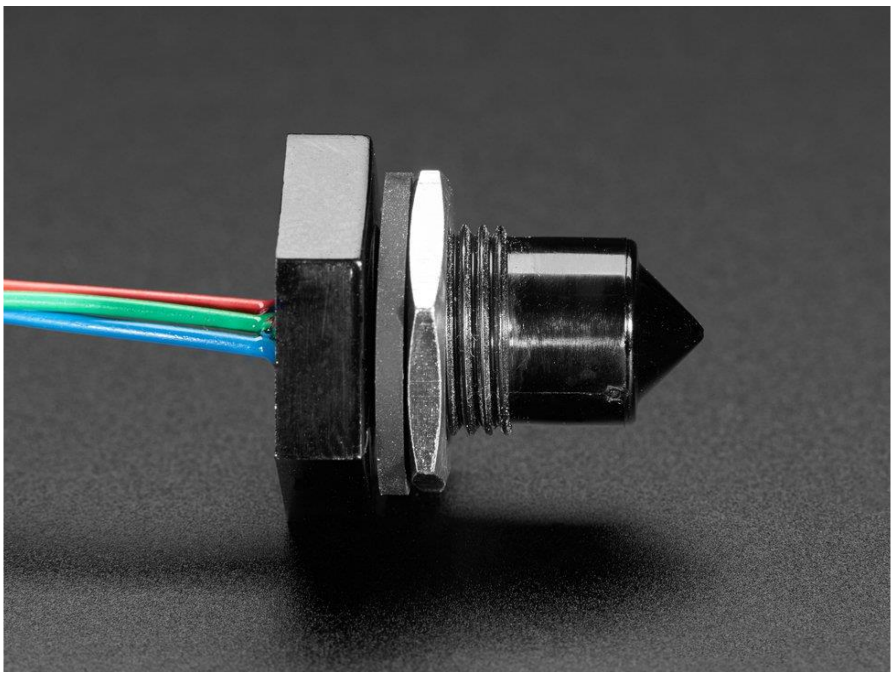

Figure 33: Sensing Tip of Optomax

Second Sensor Type:

For the second sensor type, a photo-resistor was connected in series with a 10K resistor. Photo-resistors are light sensitive resistors whose resistance decreases as the intensity of light they are exposed to increases. They are also known as light dependent resistors (LDR). When it is dark, its resistance is very high (sometimes up to one mega-ohm). When they are exposed to light, their resistance drops drastically (even down to few ohms) [32]. Figure 34 displays a photo-resistor [20]. Figure 35 displays a 10k resistor that was used in this combination [30].

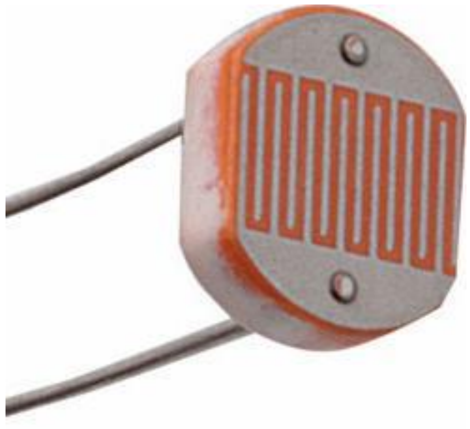

Figure 34: Photo Resistor

Figure 35: 10k Resistor

The photo-resistor and the 10k resistor were placed in series, connected to a 5V supply and ground from the micro-controller. The whole setup can be put on a breadboard and an example is displayed in Figure 36.

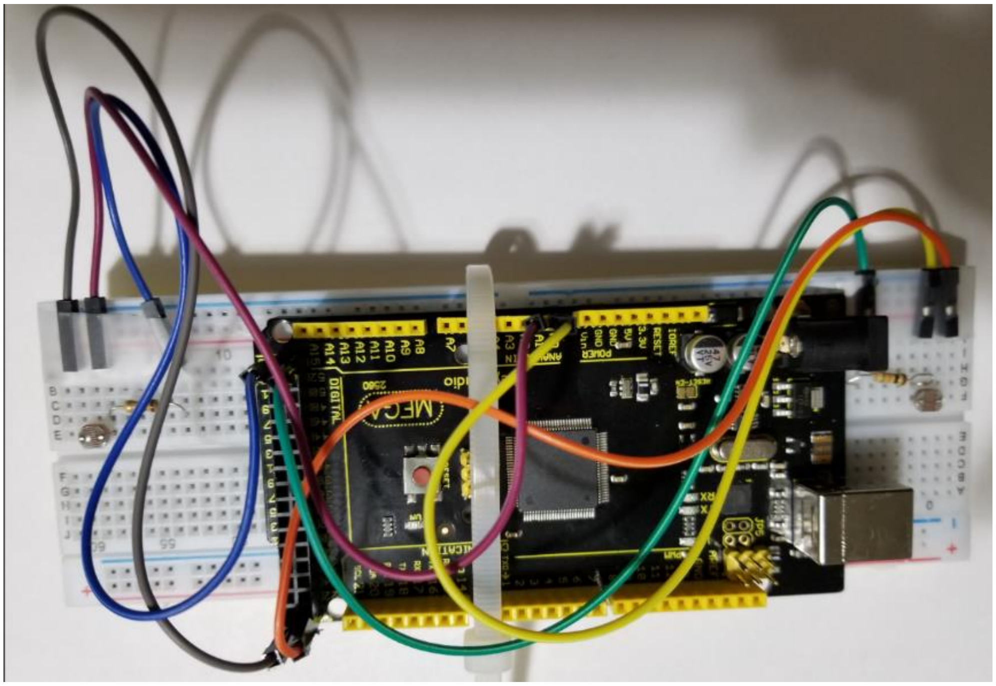

Figure 36: Combination Sensor with Photo-resistor and 10K Resistor

The photo-resistor detects a change in light intensity as its resistance changes. Again using the same code we derive a time stamp for this change. From this point, the velocity was calculated by using the distance over time formula. The reason for using a 10K resistor is to divide the voltage and have a way of comparing a voltage drop as light intensity changes. A circuit diagram for this sensor type is shown in Figure 37.

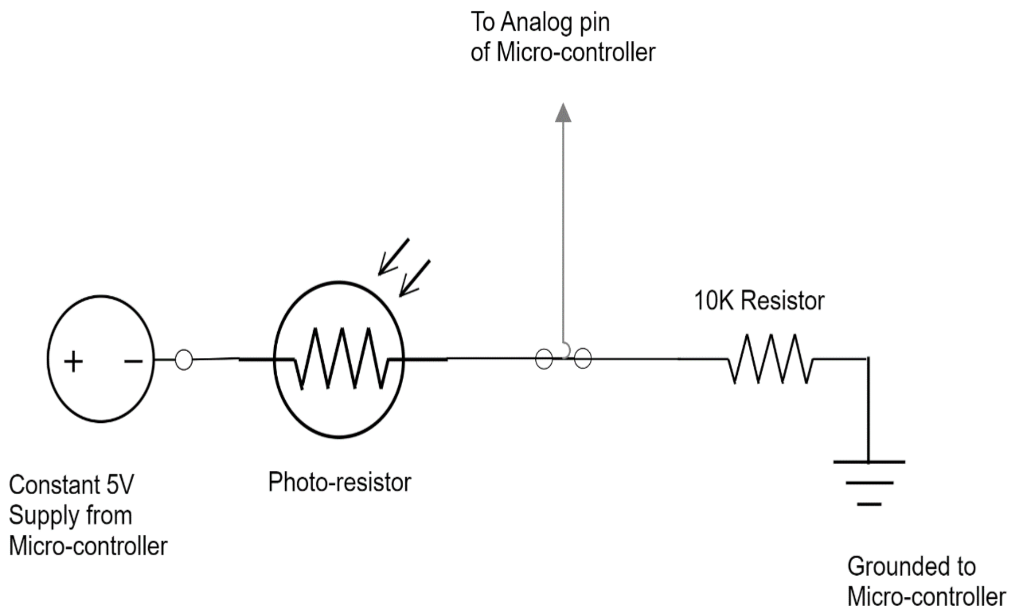

Figure 37: Circuit Diagram for Combination Sensor

Results

The sensor type 1 (Optomax sensors) successfully recorded data of the wave velocity for every experimental run. Ten sensors were distributed with a separation of one foot among each other, along the wave developmental pipe section. Using the code (written in C and can be found in Appendix A), the sensors were coupled in pairs to report velocities at 5 different sections in the pipe. Sensor type 2 (photo-resistor) did not provide accurate results due to its high dependency on light intensity. The photo-resistor outputs a certain numerical value based on the light intensity. A high number represents a higher light intensity and vice-versa. And due to mostly using clear water, this number did not fluctuate much thus sensor type 2 (photo-resistor) was unable to detect significant changes in light intensity.

The Omega pressure transducer also successfully recorded data of the air pressure in the U-section. Air pressure of 2.75 psi for a time of 0.53 second was chosen as ideal data set due to its close similarity with theoretical kinematics analysis.

Table 3 represents the different velocities for each run along with some other data in details. DL represents the development length, the pressure (psi) data in the second column is the air pressure inside the air pressure chamber, and Avg_Pressure is the average of the pressure data recorded by the pressure transducer in the U-section. Each velocity is measured over a two feet distance.

Figure 38 shows the velocity of the water jet along the various locations of the pipe where the sensors were placed for 2.75 psig runs. Figure 39 shows the relationship between the pressure in the chamber and the pressure in the U-tube section for 2.75 psig runs. As the pressure in the chamber increases the pressure in the U-section increases as well. The pressure in the U-section is lower than the pressure in the chamber because as the pressure is released from the chamber, the overall volume increases and thus pressure decreases.

Table 3: Detailed Velocity and Pressure Data

				Velocity (ft/s)					
Run	**Pressure (psi)**	**DL (ft)**	**Time(s)**	**2**	**4**	**6**	**8**	**10**	**Avg_Pressure (psi)**
1	5	2	0.4	15.63	16.95	11.36	13.70	14.56	2.22
2	3	2	0.4	12.35	12.50	12.99	12.82	14.56	1.64
3	2.5	2	0.4	21.74	12.50	12.82	10.53	6.97	1.41
4	1.5	3	0.63	6.25	10.87	10.20	8.26	15.37	0.82
5	1.5	3	0.75	11.63	14.49	12.35	11.49	9.76	1.19
6	1.5	3	0.75	7.75	7.94	7.63	6.49	6.10	0.5
7	3	3	0.75	8.26	15.15	11.49	9.52	8.06	0.41
8	3	3	0.75	13.70	13.25	10.42	12.50	11.53	1.14
9	3	2.5	0.5	16.67	10.42	10.20	12.35	11.22	1.32
10	1.5	3	0.58	8.33	8.06	8.33	7.19	7.76	0.68
11	3	3	0.58	16.13	11.49	12.20	10.10	11.22	1.12
12	3	3	0.58	18.87	15.63	12.35	12.20	9.43	1.19
13	3	3	0.53	14.08	15.63	9.71	12.20	11.53	1.18
14	2.75	3	0.53	10.10	12.82	10.64	10.64	10.25	1.09
15	2.75	3	0.53	11.63	12.82	12.35	10.10	8.3	1.11
16	2.75	3	0.53	11.49	14.08	11.11	11.36	10.64	1.13
17	2.75	3	0.53	11.24	12.2	11.76	9.35	12.39	1.09
18	2.75	3	0.53	11.57	11.24	10.63	11.11	10.57	1.11
19	2.75	3	0.53	11.76	13.16	10.42	10.35	9.71	1.14
20	4	3	0.53	20	12.99	16.13	14.08	10.78	1.56
21	5	3	0.53	28.57	11.36	16.95	16.67	16.6	1.85
22	10	3	0.53	22.73	12.05	38.46	27.78	25.94	2.89

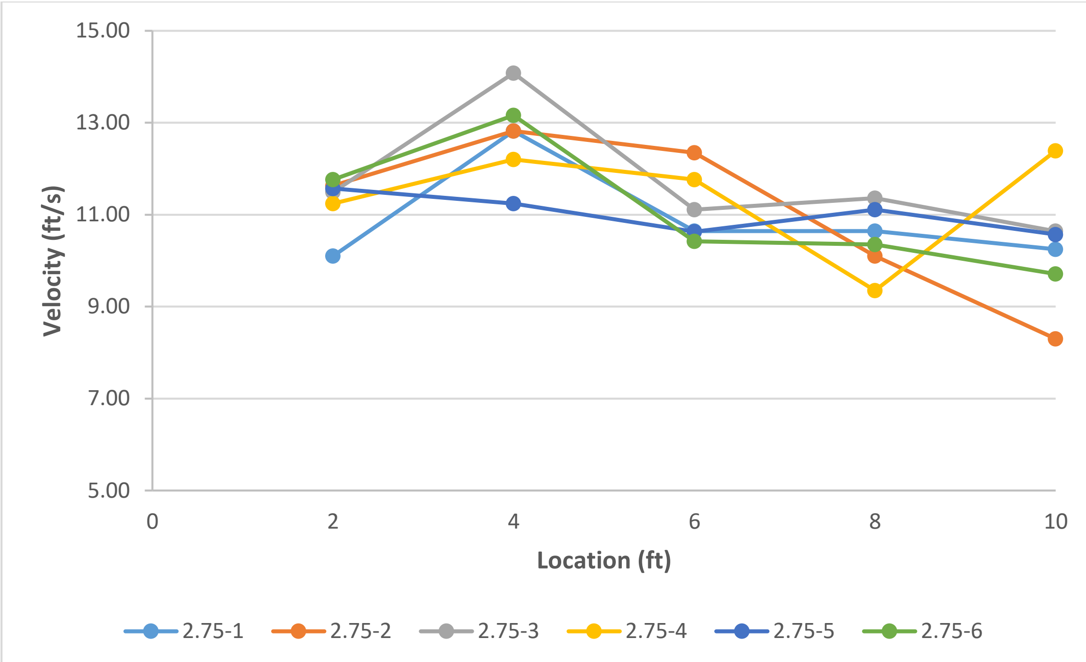

Figure 38: Velocity of Jet at Different Locations for 2.75 psig Runs

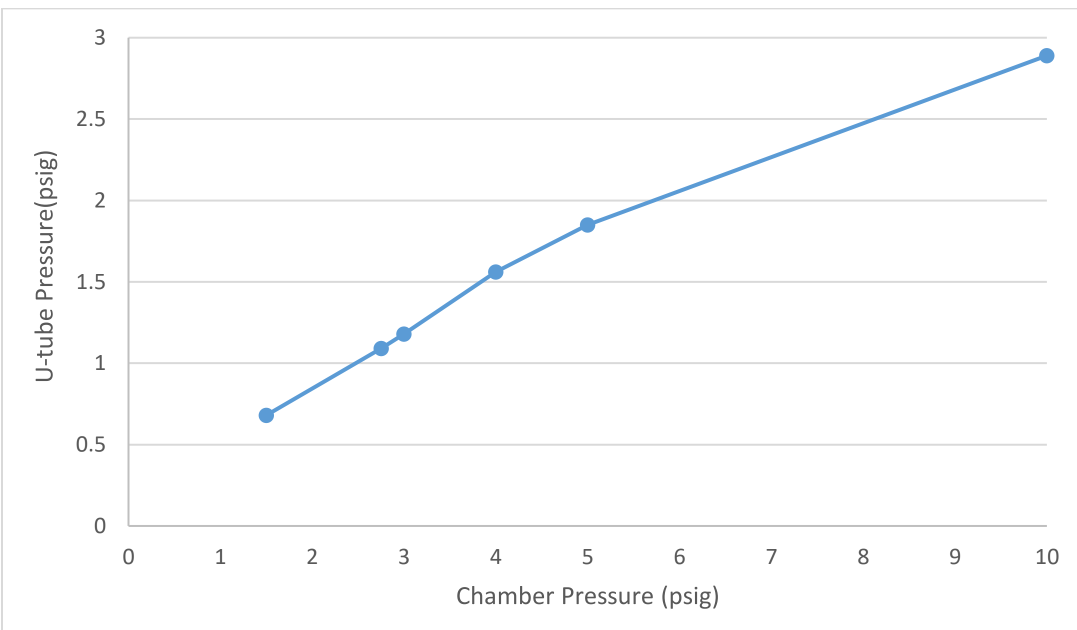

Figure 39: Relation between the Chamber Pressure and U-tube Pressure

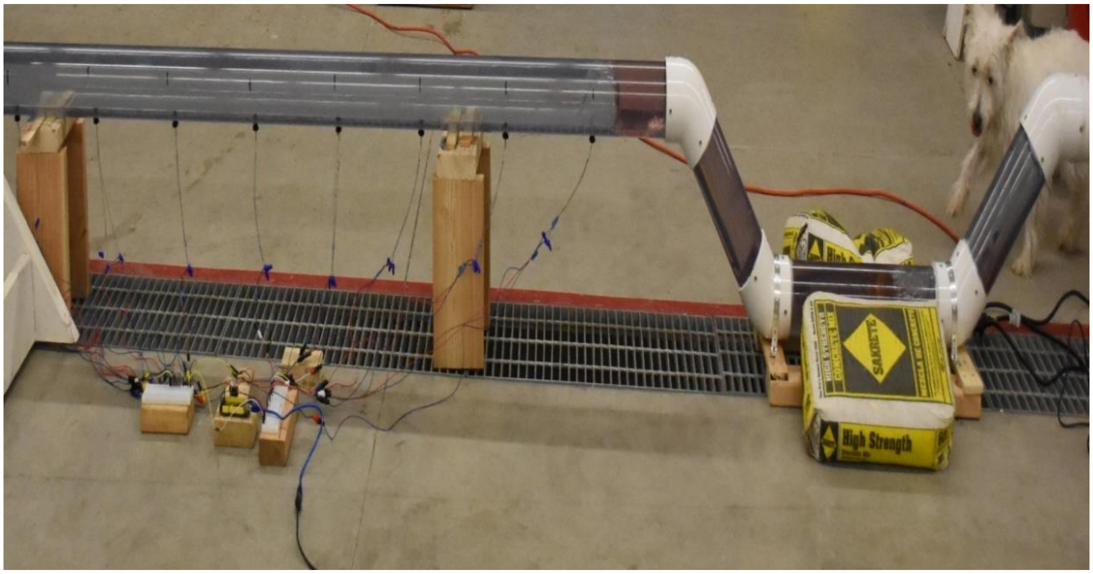

Figure 40: Wave Generated during 2.75 psi Experimental Run

Standard deviation for the pressure in the U-tube section was also computed. It was computed for three runs of 2.75 psi pressure (air pressure chamber). The results are tabulated in Table 4.

Table 4: Standard Deviation for Three Experimental Runs

	2.75psi_Run 6	**2.75psi_Run 5**	**2.75psi_Run 3**
Average Pressure in U-tube	1.14	1.11	1.13
Standard Deviation	0.75	0.77	0.74

The goal was to generate a water jet with constant velocity. Referring to Table 3, it can be seen clearing the velocity is not constant. The reason being the pressure inside the U-tube section is not constant. Another explanation can be, gravity acts on the wave front and produces a tongue in the bottom portion, which might be a reason for the velocity to increase as water is accelerated by gravity. As the tongue is produced, the wetted perimeter of the water jet is reduced, as the top portion of the wave is dragged down by gravity. With the smaller surface area in contact, water might have been additionally accelerated due to the acting air pressure. Figure 41 through Figure 43 shows the plot of instantaneous velocity against time for three of the 2.75 psi chamber air pressure runs.

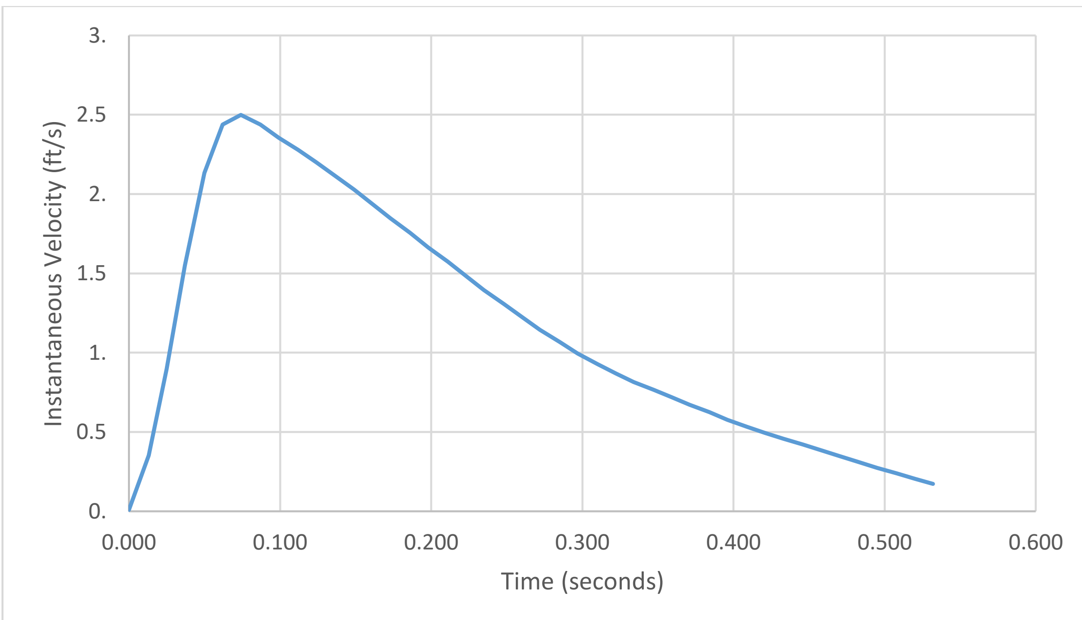

Figure 41: Instantaneous Velocity versus Time for 2.75psi_Run 6

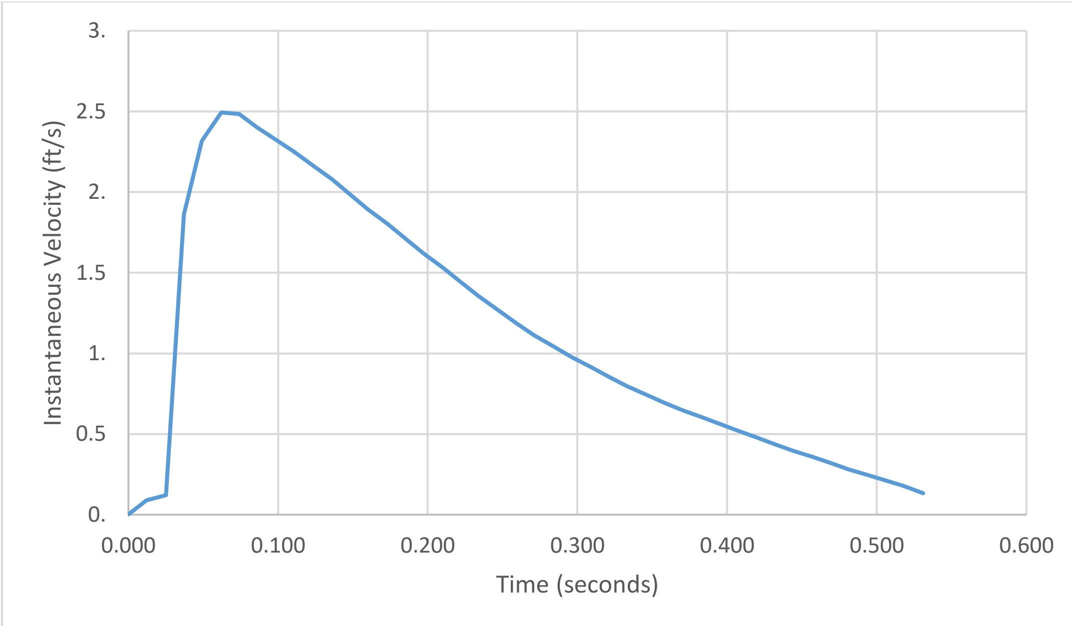

Figure 42: Instantaneous Velocity versus Time for 2.75psi_Run 5

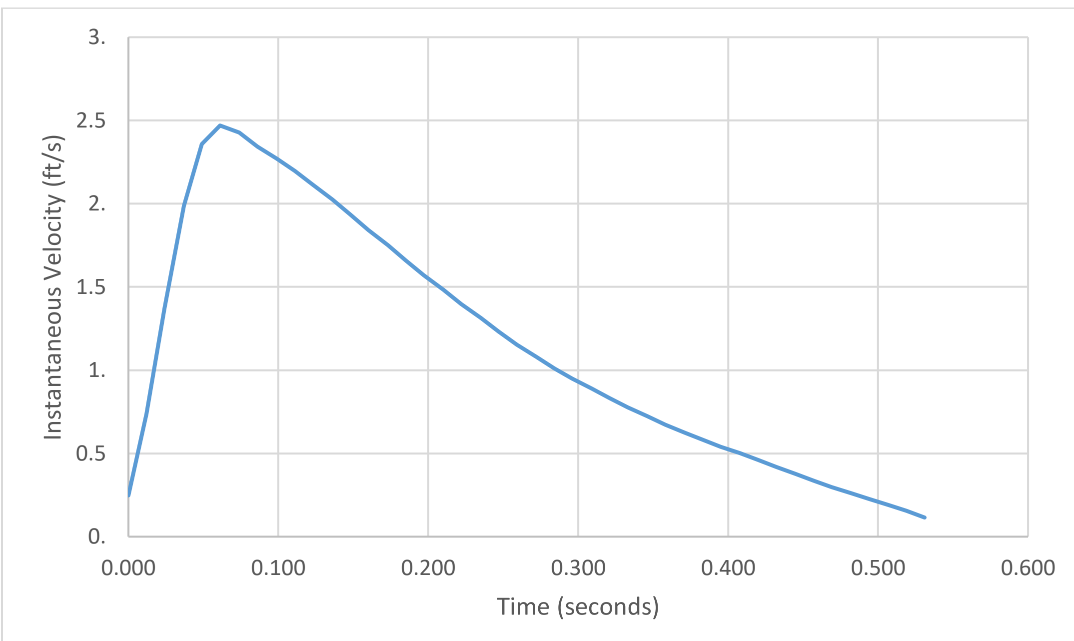

Figure 43: Instantaneous Velocity versus Time for 2.75psi_Run 3

Uncertainty and Calculated to Experimental Velocity Ratio Calculation:

$$Velocity = \frac{Distance}{Time} = \frac{d_2 - d_1}{t_2 - t_1} = \frac{\Delta d}{\Delta t}$$

$$Distance\ uncertainty\ (u) = \frac{0.25\ inch}{12\ inch} \approx 2.1\%$$

Assuming time uncertainty ≈ 1%

So,

$$\Delta d\ uncertainty\ (X) = \sqrt{0.021^2 + 0.021^2} \approx 2.9\%$$

$$\Delta t\ uncertainty\ (Y) = \sqrt{0.01^2 + 0.01^2} \approx 1.4\%$$

Therefore,

$$\boldsymbol{Velocity\ uncertainty} = \sqrt{X^2 + Y^2} = \sqrt{0.029^2 + 0.014^2} \approx \mathbf{3.2}\%$$

The expected velocity at 3 feet (developmental length of wave) was calculated to be 11.36 feet/second. This value was calculated by Rojin Tuladhar during the theoretical kinematic analysis. The measured velocity (from experiments recorded by sensors) was 11.40 feet/second at 3 feet. Thus the calculated to experimental velocity ratio is computed as follows:

$$\frac{Calculated\ velocity}{Experimental\ velocity} = \frac{11.36\ feet/second}{11.40\ feet/second} = 0.996 \approx 99.6\%$$

Conclusions and Future Work

In summary, our team was successfully able to design a small-scale physical model to generate a jet that can be used to simulate a wave section, utilizing air pressure and U-tubed section. Air pressure of 2.75 psi for a time of 0.53 second was chosen as ideal data set due to its close similarity with theoretical kinematics analysis. As expected the primary sensor i.e. sensor type 1 (Optomax sensors) gave velocity measurements every single time without any discrepancies. Hence, sensor type 1 (Optomax sensors) is recommended as the main sensor type to be used for measuring wave velocity generated by the physical model. Sensor type 2 (photo-resistor) did not provide reliable results due to its high dependency on light intensity. And due to mostly using clear water, sensor type 2 (photo-resistor) was unable to detect significant changes in light intensity. Even tough water with dye was used, the change in light intensity was insignificant.

Additional research work is required in order to find more ideal sensor type for future designs, where the physical model is expected to be built with more complexity. These sensors should be a single component sensor. Sensors with dependency on light intensity are not deemed suitable. Less complex electrical circuit requirement will be advantageous for overall accuracy. It prevents unnecessary contact between connection wires thereby preventing short-circuiting. Also reducing the distance between the sensors is suggested. This will allow measuring instantaneous velocity rather than average velocity.

References

[1] Abrahams, A. D., Parsons, A. J., & Luk, S. (1986). Field measurement of the velocity of overland flow using dye tracing. *Earth Surface Processes and Landforms, 11*(6), 653-657. doi:10.1002/esp.3290110608

[2] Annoni, M., Cristaldi, L., Norgia, M., & Svelto, C. (2008). Efficiency Measurement of Water Jet Orifices by a Novel Electrooptical Technique. *IEEE Transactions on Instrumentation and Measurement, 57*(1), 48-54. doi:10.1109/tim.2007.909620

[3] Chen, W., & Geskin, E. (1991). Measurement of the velocity of abrasive waterjet by the use of laser transit anemometer. *Proc. 10th Int. Conf. Jet Cutting Technol.,* 23-36.

[4] Cheng, C., Liao, W., He, K., & Lin, J. (2011). Empirical study on drainage stack terminal water velocity. *Building Services Engineering Research and Technology, 32*(2), 171-181. doi:10.1177/0143624410386063

[5] CONESA, O., DIETRICH, N., COCKX, A., & GUIRAUD, P. (2010). *In the wake of bubbles: Velocity Field Measurement by PIV Technique* (Unpublished master's thesis). Université de Toulouse INSA.

[6] Directional Wave Basin. (2015). *Oregon State University, College of Engineering O. H. Hinsdale Wave Research Laboratory, Facilities*. Retrieved from

http://wave.oregonstate.edu/sites/wave.oregonstate.edu/files/hwrl_data_sheet_dwb_2015_for_website.pdf

[7] Donati, S. (2004). Electro-Optical InstrumentationSensing and Measuring With Lasers. *Englewood Cliffs:Prentice-Hall, NJ*.

[8] Dorle, A., Tyler, L., & Summers, D. (2003). Measurement of particle velocities in high speed waterjet technology. *WJTA American Waterjet Conf.*

[9] Florez, F., Prenner, R., & Krouzecky, N. (2016). Measurements of air concentration and velocities in a free falling water jet. *Transactions Of Famena, 40(1),* 57-68.

[10] Goseberg, N., Wurpts, A., & Schlurmann, T. (2013). Laboratory-scale generation of tsunami and long waves. *Coastal Engineering, 79*, 57-74. doi:10.1016/j.coastaleng.2013.04.006

[11] Himmelreich, U., & Riess, W. (1991). Laser-velocimetry investigations of the flow in abrasive water jets with varying cutting head geometry. *Proc. 6th Amer. Water Jet Conf.,* 305-313.

[12] Large Wave Flume. (2015). *Oregon State University, College of Engineering O. H. Hinsdale Wave Research Laboratory, Facilities*. Retrieved from

http://wave.oregonstate.edu/sites/wave.oregonstate.edu/files/hwrl_data_sheet_lwf_2015_for_website.pdf

[13] Lei, T., Yan, Y., Shi, X., Chuo, R., & Zhao, J. (2013). Measuring velocity of water flow within a gravel layer using an electrolyte tracer method with a Pulse Boundary Model. *Journal of Hydrology, 500*, 37-44. doi:10.1016/j.jhydrol.2013.07.025

[14] Malek-Mohammadi, S., & Testik, F. Y. (2010). New Methodology for Laboratory Generation of Solitary Waves. *Journal of Waterway, Port, Coastal, and Ocean Engineering, 136*(5), 286-294. doi:10.1061/(asce)ww.1943-5460.0000046

[15] Miller, A., & Archibald, J. (1991). Measurement of particle velocities in an abrasive jet cutting system. *Proc. 6th Amer. Water Jet Conf.,* 24-27.

[16] Mohammadi, S. M. (2009). *Laboratory generation and physics of propagation of solitary waves and water surface depressions* (Unpublished doctoral dissertation).

[17] Osman, A., & Thry, B. (1998). Velocity Doppler investigations of the flow in abrasive water jet (AWJ) using a Fabry–Pérot interferometer. *Proc. 5th Pacific Rim Int. Conf. Water Jet Technol.,* 148-157.

[18] Planchon, O., Silvera, N., Gimenez, R., Favis-Mortlock, D., Wainwright, J., Bissonnais, Y. L., & Govers, G. (2005). An automated salt-tracing gauge for flow-velocity measurement. *Earth Surface Processes and Landforms, 30*(7), 833-844. doi:10.1002/esp.1194

[19] Pope, C. L., Savage, B., Johnson, B., Muchmore, C., Nichols, L., Roberts, G., Smith, C. (2017). Nuclear Power Plant Mechanical Component Flooding Fragility Experiments Status. doi:10.2172/1376902

[20] Rammohan, A., & Kumar, C. R. (2017). Performance analysis of photoresistor and phototransistor for automotive's halogen and xenon bulbs light output. *IOP Conference Series: Materials Science and Engineering, 263*, 062056. doi:10.1088/1757-899x/263/6/062056

[21] Roberts, G. (2017). *Research and Development of a Wave Impact Simulation Device for the Idaho State University Component Flooding Evaluation Laboratory* (Unpublished master's thesis). Idaho State University.

[22] Tingwu, L., Xia, W., Zhao, J., Liu, Z., & Zhang, Q. (2005). Method for measuring velocity of shallow water flow for soil erosion with an electrolyte tracer. *Journal of Hydrology, 301*(1-4), 139-145. doi:10.1016/j.jhydrol.2004.06.025

[23] Van Gent, M. (2015). The New Delta Flume for Large Scale Testing. *Deltares Facilities*. Retrieved from https://www.deltares.nl/app/uploads/2015/02/THENEW- DELTA-FLUME-FOR-large-scale-testing.pdf

[24] Ventura, E., Nearing, M. A., & Norton, L. (2001). Developing a magnetic tracer to study soil erosion. *Catena, 43*(4), 277-291. doi:10.1016/s0341-8162(00)00149-1

[25] Yang, Z., & Johnson, M. (2017). Hybrid particle image velocimetry with the combination of cross-correlation and optical flow method. *Journal of Visualization, 20*(3), 625-638. doi:10.1007/s12650-017-0417-7

Website References

[26] http://www.world-nuclear.org/ - World Nuclear Association

[27] https://www.aoe.vt.edu/ - Department of Aerospace and Ocean Engineering - Virginia Tech

[28] https://www.asce.org/ - American Society of Civil Engineers

[29] http://hyperphysics.phy-astr.gsu.edu – Department of Physics – Georgia State University

[30] https://www.adafruit.com/

[31] https://www.arduino.cc/

[32] http://www.resistorguide.com/photoresistor/

[33] http://www.omega.com/

Appendix A: Code

```
unsigned long t0=0;
unsigned long t1=0;
bool x0 = false;
bool x1 = false;
bool v0 = false;
bool v1 = false;
int s0;
int s1;
float distance01 = 1; //ft
float velocity01 = 0;

unsigned long t2=0;
unsigned long t3=0;
bool x2 = false;
bool x3 = false;
bool v2 = false;
bool v3 = false;
int s2;
int s3;
float distance23 = 1; //ft
float velocity23 = 0;

unsigned long t4=0;
unsigned long t5=0;
bool x4 = false;
bool x5 = false;
bool v4 = false;
```

```
bool v5 = false;
int s4;
int s5;
float distance45 = 1; //ft
float velocity45 = 0;

unsigned long t6=0;
unsigned long t7=0;
bool x6 = false;
bool x7 = false;
bool v6 = false;
bool v7 = false;
int s6;
int s7;
float distance67 = 1; //ft
float velocity67 = 0;

unsigned long t8=0;
unsigned long t9=0;
bool x8 = false;
bool x9 = false;
bool v8 = false;
bool v9 = false;
int s8;
int s9;
float distance89 = 10; //Inch
float velocity89 = 0;

unsigned long t10=0;
```

```
unsigned long t11=0;
bool x10 = false;
bool x11 = false;
bool v10 = false;
bool v11 = false;
int s10;
int s11;
float distance1011 = 11; //Inch
float velocity1011 = 0;

int threshold = 700;

void setup()
{
 Serial.begin(9600); // // initialize serial communications at 9600 bps:
}

void loop()
{

 s0 = analogRead(A0);
 if (s0>=threshold) x0 = false; //
 if(s0<threshold && x0 == false)
 {
  Serial.print("Sensor0: ");
  Serial.println(s0);
  Serial.print("Time0: ");
  t0 = millis();
  Serial.println(t0);
```

```
  Serial.println();
  x0 = true;
  v0 = true;
  }
 s1 = analogRead(A1);
 if (s1>=threshold) x1 = false;
 if(s1<threshold && x1 == false)
 {
  Serial.print("Sensor1: ");
  Serial.println(s1);
  Serial.print("Time1: ");
  t1 = millis();
  Serial.println(t1);
  Serial.println();
  x1 = true;
  if(v0) v1 = true;
  }
if(v0 && v1)
{
 v0 = false;
 v1 = false;
 velocity01= 1000*(distance01/(t1 - t0));
 Serial.print("Velocity01 in ft/sec: ");
 Serial.println(velocity01);
 }

 s2 = analogRead(A2);
 if (s2>=threshold) x2 = false; //
 if(s2<threshold && x2 == false)
```

```
{
  Serial.print("Sensor2: ");
  Serial.println(s2);
  Serial.print("Time2: ");
  t2 = millis();
  Serial.println(t2);
  Serial.println();
  x2 = true;
  v2 = true;
  }
 s3 = analogRead(A3);
 if (s3>=threshold) x3 = false;
 if(s3<threshold && x3 == false)
 {
  Serial.print("Sensor3: ");
  Serial.println(s3);
  Serial.print("Time3: ");
  t3 = millis();
  Serial.println(t3);
  Serial.println();
  x3 = true;
  if(v2) v3 = true;
  }
if(v2 && v3)
{
 v2 = false;
 v3 = false;
 velocity23= 1000*(distance23/(t3 - t2));
 Serial.print("Velocity23 in ft/sec: ");
```

```
Serial.println(velocity23);
}
s4 = analogRead(A4);
if (s4>=threshold) x4 = false; //
if(s4<threshold && x4 == false)
{
  Serial.print("Sensor4: ");
  Serial.println(s4);
  Serial.print("Time4: ");
  t4 = millis();
  Serial.println(t4);
  Serial.println();
  x4 = true;
  v4 = true;
  }
s5 = analogRead(A5);
if (s5>=threshold) x5 = false;
if(s5<threshold && x5 == false)
{
  Serial.print("Sensor5: ");
  Serial.println(s5);
  Serial.print("Time5: ");
  t5 = millis();
  Serial.println(t5);
  Serial.println();
  x5 = true;
  if(v4) v5 = true;
  }
if(v4 && v5)
```

```
{
 v4 = false;
 v5 = false;
 velocity45= 1000*(distance45/(t5 - t4));
 Serial.print("Velocity45 in ft/sec: ");
 Serial.println(velocity45);
 }

 s6 = analogRead(A6);
 if (s6>=threshold) x6 = false; //
 if(s6<threshold && x6 == false)
 {
   Serial.print("Sensor6: ");
   Serial.println(s6);
   Serial.print("Time6: ");
   t6 = millis();
   Serial.println(t6);
   Serial.println();
   x6 = true;
   v6 = true;
   }
 s7 = analogRead(A7);
 if (s7>=threshold) x7 = false;
 if(s7<threshold && x7 == false)
 {
   Serial.print("Sensor7: ");
   Serial.println(s7);
   Serial.print("Time7: ");
   t7 = millis();
```

```
  Serial.println(t7);
  Serial.println();
  x7 = true;
  if(v6) v7 = true;
  }
if(v6 && v7)
{
 v6 = false;
 v7 = false;
 velocity67= 1000*(distance67/(t7 - t6));
 Serial.print("Velocity67 in ft/sec: ");
 Serial.println(velocity67);
 }

 s8 = analogRead(A8);
 if (s8>=threshold) x8 = false; //
 if(s8<threshold && x8 == false)
 {
  Serial.print("Sensor8: ");
  Serial.println(s8);
  Serial.print("Time8: ");
  t8 = millis();
  Serial.println(t8);
  Serial.println();
  x8 = true;
  v8 = true;
  }
 s9 = analogRead(A9);
 if (s9>=threshold) x9 = false;
```

```
if(s9<threshold && x9 == false)
{
  Serial.print("Sensor9: ");
  Serial.println(s9);
  Serial.print("Time9: ");
  t9 = millis();
  Serial.println(t9);
  Serial.println();
  x9 = true;
  if(v8) v9 = true;
  }
if(v8 && v9)
{
 v8 = false;
 v9 = false;
 velocity89= (1000/12)*(distance89/(t9 - t8));
 Serial.print("Velocity89 in ft/sec: ");
 Serial.println(velocity89);
 }

 s10 = analogRead(A10);
 if (s10>=threshold) x10 = false; //
 if(s10<threshold && x10 == false)
 {
  Serial.print("Sensor10: ");
  Serial.println(s10);
  Serial.print("Time10: ");
  t10 = millis();
  Serial.println(t10);
```

```
  Serial.println();
  x10 = true;
  v10 = true;
  }
 s11 = analogRead(A11);
 if (s11>=threshold) x11 = false;
 if(s11<threshold && x11 == false)
 {
  Serial.print("Sensor11: ");
  Serial.println(s11);
  Serial.print("Time11: ");
  t11 = millis();
  Serial.println(t11);
  Serial.println();
  x11 = true;
  if(v10) v11 = true;
  }
if(v10 && v11)
{
 v10 = false;
 v11 = false;
 velocity1011= (1000/12)*(distance1011/(t11 - t10));
 Serial.print("Velocity1011 in ft/sec: ");
 Serial.println(velocity1011);
 }

}
```

Appendix B: Additional Wave Generation (Experimental Runs) Photos

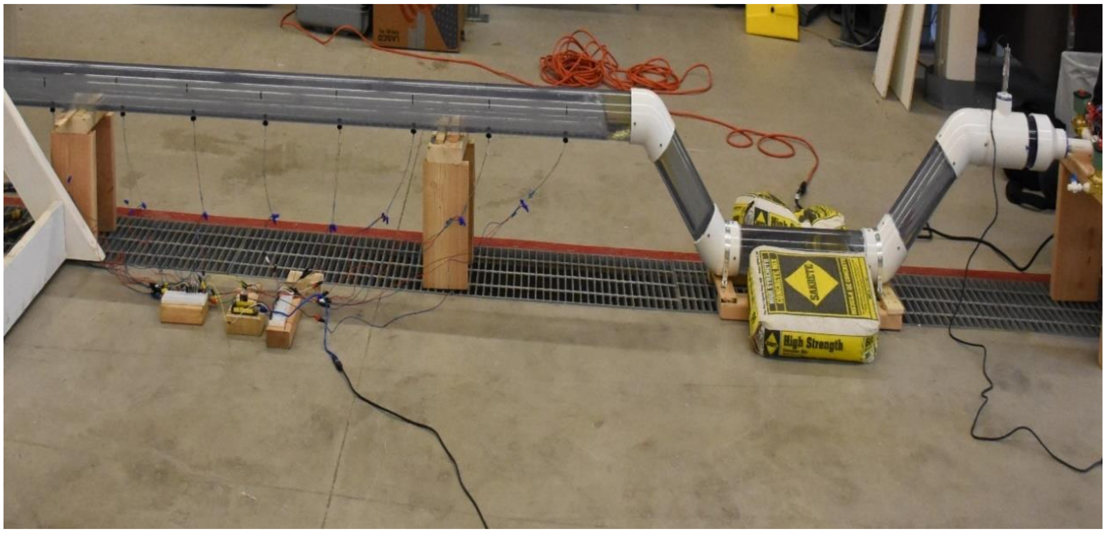

Figure 44: Water Jet for Run 13

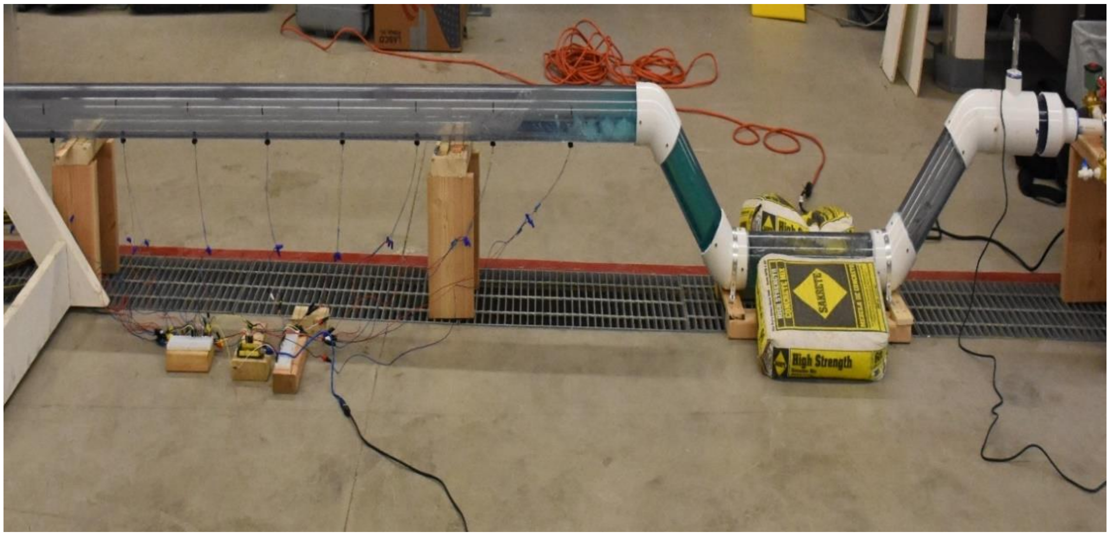

Figure 45: Water Jet for Run 15

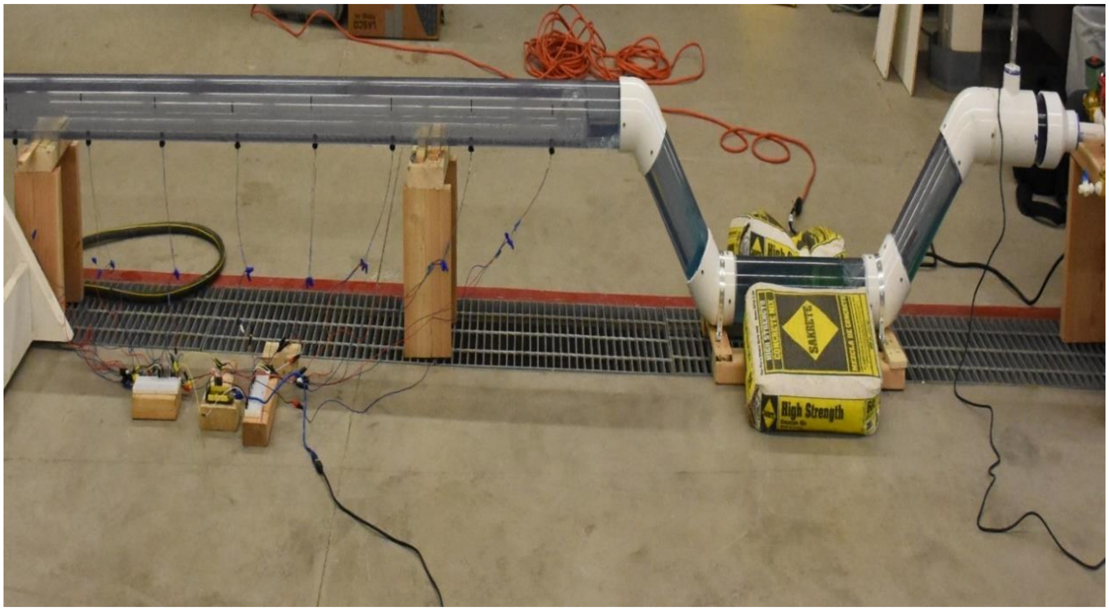

Figure 46: Water Jet for Run 16

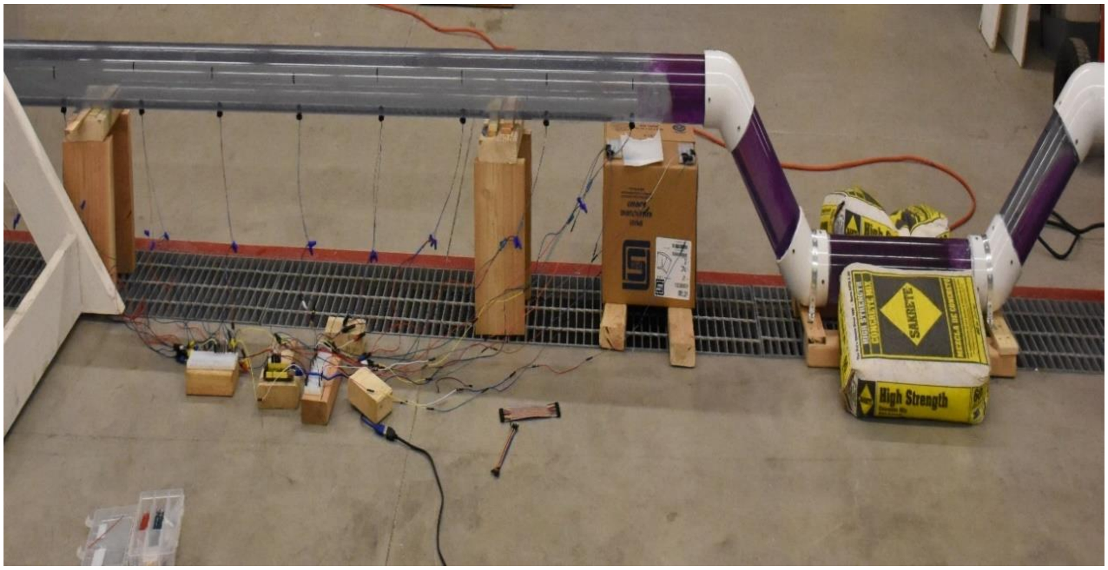

Figure 47: Water Jet for Run 20

Appendix C: Sectional Model

Sectional Model

S.no.	Description	Quantity	Drawing No.
1	Inclined Inlet 25 ° 35 ° 45 °	 1 1 1	2-10
2	Gate Channel	1	11-13
3	Outlet box	1	14-17
4	Additional Length component 0.2' 0.4' 1'	 2 4 2	18-26
5	Flanges	22	27-28

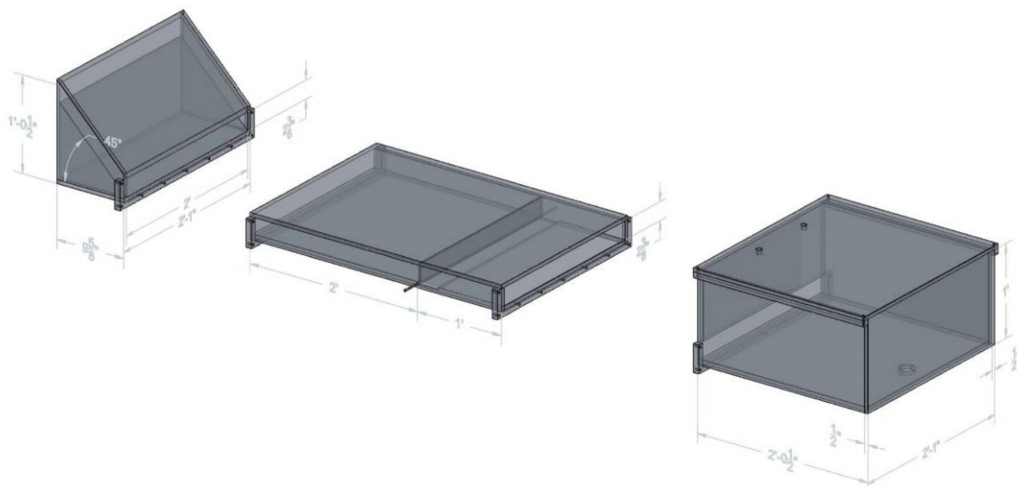
45°
2'
2'-1"
2'
1'
1"
2'-1"

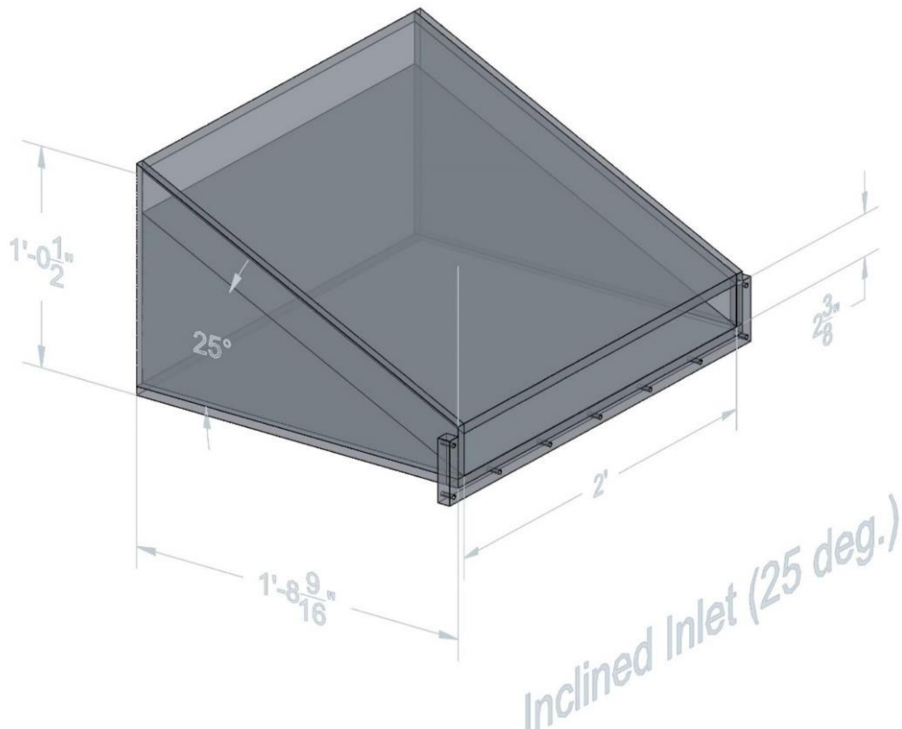
1'-0 1/2"
25°
2 3/8"
2'
1'-8 9/16"
Inclined Inlet (25 deg.)

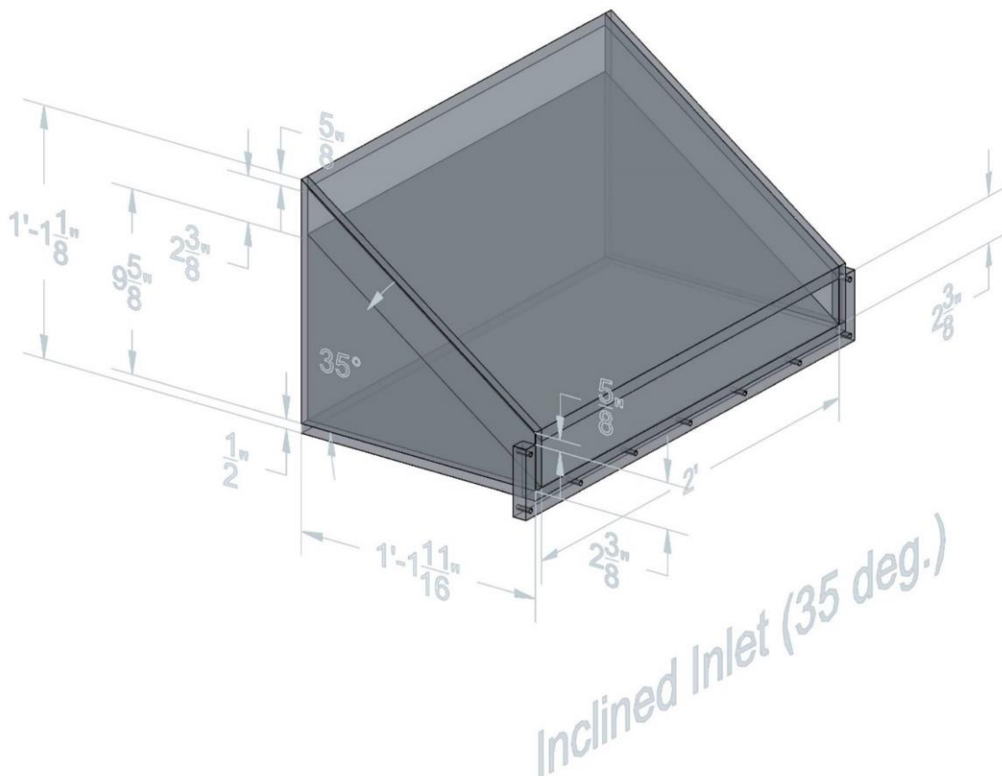

5"/8
1'-1 1"/8
9 5"/8
2 3"/8
35°
5"/8
2 3"/8
2'
1"/2
1'-1 11"/16
2 3"/8
Inclined Inlet (35 deg.)

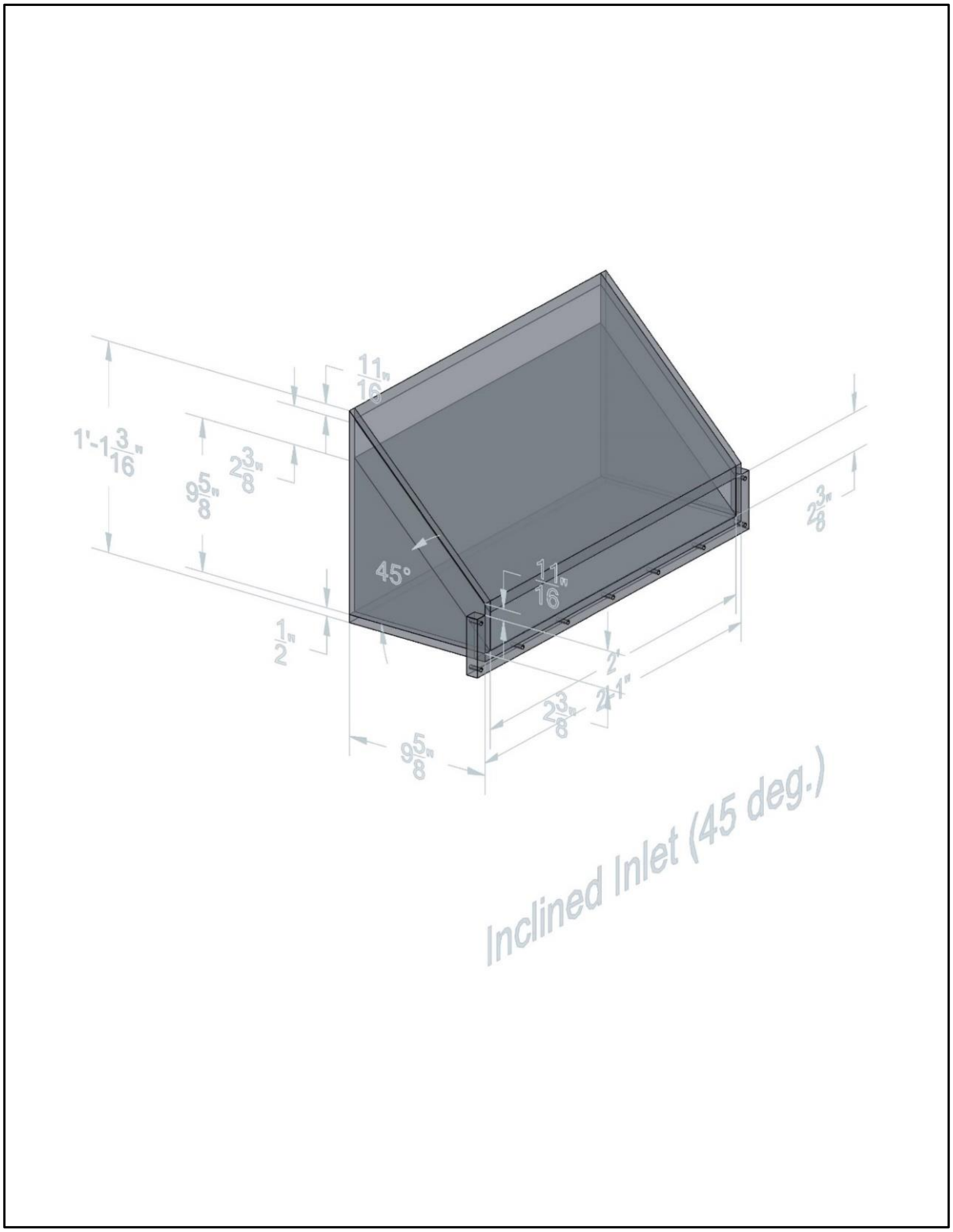
1'-1 3/16"
9 5/8"
2 3/8"
11/16"
1/2"
45°
11/16"
2 3/8"
2'
2'-1"
2 3/8"
9 5/8"
Inclined Inlet (45 deg.)

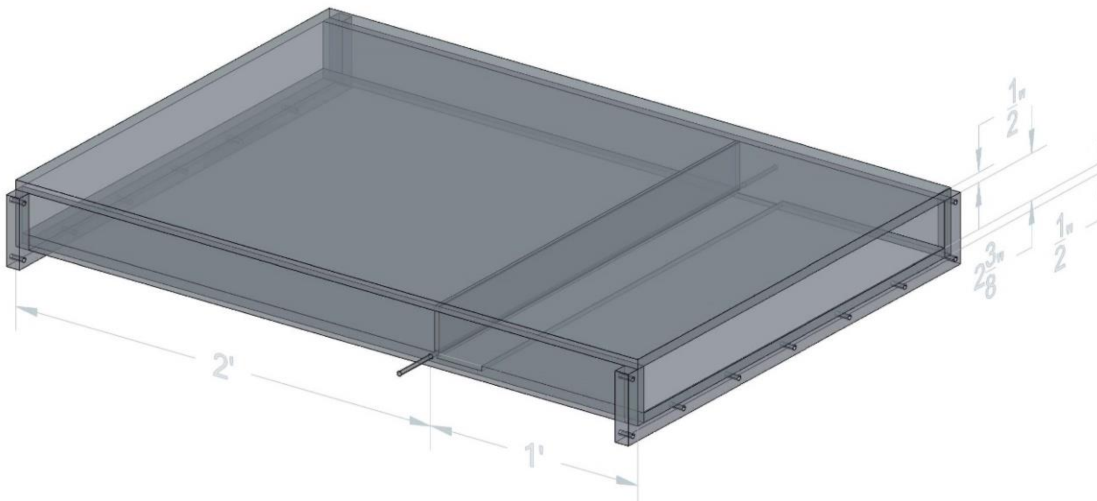

1"/2
2 3"/8
1"/2
2'
1'

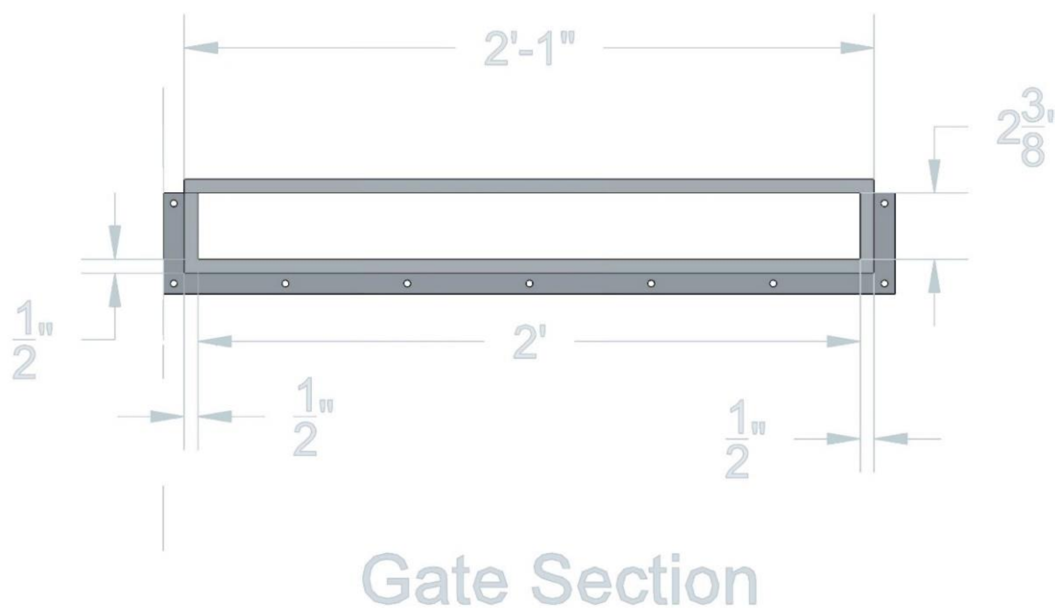
2'-1"
2 3/8"
1/2"
2'
1/2"
1/2"
Gate Section

Gate Channel

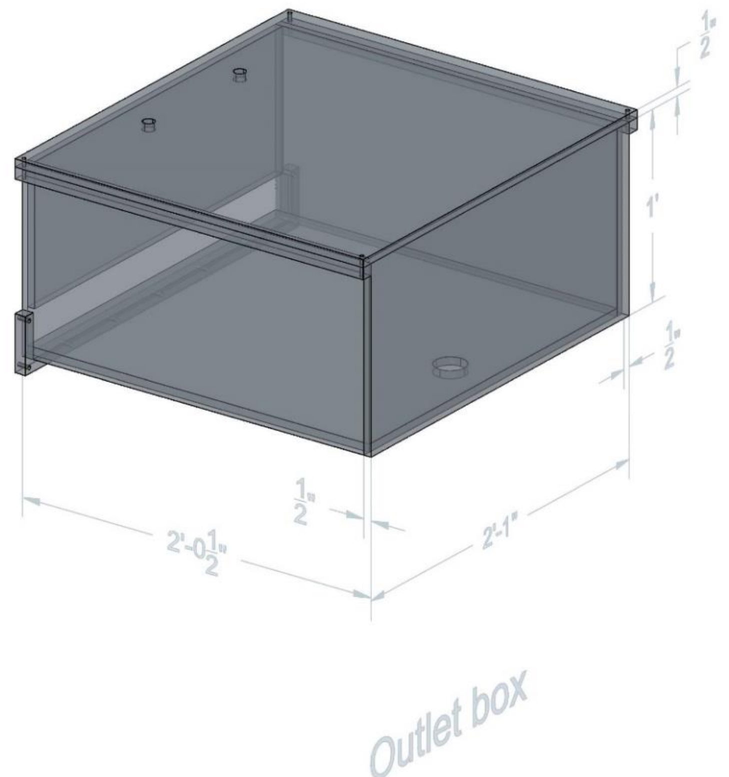

1/2"
1'
1/2"
1/2"
2'-0 1/2"
2'-1"
Outlet box

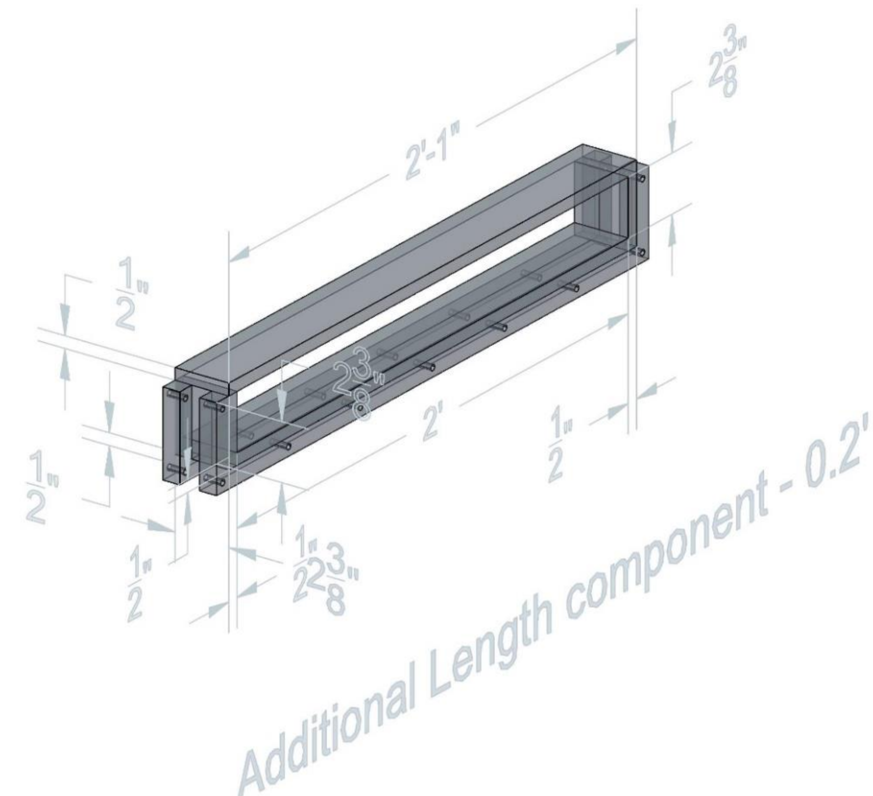
2'-1"
2'
Additional Length component - 0.2'

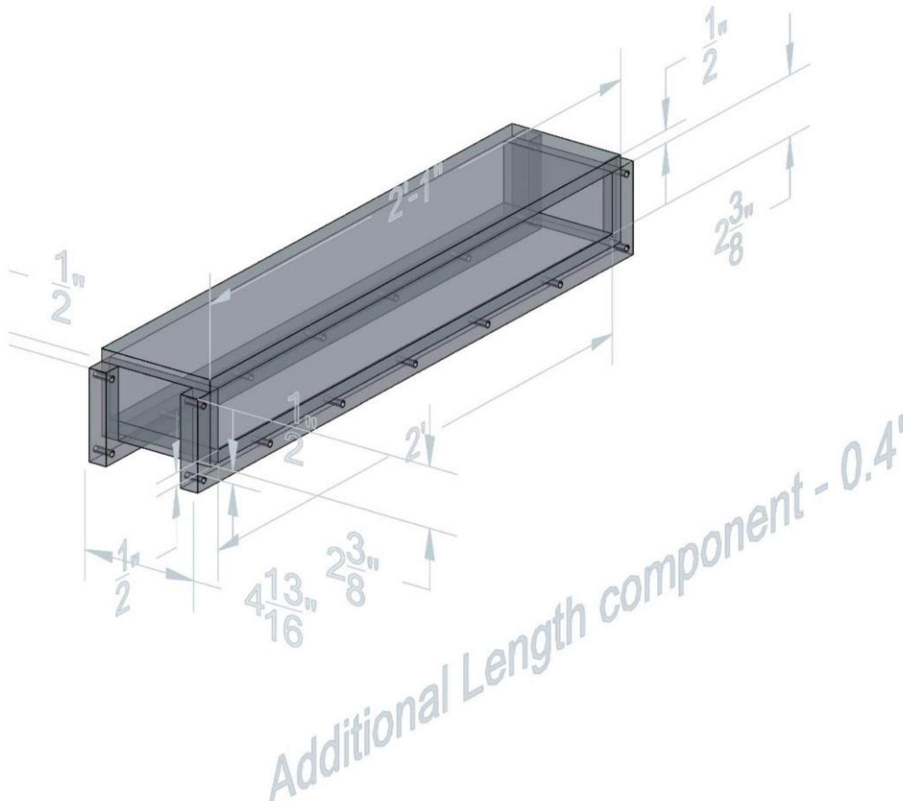
2'-1"
1/2"
2 3/8"
1/2"
1/2"
2'
1/2"
4 13/16"
2 3/8"
Additional Length component - 0.4'

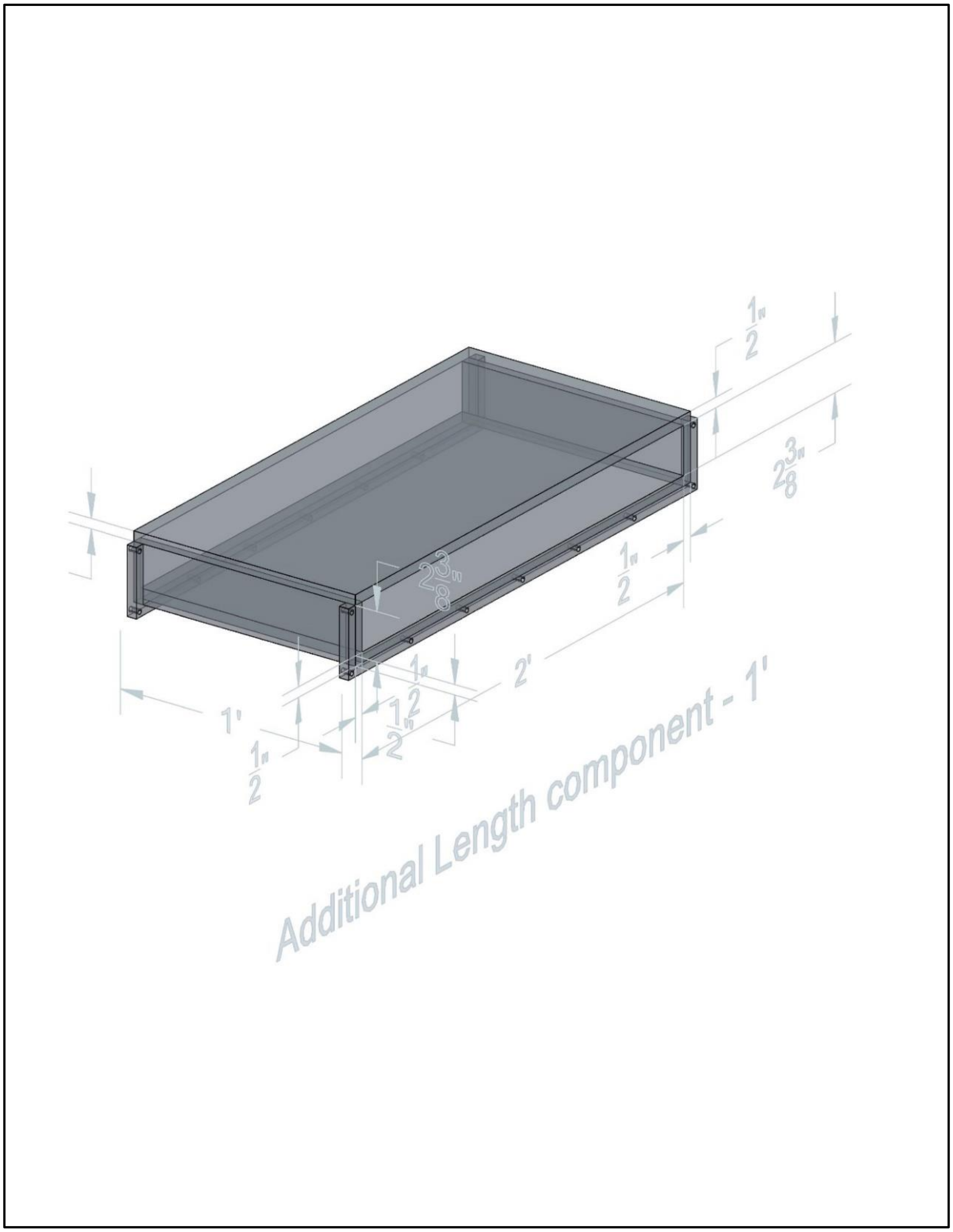

1"
2
2 3/8"
2 3/8"
1"
2
2'
1'
1"
2
1"
2
1"
2
Additional Length component - 1'

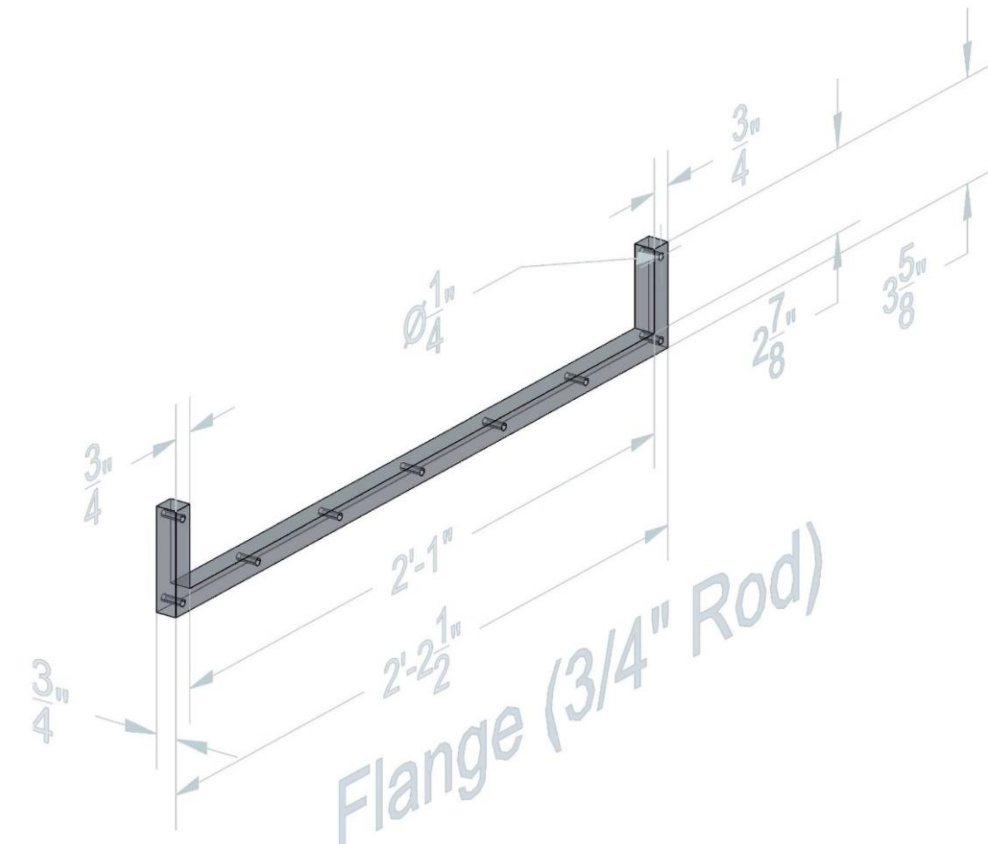

3"/4
Ø1/4"
2 7/8"
3 5/8"
3"/4
2'-1"
2'-2 1/2"
3"/4
Flange (3/4" Rod)

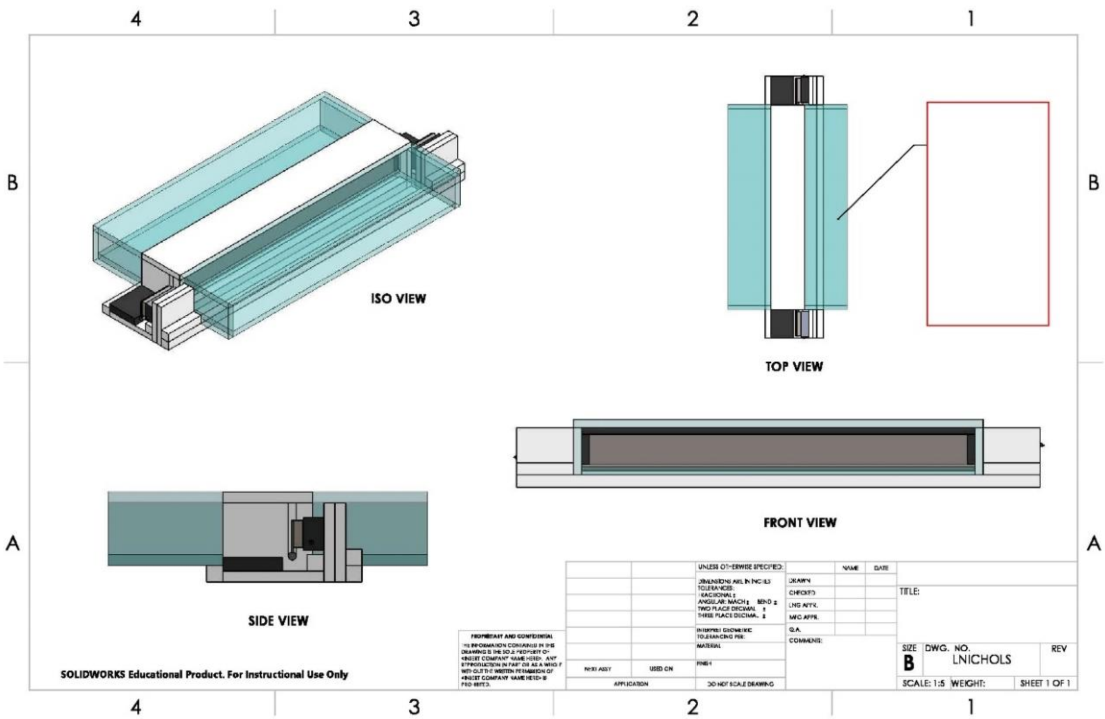
ISO VIEW
TOP VIEW
FRONT VIEW
SIDE VIEW
SOLIDWORKS Educational Product. For Instructional Use Only
UNLESS OTHERWISE SPECIFIED:
NAME
DATE
DRAWN
CHECKED
ENG APPR.
MFG APPR.
Q.A.
COMMENTS:
TITLE:
SIZE
B
DWG. NO.
LNICHOLS
REV
SCALE: 1:5
WEIGHT:
SHEET 1 OF 1
PROPRIETARY AND CONFIDENTIAL
NEXT ASSY
USED ON
APPLICATION
DO NOT SCALE DRAWING
MATERIAL
FINISH

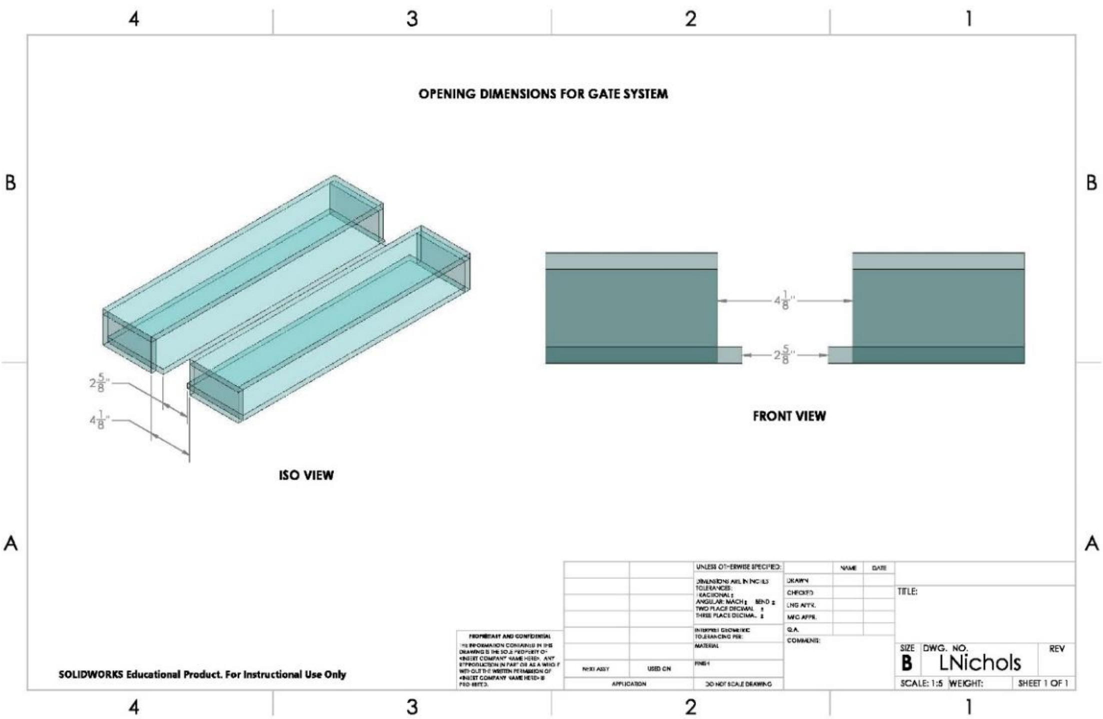
OPENING DIMENSIONS FOR GATE SYSTEM
2 5/8"
4 1/8"
ISO VIEW
4 1/8"
2 5/8"
FRONT VIEW
SOLIDWORKS Educational Product. For Instructional Use Only
UNLESS OTHERWISE SPECIFIED:
NAME
DATE
DRAWN
CHECKED
Q.A.
COMMENTS:
TITLE:
SIZE
DWG. NO.
B
LNichols
REV
SCALE: 1:5
WEIGHT:
SHEET 1 OF 1
APPLICATION
DO NOT SCALE DRAWING

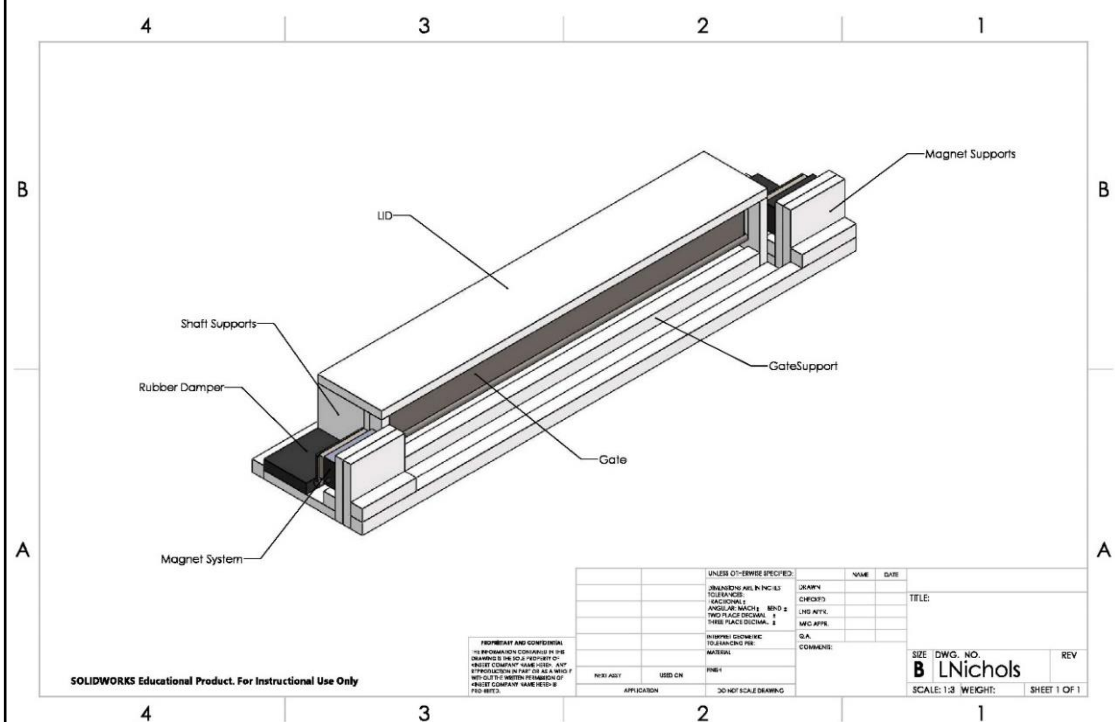
LID
Magnet Supports
Shaft Supports
GateSupport
Rubber Damper
Gate
Magnet System
SOLIDWORKS Educational Product. For Instructional Use Only
B LNichols
SCALE: 1:3
SHEET 1 OF 1

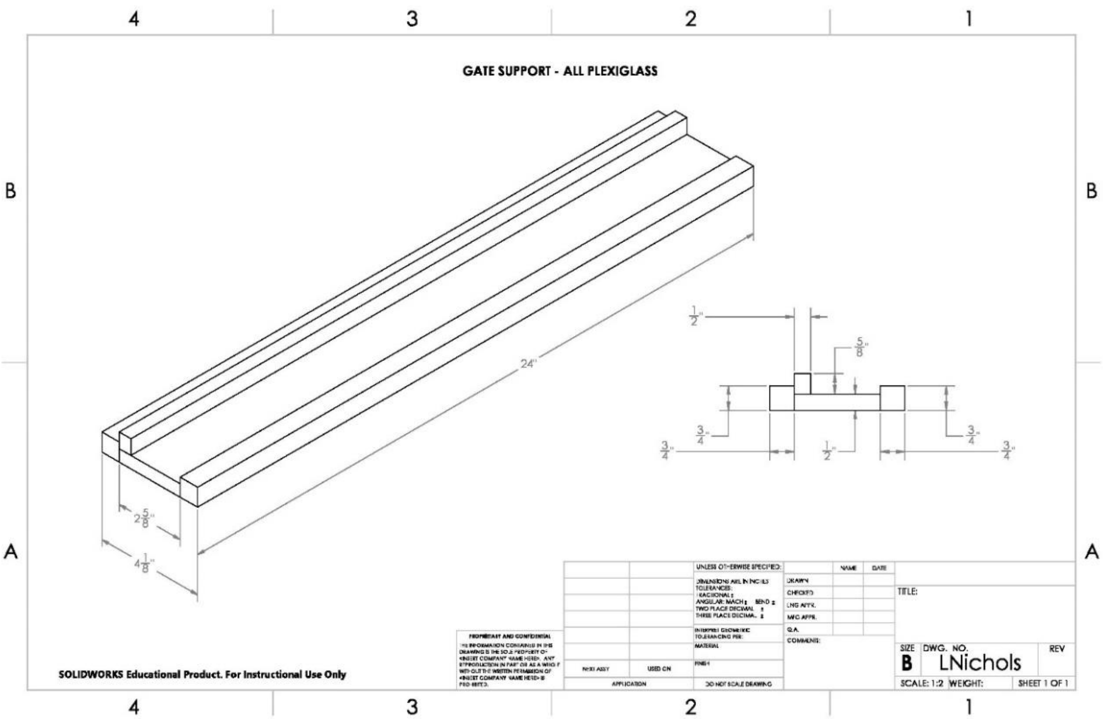
GATE SUPPORT - ALL PLEXIGLASS
24"
SOLIDWORKS Educational Product. For Instructional Use Only
UNLESS OTHERWISE SPECIFIED:
NAME
DATE
DRAWN
CHECKED
TITLE:
SIZE
DWG. NO.
B
LNichols
REV
SCALE: 1:2
WEIGHT:
SHEET 1 OF 1

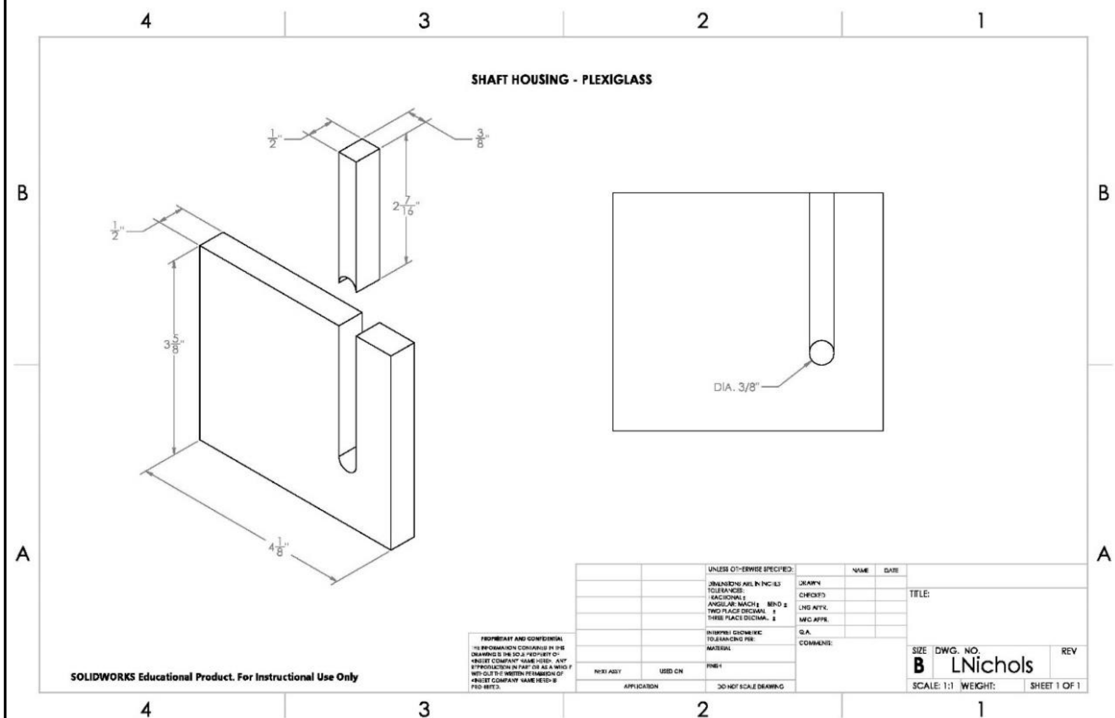
SHAFT HOUSING - PLEXIGLASS
1/2"
3/8"
2 7/16"
1/2"
3 5/8"
4 1/8"
DIA. 3/8"
SOLIDWORKS Educational Product. For Instructional Use Only
UNLESS OTHERWISE SPECIFIED:
NAME
DATE
DRAWN
CHECKED
ENG APPR.
MFG APPR.
Q.A.
COMMENTS:
TITLE:
SIZE
DWG. NO.
REV
B
LNichols
SCALE: 1:1
WEIGHT:
SHEET 1 OF 1
NEXT ASSY
USED ON
APPLICATION
DO NOT SCALE DRAWING
PROPRIETARY AND CONFIDENTIAL

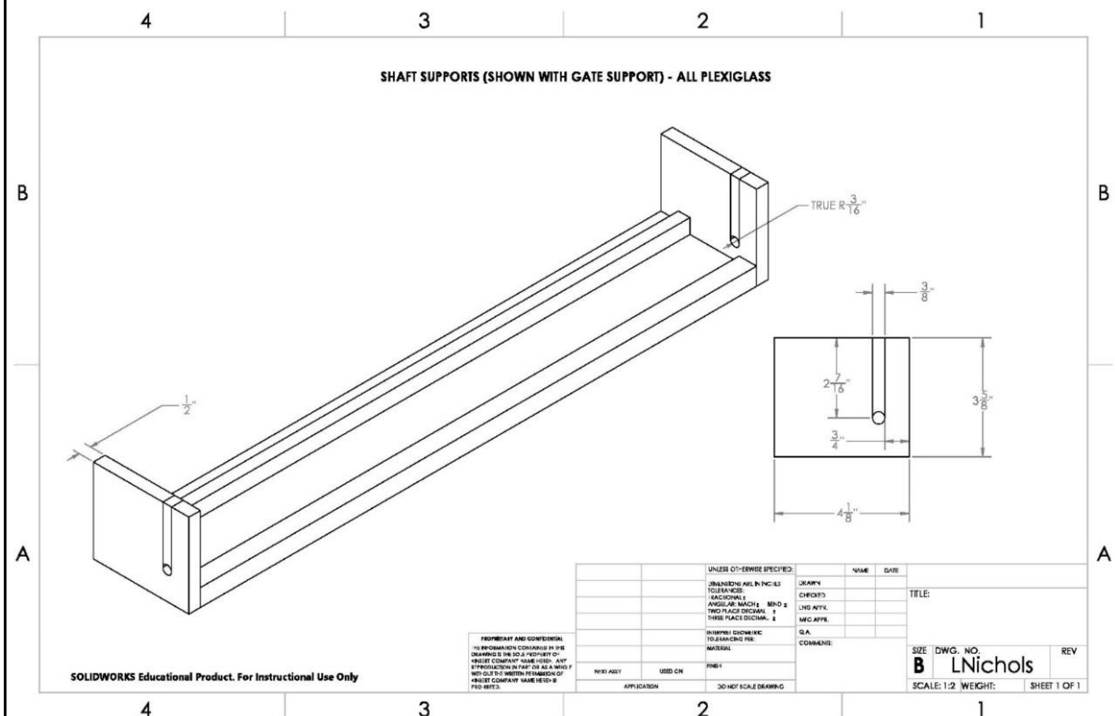

SHAFT SUPPORTS (SHOWN WITH GATE SUPPORT) - ALL PLEXIGLASS
TRUE R 3/16"
1/2"
3/8"
2 7/16"
3 5/8"
3/4"
4 1/8"
UNLESS OTHERWISE SPECIFIED:
NAME
DATE
DRAWN
CHECKED
ENG APPR.
MFG APPR.
Q.A.
COMMENTS:
TITLE:
MATERIAL
FINISH
NEXT ASSY
USED ON
APPLICATION
DO NOT SCALE DRAWING
PROPRIETARY AND CONFIDENTIAL
SIZE
B
DWG. NO.
LNichols
REV
SCALE: 1:2
WEIGHT:
SHEET 1 OF 1
SOLIDWORKS Educational Product. For Instructional Use Only

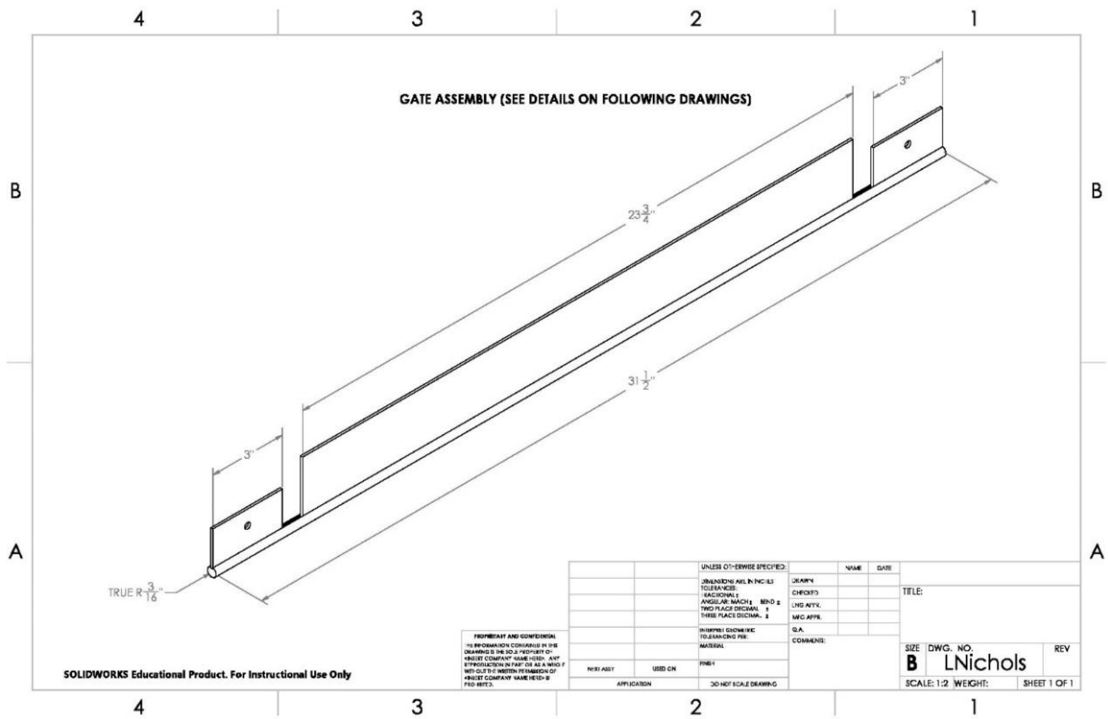

GATE ASSEMBLY (SEE DETAILS ON FOLLOWING DRAWINGS)
3"
23 3/4"
3"
31 1/2"
TRUE R 3/16"
SOLIDWORKS Educational Product. For Instructional Use Only
UNLESS OTHERWISE SPECIFIED:
NAME
DATE
DRAWN
CHECKED
ENG APPR.
MFG APPR.
Q.A.
COMMENTS:
TITLE:
MATERIAL
FINISH
NEXT ASSY
USED ON
APPLICATION
DO NOT SCALE DRAWING
PROPRIETARY AND CONFIDENTIAL
SIZE
DWG. NO.
B
LNichols
REV
SCALE: 1:2
WEIGHT:
SHEET 1 OF 1

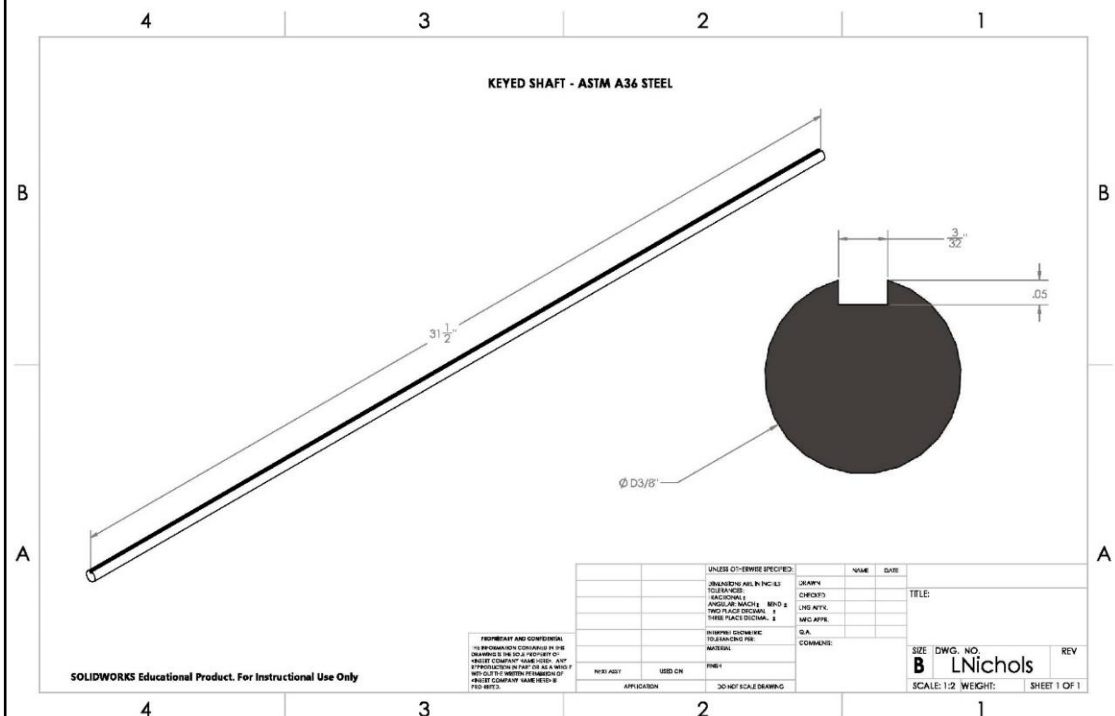

KEYED SHAFT - ASTM A36 STEEL
31 1/2"
3/32"
.05
Ø D3/8"
SOLIDWORKS Educational Product. For Instructional Use Only
UNLESS OTHERWISE SPECIFIED:
NAME
DATE
DRAWN
CHECKED
TITLE:
SIZE
B
DWG. NO.
LNichols
REV
SCALE: 1:2
WEIGHT:
SHEET 1 OF 1
APPLICATION
DO NOT SCALE DRAWING

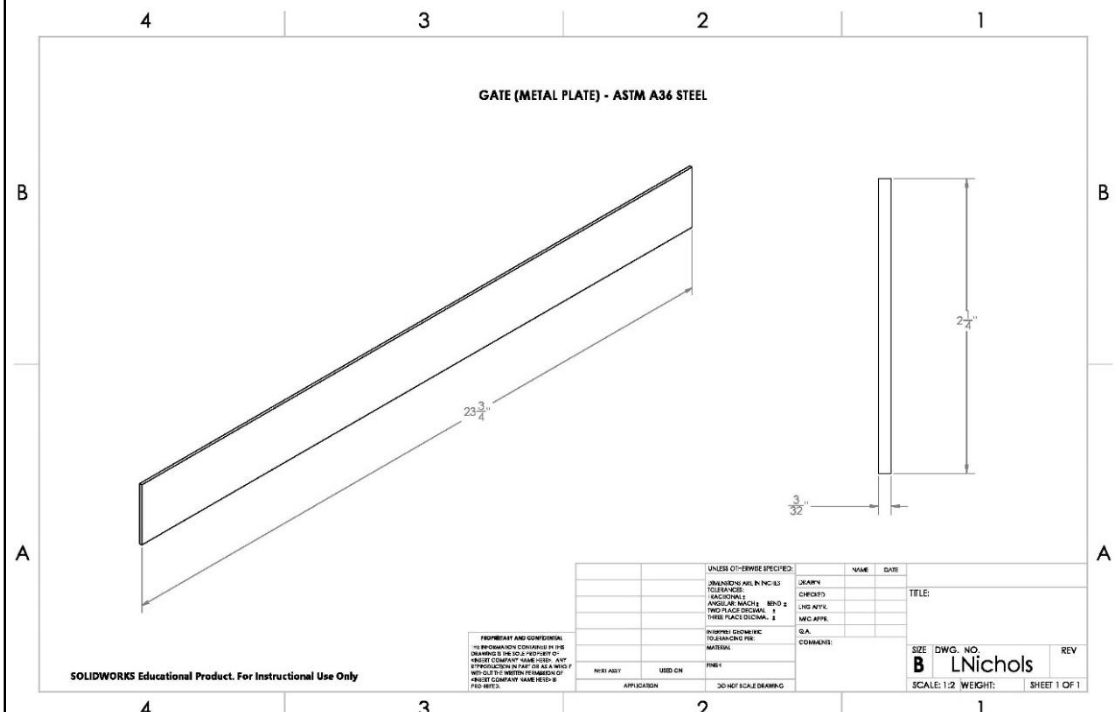
GATE (METAL PLATE) - ASTM A36 STEEL
23 3/4"
2 1/4"
3/32"
UNLESS OTHERWISE SPECIFIED:
DIMENSIONS ARE IN INCHES
TOLERANCES:
FRACTIONAL ±
ANGULAR: MACH ± BEND ±
TWO PLACE DECIMAL ±
THREE PLACE DECIMAL ±
INTERPRET GEOMETRIC TOLERANCING PER:
MATERIAL
FINISH
NEXT ASSY
USED ON
APPLICATION
DO NOT SCALE DRAWING
NAME
DATE
DRAWN
CHECKED
ENG APPR.
MFG APPR.
Q.A.
COMMENTS:
TITLE:
SIZE
B
DWG. NO.
LNichols
REV
SCALE: 1:2
WEIGHT:
SHEET 1 OF 1
PROPRIETARY AND CONFIDENTIAL
SOLIDWORKS Educational Product. For Instructional Use Only

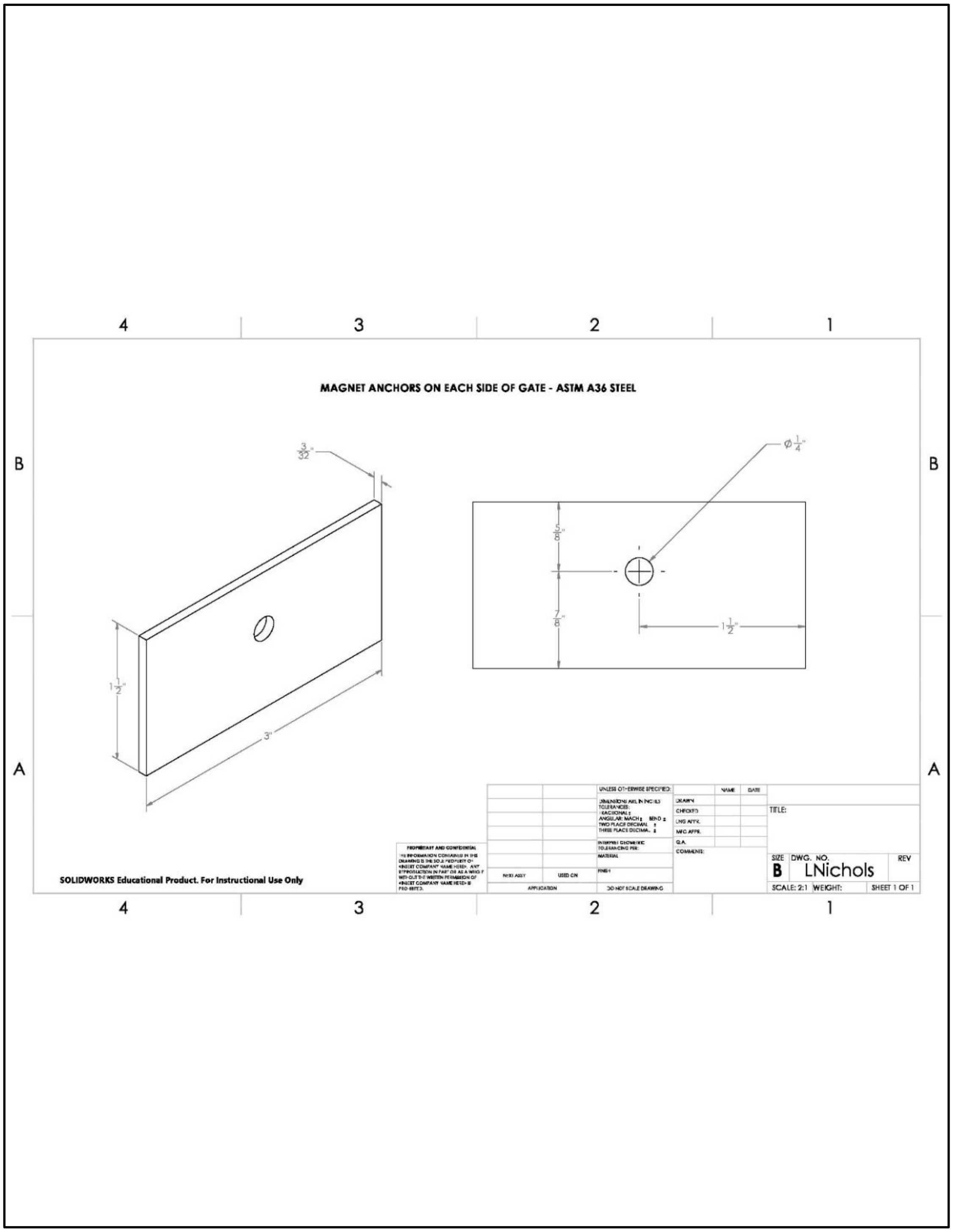

MAGNET ANCHORS ON EACH SIDE OF GATE - ASTM A36 STEEL
3/32"
Ø 1/4"
5/8"
7/8"
1 1/2"
1 1/2"
3"
SOLIDWORKS Educational Product. For Instructional Use Only
UNLESS OTHERWISE SPECIFIED:
NAME
DATE
DRAWN
CHECKED
ENG APPR.
MFG APPR.
Q.A.
COMMENTS:
TITLE:
SIZE
DWG. NO.
REV
B
LNichols
SCALE: 2:1
WEIGHT:
SHEET 1 OF 1
NEXT ASSY
USED ON
APPLICATION
DO NOT SCALE DRAWING

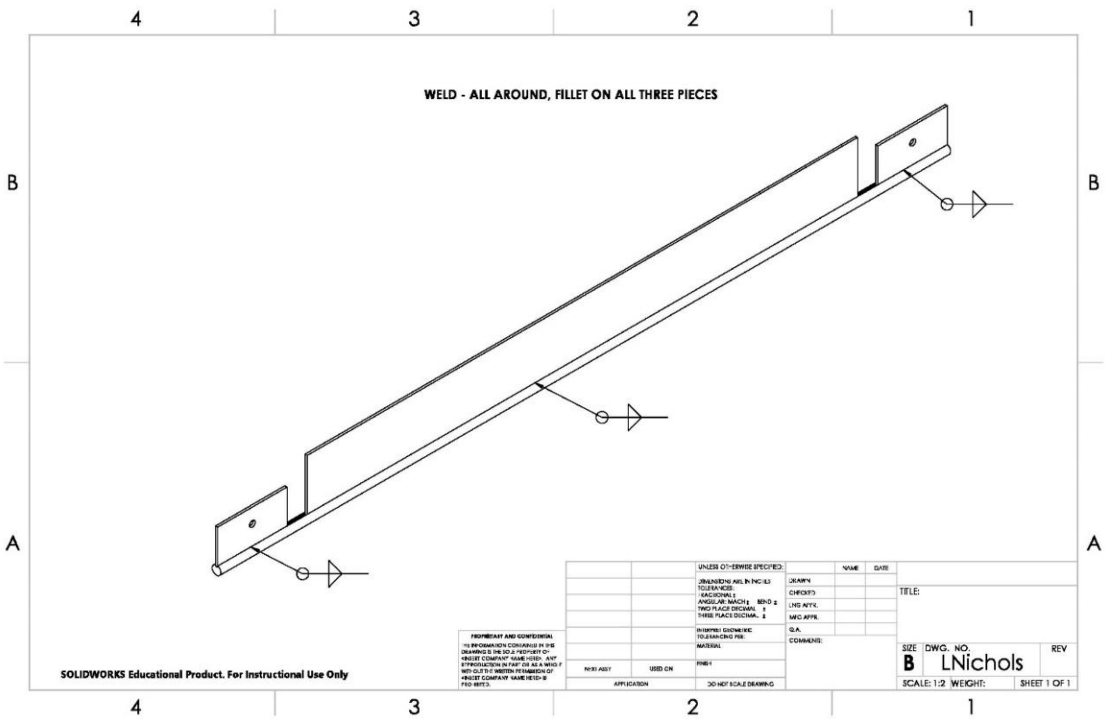
WELD - ALL AROUND, FILLET ON ALL THREE PIECES
SOLIDWORKS Educational Product. For Instructional Use Only
PROPRIETARY AND CONFIDENTIAL
UNLESS OTHERWISE SPECIFIED:
NAME
DATE
DRAWN
CHECKED
ENG APPR.
MFG APPR.
Q.A.
COMMENTS:
MATERIAL
FINISH
NEXT ASSY
USED ON
APPLICATION
DO NOT SCALE DRAWING
TITLE:
SIZE
DWG. NO.
REV
B
LNichols
SCALE: 1:2
WEIGHT:
SHEET 1 OF 1

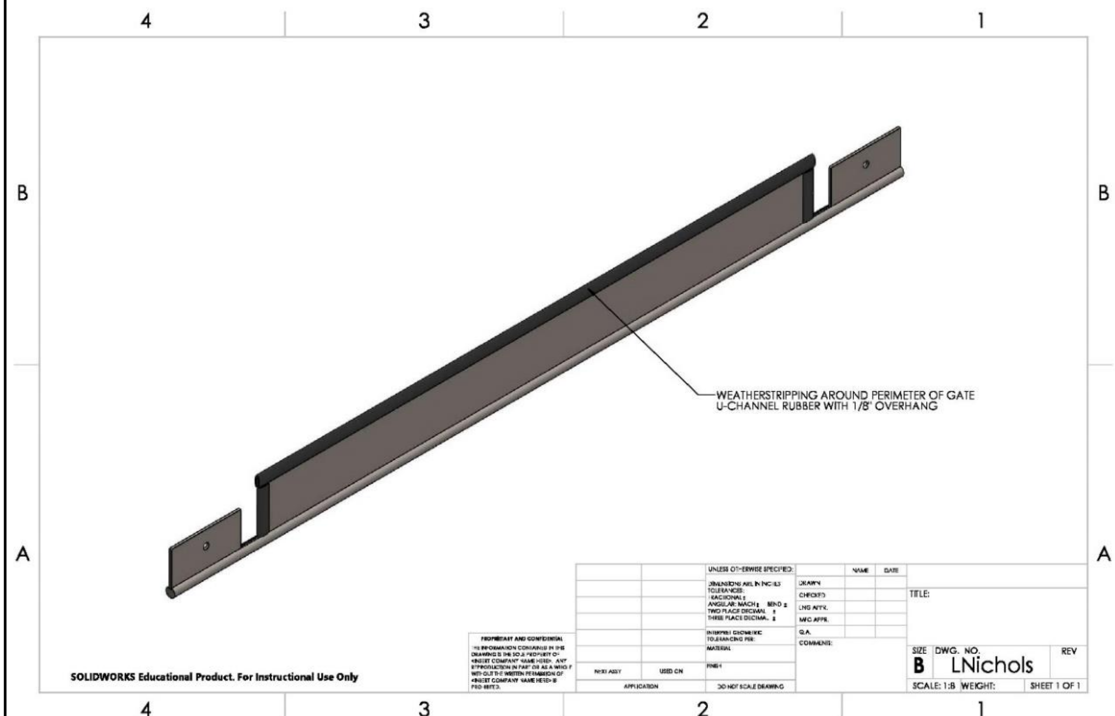
WEATHERSTRIPPING AROUND PERIMETER OF GATE
U-CHANNEL RUBBER WITH 1/8" OVERHANG
SOLIDWORKS Educational Product. For Instructional Use Only
UNLESS OTHERWISE SPECIFIED:
NAME
DATE
DRAWN
CHECKED
ENG APPR.
MFG APPR.
Q.A.
COMMENTS:
TITLE:
PROPRIETARY AND CONFIDENTIAL
NEXT ASSY
USED ON
APPLICATION
MATERIAL
FINISH
DO NOT SCALE DRAWING
SIZE
B
DWG. NO.
LNichols
REV
SCALE: 1:8
WEIGHT:
SHEET 1 OF 1

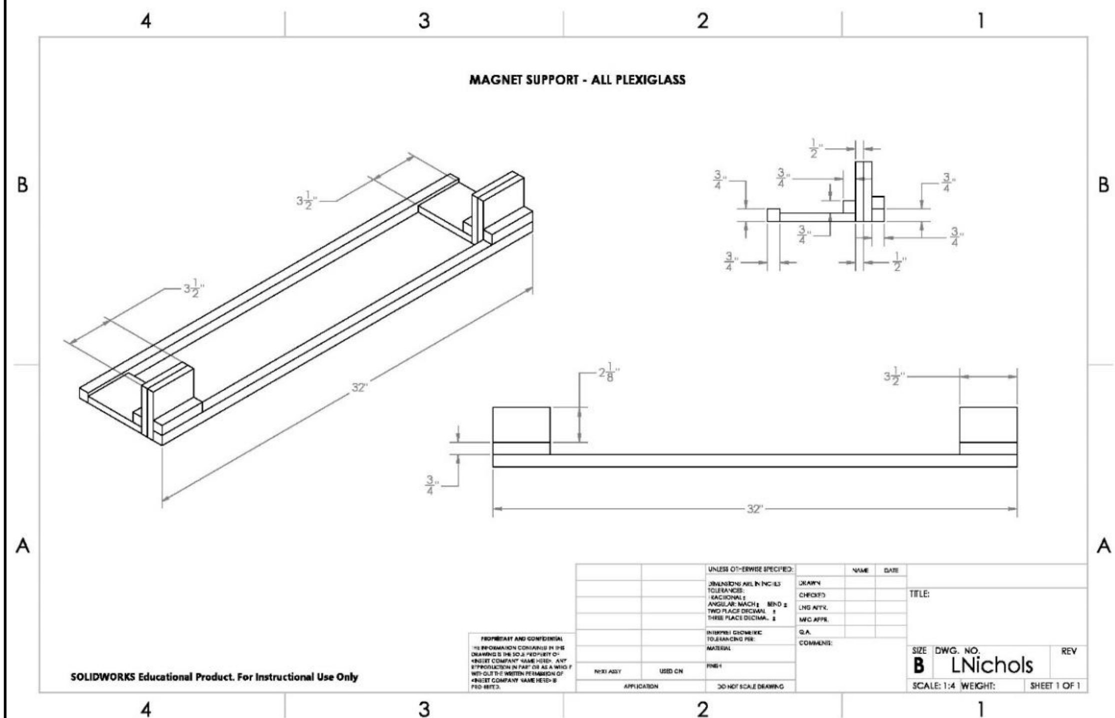
MAGNET SUPPORT - ALL PLEXIGLASS
32"
2 1/8"
3 1/2"
3/4"
1/2"
UNLESS OTHERWISE SPECIFIED:
NAME
DATE
DRAWN
CHECKED
ENG APPR.
MFG APPR.
Q.A.
COMMENTS:
MATERIAL
FINISH
NEXT ASSY
USED ON
APPLICATION
DO NOT SCALE DRAWING
PROPRIETARY AND CONFIDENTIAL
TITLE:
SIZE DWG. NO. REV
B LNichols
SCALE: 1:4 WEIGHT: SHEET 1 OF 1
SOLIDWORKS Educational Product. For Instructional Use Only

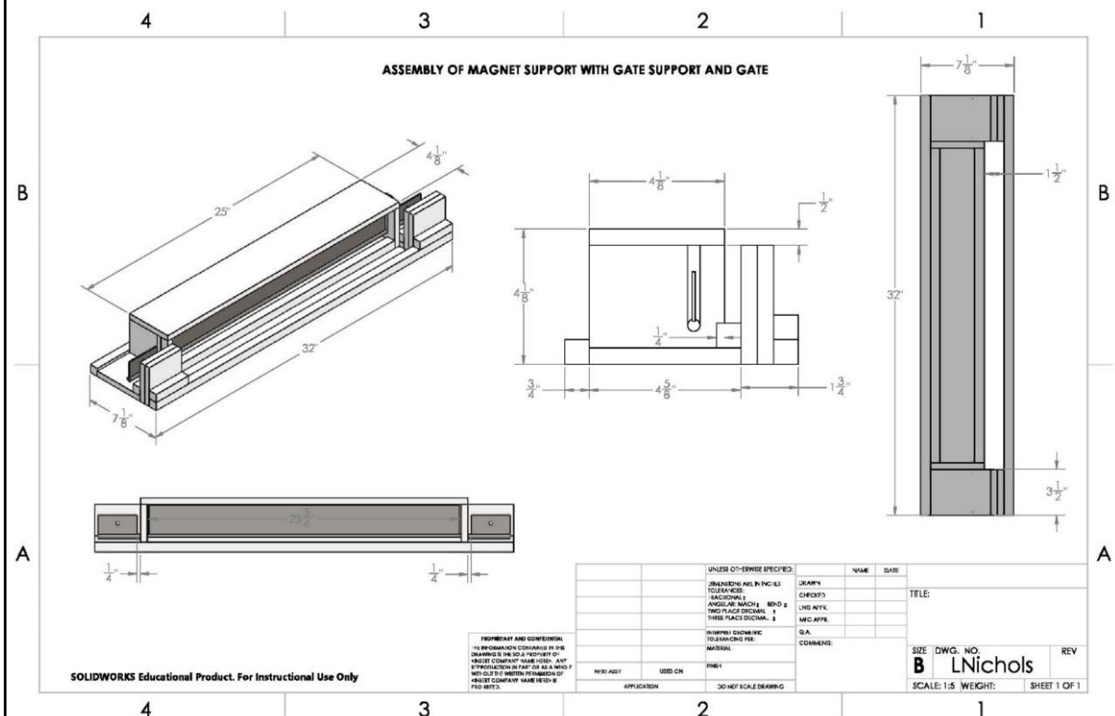
ASSEMBLY OF MAGNET SUPPORT WITH GATE SUPPORT AND GATE
SOLIDWORKS Educational Product. For Instructional Use Only
LNichols
SCALE: 1:5
SHEET 1 OF 1

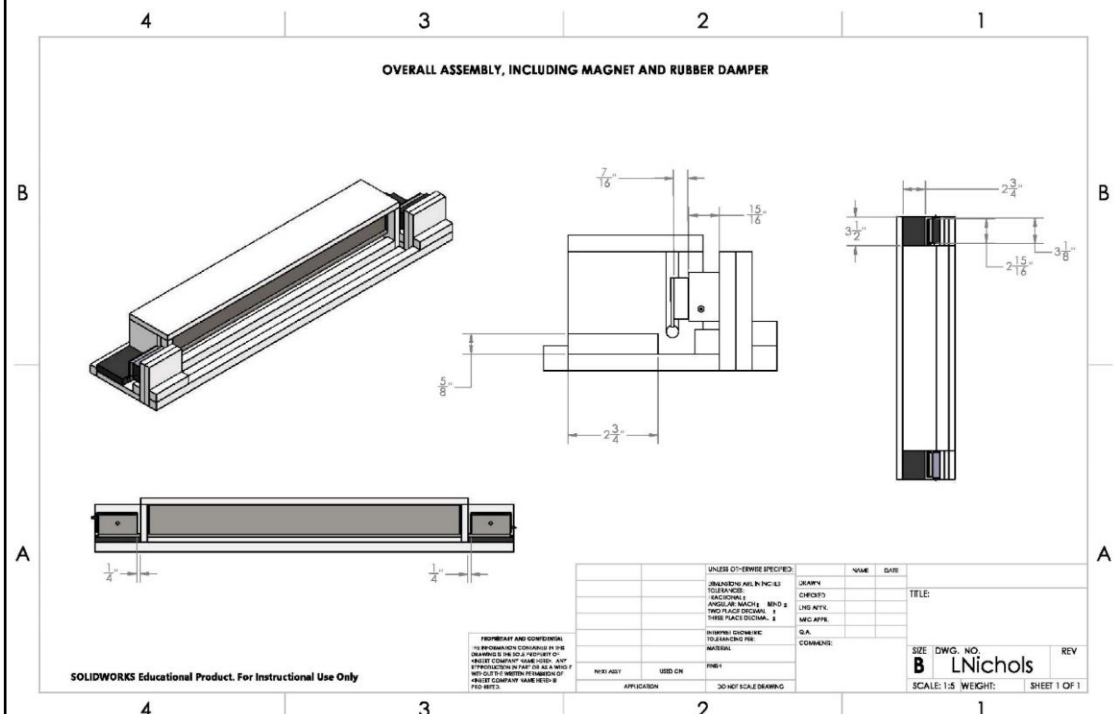
OVERALL ASSEMBLY, INCLUDING MAGNET AND RUBBER DAMPER
SOLIDWORKS Educational Product. For Instructional Use Only
UNLESS OTHERWISE SPECIFIED:
DIMENSIONS ARE IN INCHES
TITLE:
SIZE
B
DWG. NO.
LNichols
REV
SCALE: 1:5
WEIGHT:
SHEET 1 OF 1
DO NOT SCALE DRAWING
PROPRIETARY AND CONFIDENTIAL

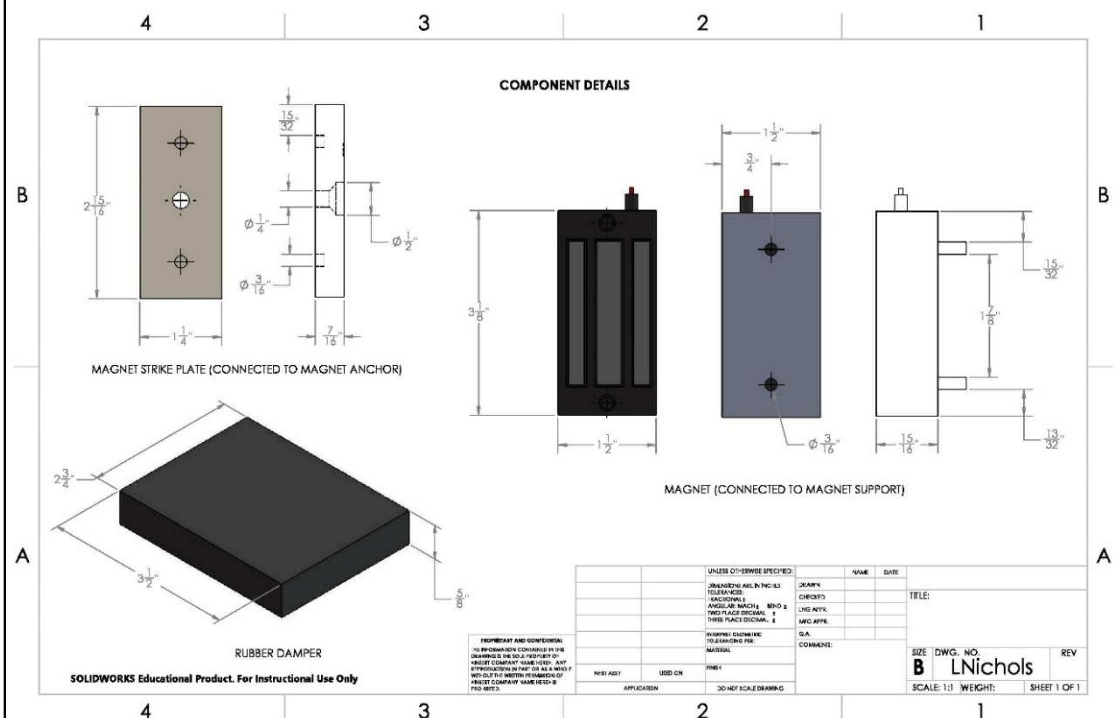

COMPONENT DETAILS
MAGNET STRIKE PLATE (CONNECTED TO MAGNET ANCHOR)
RUBBER DAMPER
MAGNET (CONNECTED TO MAGNET SUPPORT)
SOLIDWORKS Educational Product. For Instructional Use Only
UNLESS OTHERWISE SPECIFIED:
NAME
DATE
DRAWN
CHECKED
ENG APPR.
MFG APPR.
Q.A.
COMMENTS:
TITLE:
SIZE
DWG. NO.
REV
B
LNichols
SCALE: 1:1
WEIGHT:
SHEET 1 OF 1
NEXT ASSY
USED ON
APPLICATION
DO NOT SCALE DRAWING
MATERIAL
FINISH
PROPRIETARY AND CONFIDENTIAL

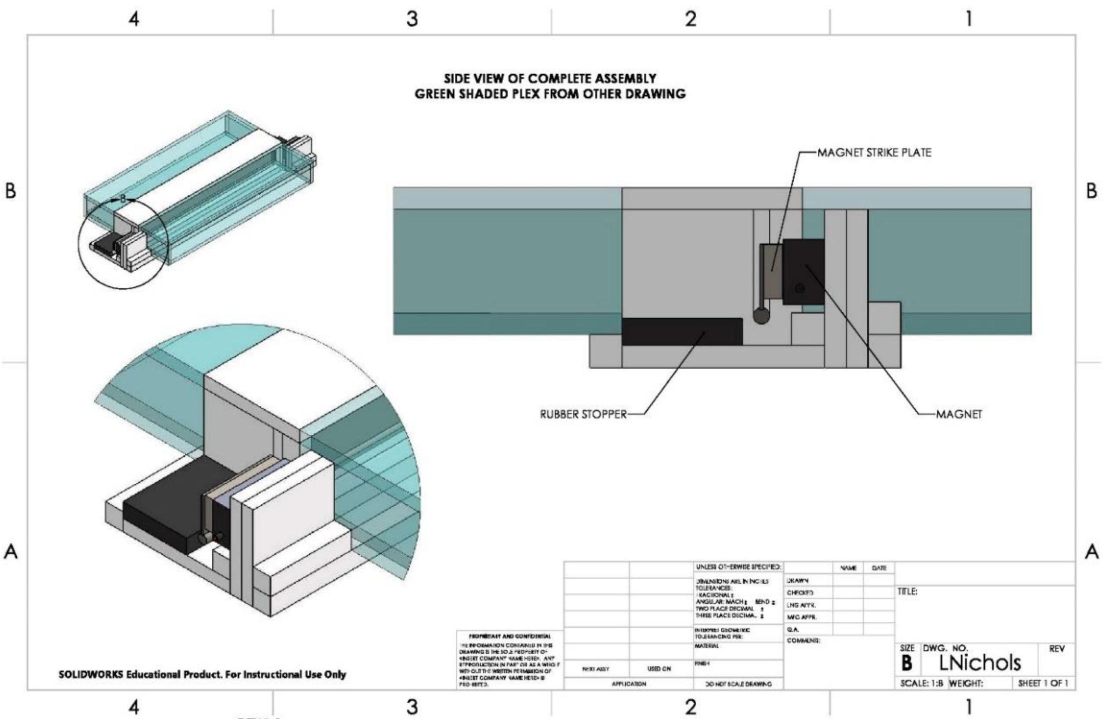

SIDE VIEW OF COMPLETE ASSEMBLY
GREEN SHADED PLEX FROM OTHER DRAWING
MAGNET STRIKE PLATE
RUBBER STOPPER
MAGNET
SOLIDWORKS Educational Product. For Instructional Use Only
UNLESS OTHERWISE SPECIFIED:
NAME
DATE
DRAWN
CHECKED
MFG APPR.
Q.A.
COMMENTS:
TITLE:
MATERIAL
NEXT ASSY
USED ON
APPLICATION
DO NOT SCALE DRAWING
SIZE
B
DWG. NO.
LNichols
REV
SCALE: 1:8
WEIGHT:
SHEET 1 OF 1

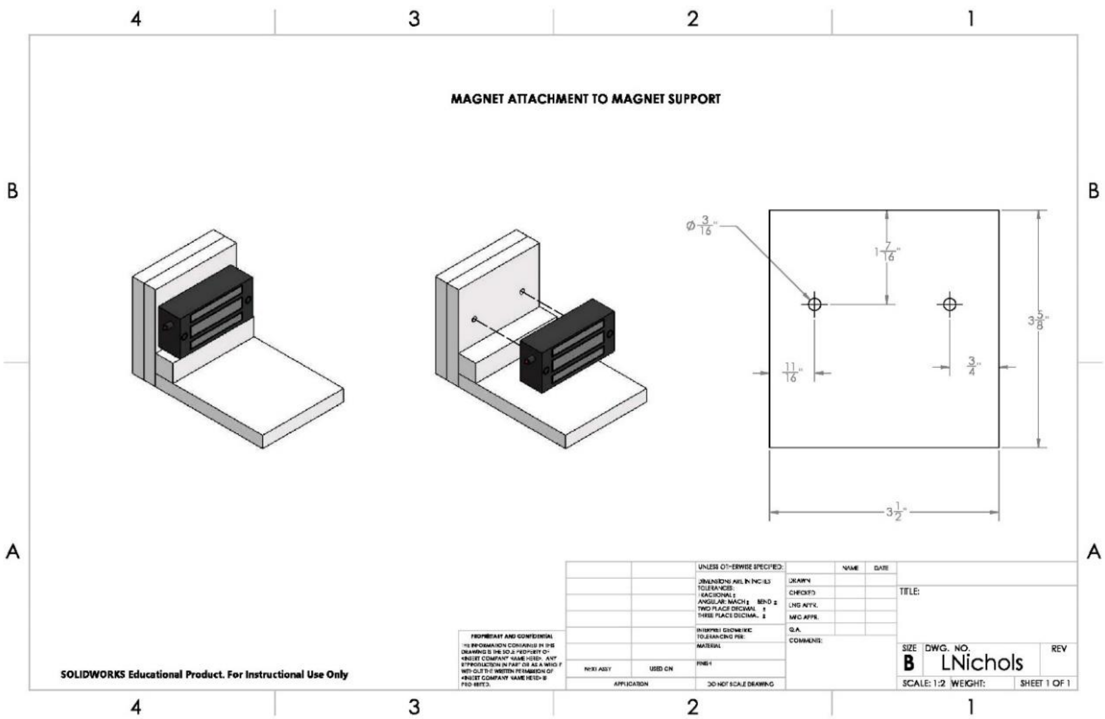
MAGNET ATTACHMENT TO MAGNET SUPPORT
SOLIDWORKS Educational Product. For Instructional Use Only
TITLE:
SIZE
B
DWG. NO.
LNichols
REV
SCALE: 1:2
WEIGHT:
SHEET 1 OF 1
DO NOT SCALE DRAWING
APPLICATION
PROPRIETARY AND CONFIDENTIAL

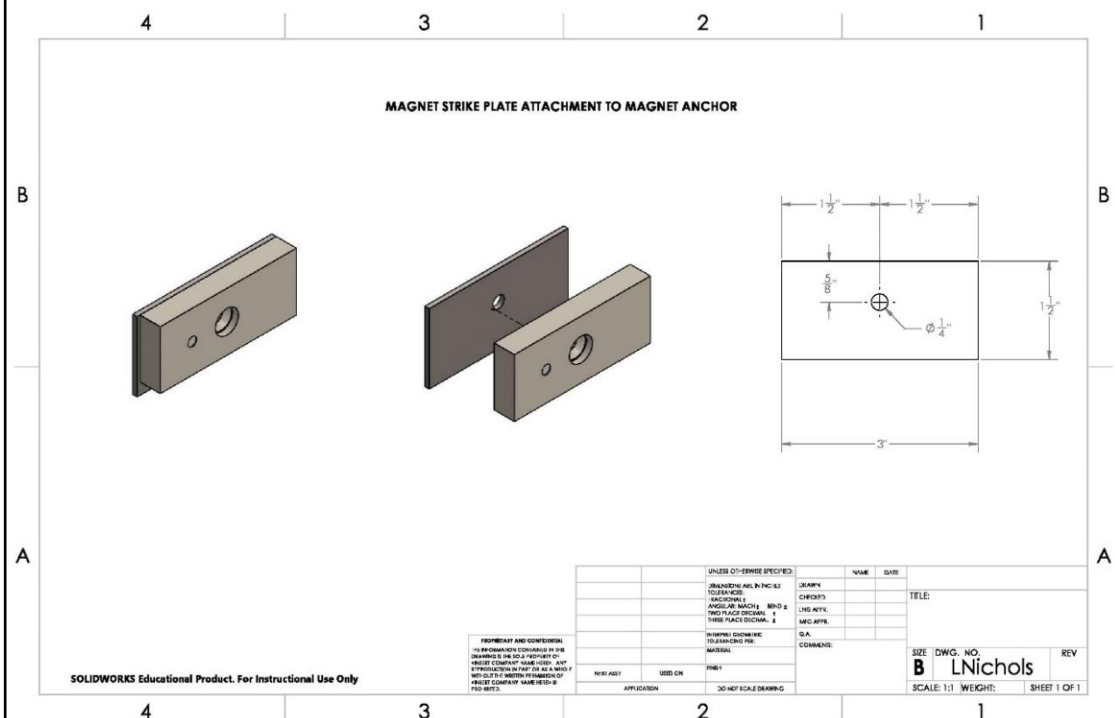

MAGNET STRIKE PLATE ATTACHMENT TO MAGNET ANCHOR
SOLIDWORKS Educational Product. For Instructional Use Only
DWG. NO.
LNichols
SCALE: 1:1
WEIGHT:
SHEET 1 OF 1
TITLE:

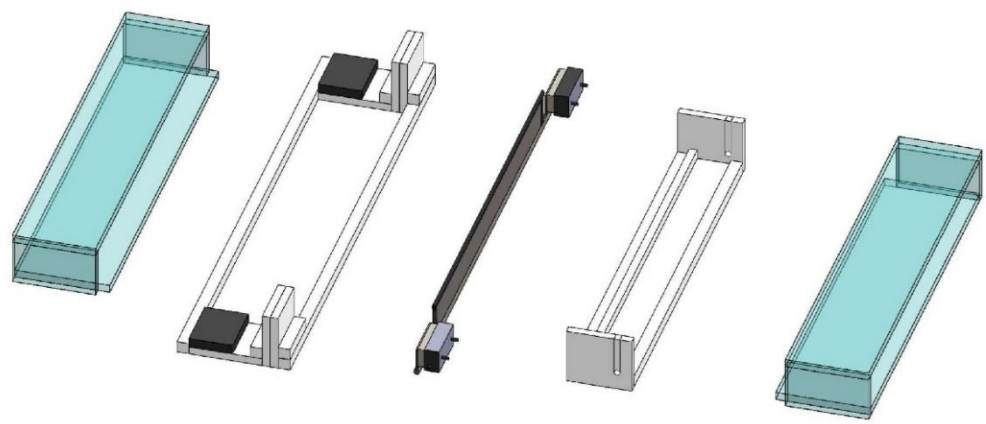

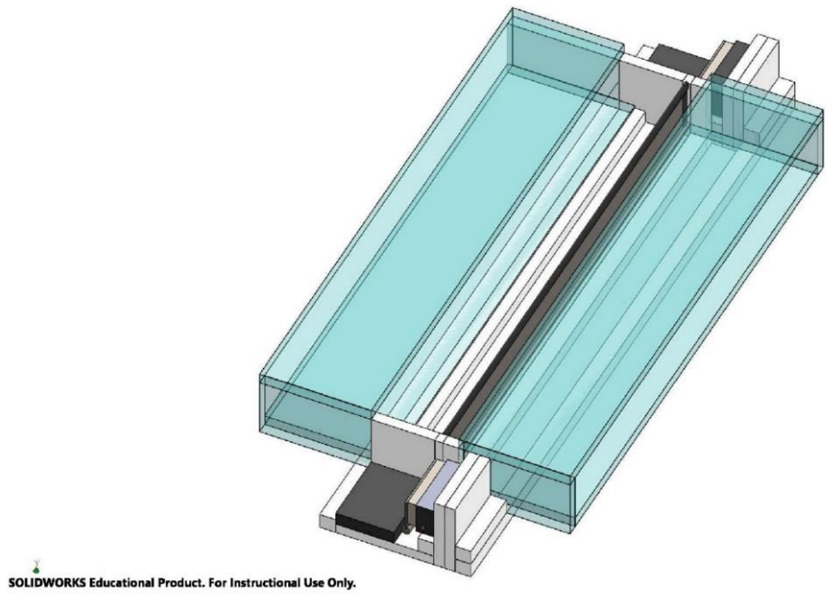
SOLIDWORKS Educational Product. For Instructional Use Only.

Appendix D: Artificial Wave Generation

O. H. HINSDALE

WAVE RESEARCH LABORATORY

OREGON STATE UNIVERSITY

Large Wave Flume

The Large Wave Flume is the largest of its kind in North America. Because of its size and ability to operate in high Reynolds regimes, the flume is ideally suited for:

- Scaled shallow water hurricane and storm wave conditions
- Long wave and tsunami generation
- Active wave absorption for large reflected waves
- Minimizing tank seiche for long duration studies

Wave Flume

• Length:	104 m	342 ft
• Width:	3.7 m	12 ft
• Depth:	4.6 m	15 ft

Wavemaker

- Type: Piston-type, Hydraulic Actuator Assembly
- Wave Types: Regular, Irregular, Tsunami, User Defined
- Period Range: 0.8 to 12 seconds
- Max Wave: 1.7 m (5.6 ft) @ 5 sec in max 2.7 m water
  1.4 m (3.9ft) tsunami in max 2.0 m water
- Max Stroke: 4 m (13.1 ft) at 4 m/s (13.1 ft/s)

Instrumentation Carriage

- Powered carriage with full cross-shore traverse
- Carriage-mounted vertical instrument deployment frame
- Lightweight carriage for video and lighting applications

Oregon State UNIVERSITY OSU College of Engineering

Web: http://wave.oregonstate.edu
Tel: +1 (541) 737 – 2875 | Fax: +1 (541) 737 – 6974

O. H. HINSDALE

WAVE RESEARCH LABORATORY

OREGON STATE UNIVERSITY

Directional Wave Basin

Previously known as the Tsunami Wave Basin, was designed to understand the fundamental nature of tsunami inundation, tsunami-structure impact, harbor resonance and to improve the numerical tools for tsunami mitigation.

In addition to tsunami research, the facility is particularly suited for general testing of coastal infrastructures, nearshore processes research, wave hydrodynamics, floating structures and renewable energy devices.

The wave machine is a unique powerful snake-type system made of 29 boards with up to 2.1 m long stroke. It has been designed to generate short- and long-period multidirectional high quality waves.

Wave Basin Dimensions

• Length:	48.8 m	160 ft
• Width:	26.5 m	87 ft
• Max depth:	1.37 m	4.5 ft
• Freeboard:	0.6 m	2.0 ft

Wavemaker

• Type:	Piston-type, Electric motor
• Waveboards:	29 boards, 2.0 m (6.6 ft) high
• Wave types:	Regular, Irregular, Tsunami, Multidirectional, User defined
• Period range:	0.5 to 10 seconds
• Max. Wave:	0.75 m (2.5 ft) in 1.37 m (4.5 ft) depth
• Max. Stroke:	2.1 m (6.9 ft)
• Max. Velocity:	2.0 m/s (6.6 ft/s)

Supporting infrastructure

- 7.5 T capacity bridge crane
- Instrumentation carriage, spans 26.5 m
- Unistrut installed in floor and sides to secure models
- Two access ramps, 14 ft width (4.2 m)
- Steady flow currents installed on project-by-project basis

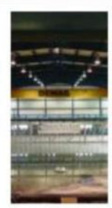

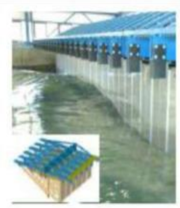

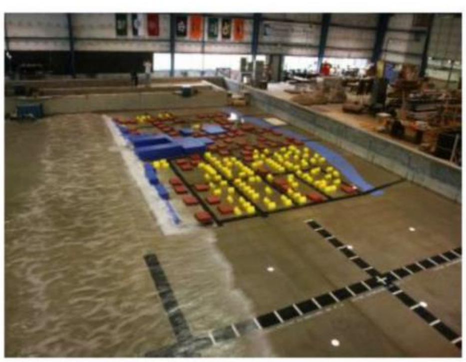

Oregon State University OSU College of Engineering

Web: http://wave.oregonstate.edu
Tel: +1 (541) 737 – 2875 | Fax: +1 (541) 737 – 6974

THE NEW DELTA FLUME FOR LARGE-SCALE TESTING

BY MARCEL R.A. VAN GENT

The new Delta Flume in Delft was constructed to facilitate large-scale physical model testing. The new Delta Flume has a length of about 300m, a width of 5m and a height of 9.5m. The maximum significant wave height that can be generated is about $H_s = 2.2$m and maximum individual wave heights in the range between $H_{max} = 4$m and 4.5m. This unique facility enables physical modelling at prototype-scale or at close-to-prototype scale. Preventing or diminishing scale-effects is especially important for coastal structures in which sand, clay, grass or other natural construction material is being applied. Besides projects with dikes and dunes, structures such as breakwaters, bed protections, monopiles, offshore wind farms, and storm surge barriers are scheduled to be tested. Along with new facilities also new measurement techniques have been developed, both for the new Delta Flume and for the other wave facilities (*e.g.* wave basins). The new Delta Flume completes a set of wave facilities for physical model testing consisting of small and large-scale test facilities and 2D (wave flumes) and 3D (wave basins) facilities.

Introduction

To determine the response of coastal structures such as dikes, dunes, dune-revetments, breakwaters, cobble & gravel beaches, intake & outfall structures, offshore windfarms and bed protections, under loading of waves and/or currents physical model testing is an essential part of the design and evaluation process of such structures. Some aspects require modelling at a large scale since the materials and/or physical processes cannot be modelled properly on a small scale using Froude's scaling law. Examples of materials that cannot be modelled properly at a small-scale are sand, clay, grass or natural construction material (*e.g.* brushwood). Physical processes that cannot be modelled properly at a small-scale are often related to flow characteristics that do not scale according to Froude's scaling law, *e.g.* for structures in which laminar (porous) flow plays an important role results may be affected by scale-effects. Nevertheless, tests at small-scale can provide valuable indicative results although for accurate quantitative results large scale models are still

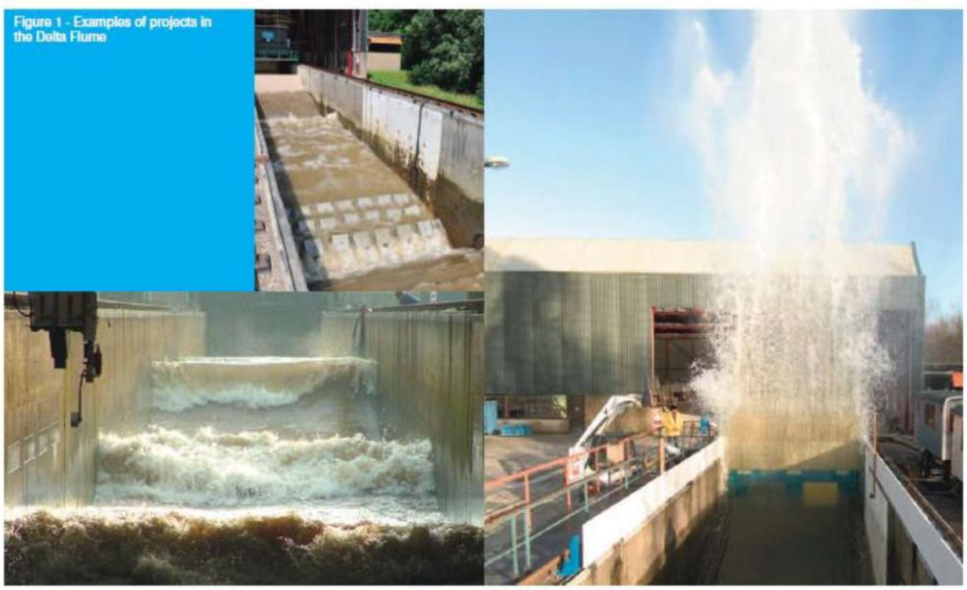

Figure 1 - Examples of projects in the Delta Flume

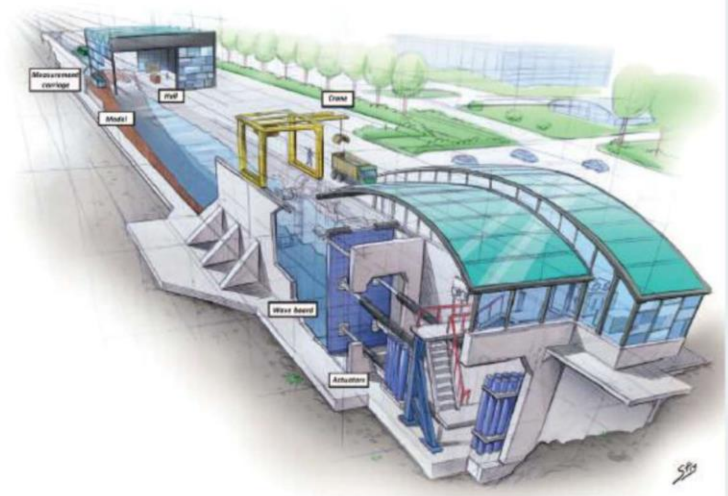

Figure 2 - Impression of the new Delta Flume (courtecy mr Stephan Timmers)

required. Many types of coastal structures can be modelled sufficiently accurate at small scales, e.g. most rubble mound breakwaters.

Besides the scale of models it is important to determine whether the structures can be modelled in a 2D model (wave flumes) or need to be modelled in a 3D model (wave basins). Often combinations of 2D and 3D models are applied, e.g. where cross-sections of structures are optimized in a wave flume, while 3D aspects are studied afterwards in a separate 3D model. Also the combination of small-scale tests and large-scale tests may be an efficient way to determine the performance of coastal structures for those structures in which some of the characteristics would be affected by scale-effects in smaller models. Therefore, it is essential to have a set of small-scale and large-scale facilities available, as well as 2D (wave flumes) and 3D facilities (wave basins). Not only the facilities are important, also the measurement equipment and experienced staff are key factors of the success of physical model tests. In Van Gent (2014) an overview of projects in the various physical model facilities is given.

Projects In The Old Delta Flume

In the old Delta Flume (240m*5m*7m) a large number of projects has been performed in the last 35 years. In these projects the choice for this facility has been based mainly on the need to limit or avoid scale-effects in physical model tests. The new Delta Flume in Delft (300m*5m*9.5m) has been constructed to facilitate measurements at an even larger scale. Figure 1 shows examples of projects performed in the old Delta Flume: Wave impacts on vertical walls, wave overtopping at dikes with grass, the dynamic behaviour of cobble beaches, the stability of placed-block revetments, the residual strength of clay-dikes, breakwater stability, dune erosion, and wave damping by brushwood mattresses. Other typical studies in the Delta Flume are related to for instance the validation of numerical models, testing and calibration of field measurement equipment, and the stability of pipeline covers.

Besides consultancy projects many research projects in the Delta Flume have been performed and resulted in information on the performance of coastal structures, for instance:

■ Placed-block revetments ■ Grass slopes under wave attack ■ Residual strength of dikes ■ Dune erosion ■ Gravel and cobble beaches ■ Wave impacts on vertical walls ■ Geotubes and geocontainers.

The New Delta Flume

The main characteristics of the new Delta Flume compared to the old Delta Flume are that the maximum wave height that can be generated is higher, the length is increased, tidal water level variations can be generated, and the new Delta Flume is close to the other wave facilities in Delft. One of the main advantages of the new Delta Flume over the old Delta Flume is that scale-effects are further reduced; a larger portion of the projects can be performed at (close-to) prototype scale. Figure 2 provides an impression of the new Delta Flume.

Flume dimensions The flume has a total length of about 300m. The size was determined based on tests that have been performed in the old Delta Flume. The modelling area has a total depth of 9.5m for a length of 183m, and an extra 75m section of 7m deep. The deep part has a length that is sufficient to model structures such as dikes while the combination with a shallower section allows for modelling of gentle foreshores over a length of about 250m in combination with for instance dunes. For the majority of the projects the water depth at the wave board will be between 2.5m and 8m. The flume is 5m wide.

Wave conditions The maximum wave heights that can be generated are about H_{m0} = 2.2m and maximum individual wave heights in the range between H_{max} = 4m and 4.5m. The optimal water depth at the wave board for reaching the highest significant wave height for which also the wave height distribution is modelled accurately, is estimated at 6.9m. Spectral significant wave heights larger than H_{m0} = 2.2m can be generated but these will cause some side wall overtopping. Irregular and regular waves, as well as some more special wave conditions can be generated (e.g. for

Tsunami modelling and focussed waves). It is expected that irregular wave conditions with standard spectral shapes (e.g. Jonswap) will be generated in the majority of experiments, so that during the design of the wave generator emphasis was put on precise specification of this type of wave conditions. Increasing wave height, wave period and water depth require more wave generating power, more wave board stroke and larger flume depths. In Hofland et al (2013) the percentage of water defences in The Netherlands that can be modelled at full scale is discussed. It is estimated that the new Delta Flume is capable of generating sufficiently large wave heights to cover about 85% of the Dutch sea dikes at prototype scale under design conditions. This means an increase in number of Dutch dike sections that can be tested at full scale of about 50% compared to the old Delta Flume.

To generate the large wave heights (e.g. $H_{m0} = 2.2$m) with the corresponding wave periods (e.g. $T_p = 9.4$s), a certain wave board stroke is needed. However, waves will reflect from the structures in the wave flume. To absorb these reflected waves with our active reflection compensation system (ARC, see also Wenneker *et al*, 2010), also a part of the wave board stroke is needed. The stroke of the new wave board is 7m, allowing for the mentioned significant wave height in combination with space to absorb waves that are reflected by structures in the flume.

Wave generator To generate the waves that are required a piston-type wave board was selected because of its good performance for coastal applications. The wave board is of the dry-back type. A hydraulic system was opted for. Four actuators are applied to better distribute the forces that the board will experience. The wave generator utilizes Degree of Freedom (DOF) control on the four actuators to accurately control the linear motion of the board while zeroing out unwanted board deflections such as twisting or bending due to hydrodynamic forces and board compliance. The length of an actuator is 24.5m when fully extended. A novelty in the new Delta Flume is that a tidal variation in the water level is possible by filling and emptying the flume during an experiment. The maximum filling discharge is 1 m³/s.

Measurements Various measurement techniques are acquired and developed to extract data from the experiments in the flume (Hofland *et al*, 2012). Besides classic point measurements, also synoptic measurement techniques (i.e. high resolution measurements of time-varying spatial fields) have been developed. For the measurements of waves (at the wall) the proven resistance-type wave probes are used. Radars will be used to obtain wave height measurements at any location. In addition, the use of laser scanners and stereo matching of video images can be used to obtain spatially distributed information of waves and/or (deformed) structures. Also good visual observation of the tests is ensured using for instance a central video observation system and many (flush) cavities in the wall near the location of most models to install instruments.

***Dr Marcel R.A. van Gent* is a specialist in the field of coastal engineering, in particular coastal structures, wave modelling, dikes and dunes. He obtained his PhD at the Delft University of Technology in 1995 on the modelling of reshaping rubble mound coastal structures and gravel beaches. Dr Marcel van Gent is now head of the department 'Coastal Structures & Waves' at Deltares, Delft. His is leading a group that consists of about 35 scientists and assistants for performing physical model tests in wave flumes and wave basins, developing numerical wave models, and providing specialist consultancy services. Since 1991 Marcel van Gent participated in various research projects, including projects for the European Union, for the Dutch Government, and in co-operation with Universities, Consultancy firms, and Contractors. Dr Marcel van Gent published about 100 international scientific papers on coastal structures, wave modelling and dune erosion.**

REFERENCES

Hofland, B., R. Hoffmann and R. Lindenbergh (2012), Wave measurement techniques for the new large-scale Delta Flume. Proc. Coastlab2012, Gent.
Hofland, B., I. Wenneker and M. van Gent (2013), Description of the new Delta Flume, Proc. Coastlines, Marine
Van Gent, M.R.A. (2014), Overview of physical modeling at Deltares including the new Delta Flume, Keynote, Proc. Coastlab 2014.
Wenneker, I., J. Meesters, R. Hoffmann and D. Francissen (2010), Active Wave Absorption System ARCH, Proc. Coastlab 2010, Barcelona.


(a)

(a) hydraulic power units for wave generator
(b) crane above flume to construct structures to be tested
(c) blue wave paddle


(b)


(c)

Appendix E: Infrared Break Beam Sensor

adafruit learning system

IR Breakbeam Sensors

Created by lady ada

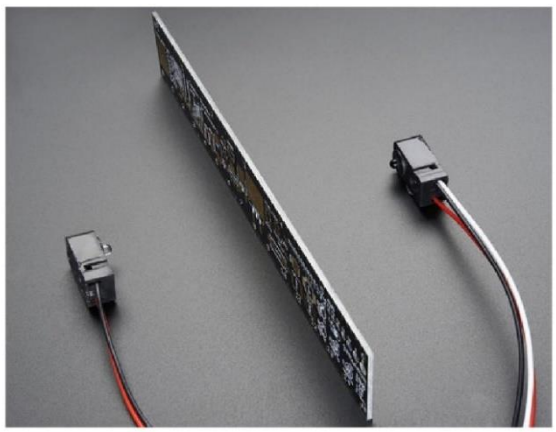

Last updated on 2017-12-08 10:32:59 PM UTC

Overview

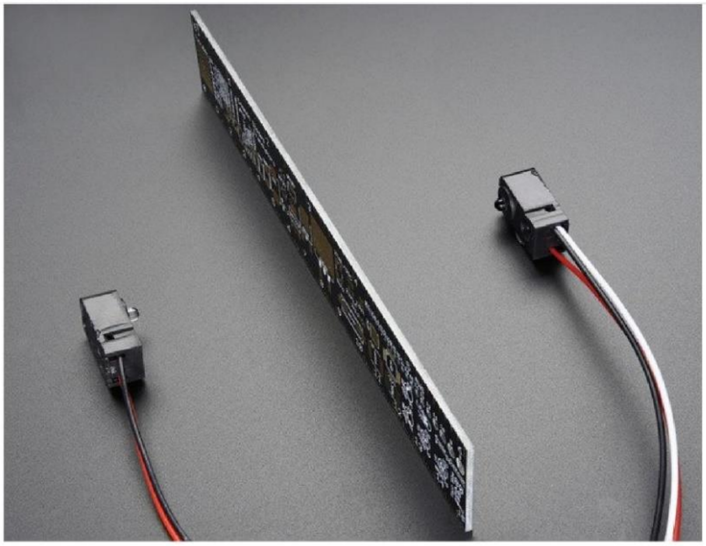

Infrared (IR) break-beam sensors are a simple way to detect motion. They work by having an emitter side that sends out a beam of human-invisible IR light, then a receiver across the way which is sensitive to that same light. When something passes between the two, and its not transparent to IR, then the 'beam is broken' and the receiver will let you know.

Compared to PIR sensors, breakbeams are faster and allow better control of where you want to detect the motion. Compared to Sonar modules, they're less expensive. However, you do need **both** emitter and receiver

The receiver is on the left, it has three wires. The transmitter is on the right, it has two wires

Arduino

Wiring these sensors for Arduino use is really easy.

First up you'll need to power the transmitter. Connect the black wire to ground and the red wire directly to 3.3V or 5V power. It will draw 9mA from 3.3V (lower power) and 20mA from 5V (better range)

Next up you'll want to connect up the receiver. Connect the black wire to ground, the red wire to 3.3V or 5V (whichever logic level you like) and then the white or yellow wire to your digital input.

Note that you do not *have* to share power supply ground or power between the two, the 'signal' is sent optically.

The receiver is **open collector** which means that you do need a pull up resistor. Most microcontrollers have the ability to turn on a built in pull up resistor. If you do not, connect a 10K resistor between the white wire of the receiver and the red wire.

On an Arduino, we'll connect the signal (yellow/white) pin to Digital #4

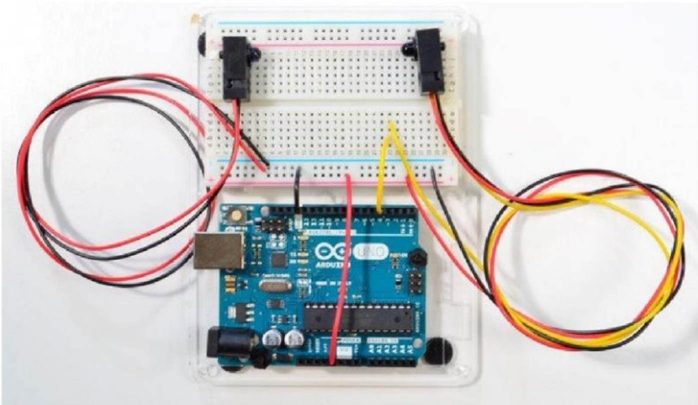

Run this demo code on your Arduino

```
/*
  IR Breakbeam sensor demo!
*/

#define LEDPIN 13
  // Pin 13: Arduino has an LED connected on pin 13
  // Pin 11: Teensy 2.0 has the LED on pin 11
  // Pin  6: Teensy++ 2.0 has the LED on pin 6
  // Pin 13: Teensy 3.0 has the LED on pin 13

#define SENSORPIN 4

// variables will change:
int sensorState = 0, lastState=0;         // variable for reading the pushbutton status

void setup() {
  // initialize the LED pin as an output:
  pinMode(LEDPIN, OUTPUT);
  // initialize the sensor pin as an input:
  pinMode(SENSORPIN, INPUT);
  digitalWrite(SENSORPIN, HIGH); // turn on the pullup

  Serial.begin(9600);
}

void loop(){
  // read the state of the pushbutton value:
  sensorState = digitalRead(SENSORPIN);

  // check if the sensor beam is broken
  // if it is, the sensorState is LOW:
  if (sensorState == LOW) {
    // turn LED on:
    digitalWrite(LEDPIN, HIGH);
  }
  else {
    // turn LED off:
    digitalWrite(LEDPIN, LOW);
  }

  if (sensorState && !lastState) {
    Serial.println("Unbroken");
  }
  if (!sensorState && lastState) {
    Serial.println("Broken");
  }
  lastState = sensorState;
}
```

With the above wiring, when you put you hand between the sensor pair, the onboard LED will turn on and the serial console will print out messages:

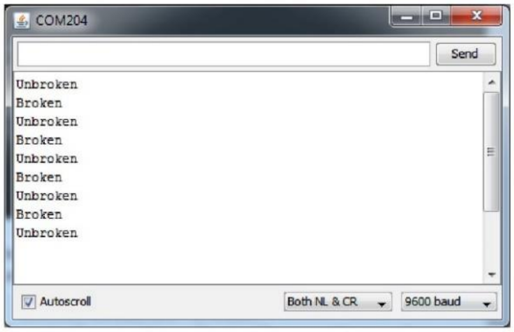
COM204
Send
Unbroken
Broken
Unbroken
Broken
Unbroken
Broken
Unbroken
Broken
Unbroken
Autoscroll
Both NL & CR
9600 baud

CircuitPython

It's easy to read a break beam sensor from CircuitPython code using built-in digital input/output capabilities.

First wire up a break beam transmitter and receiver just like you would for an Arduino. Here's an example of wiring to a Feather M0:

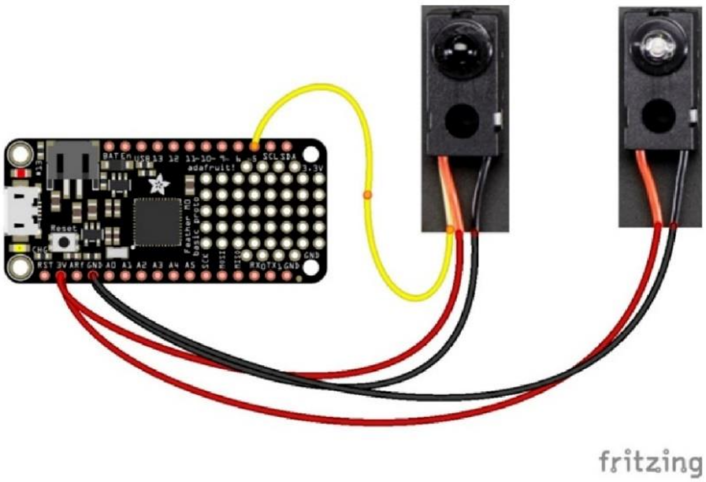

- **Board 3V** (or 5V if your board has it) to **both** receiver and transmitter **red wire**.
- **Board GND** to **both** receiver and transmitter **black wire.**
- **Board D5** (or any other digital input) to receiver **yellow wire.**

Next connect to the board's serial REPL so you are at the CircuitPython >>> prompt.

Now import the **board** and **digitalio** modules that allow you to create a digital input. Be sure you've read the CircuitPython digital I/O guide for more background too!

```
import board
import digitalio
```

Create a digital input for the pin connected to the receiver, D5 in this case:

```
break_beam = digitalio.DigitalInOut(board.D5)
break_beam.direction = digitalio.Direction.INPUT
break_beam.pull = digitalio.Pull.UP
```

Notice you set the **direction** property to input, and the **pull** property to a pull-up (just like the digital I/O guide mentions). This is necessary to configure the digital input with an internal pull-up resistor so it always reads a good value from the break beam sensor.

Checking if the sensor detects a break is as easy as reading the **value** property of the digital input. When value is true it means the input is at a high logic level which occurs when the receiver can see the transmitter and the beam is not broken. However if you get a value of false the input is at a low logic level which means the receiver cannot see the transmitter and the beam is broken!

Try reading the value with nothing blocking the transmitter and receiver:

```
break_beam.value
```

```
>>> break_beam.value
True
```

Now put something large and opaque, like your hand, in front of the transmitter to block the light. Read the value again:

```
break_beam.value
```

```
>>> break_beam.value
False
>>>
```

Awesome! Notice the digital input value was true, or at a high logic level, when nothing was blocking the beam. As soon as your hand covered the beam the input value turned false, or low logic level, to indicate an obstruction.

You can put all of this together into a complete program that prints a message whenever the beam is blocked. Save this as **main.py** on your board and examine the serial monitor for output, a message is printed when the beam is blocked:

```
import time

import board
import digitalio


# Create digital input with pull-up resistor on pin D5
# for break beam sensor.
break_beam = digitalio.DigitalInOut(board.D5)
break_beam.direction = digitalio.Direction.INPUT
break_beam.pull = digitalio.Pull.UP

# Main loop runs forever and prints a message once a second
# while the sensor is blocked/broken.
while True:
    if not break_beam.value:
        # Break beam input is at a low logic level, i.e. broken!
        print('Beam is broken!')
    time.sleep(1.0)  # Delay for 1 second and repeat again.
```

That's all there is to reading a beam break sensor with CircuitPython!

Appendix F: Arduino Micro-controller Mega 2560

Use your Arduino Mega 2560 on the Arduino Desktop IDE

If you want to program your Arduino Mega 2560 while offline you need to install the Arduino Desktop IDE

Connect your board

Connect your Mega2560 board with an A B USB cable; sometimes this cable is called a *USB printer cable*

The USB connection with the PC is necessary to program the board and not just to power it up. The Mega2560 automatically draw power from either the USB or an external power supply. Connect the board to your computer using the USB cable. The green power LED (labelled PWR) should go on.

Open your first sketch

Open the LED blink example sketch: File > Examples >01.Basics > Blink.

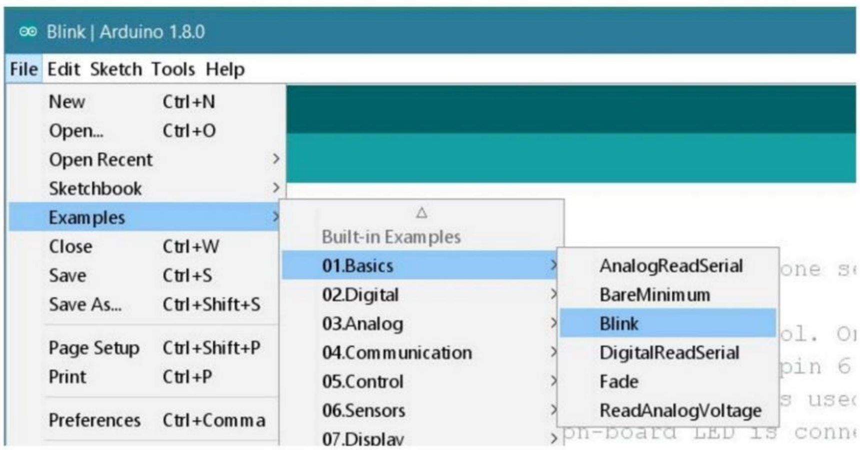

Select your board type and port

You'll need to select the entry in the Tools > Board menu that corresponds to your Arduino or Genuino board. You have a Mega2560, therefore it has an ATmega2560 microcontroller, selected by default as processor.

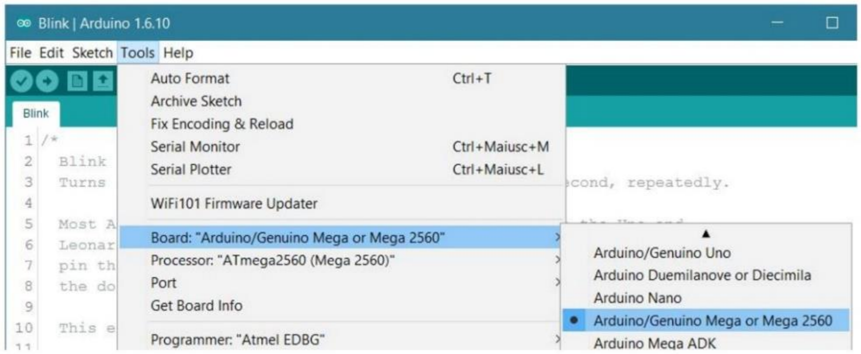

Select the serial device of the board from the Tools | Serial Port menu. This is likely to be COM3 or higher (COM1 and COM2 are usually reserved for hardware serial ports). To find out, you can disconnect your board and re-open the menu; the entry that disappears should be the Arduino or Genuino board. Reconnect the board and select that serial port.

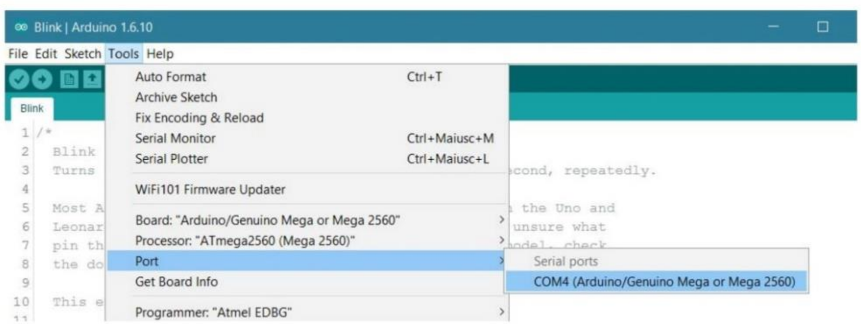

Upload the program

Now, simply click the "Upload" button in the environment. Wait a few seconds - you should see the RX and TX leds on the board flashing. If the upload is successful, the message "Done uploading." will appear in the status bar.

A few seconds after the upload finishes, you should see the pin 13 (L) LED on the board start to blink (in orange). If it does, congratulations! Your board is up-and-running.

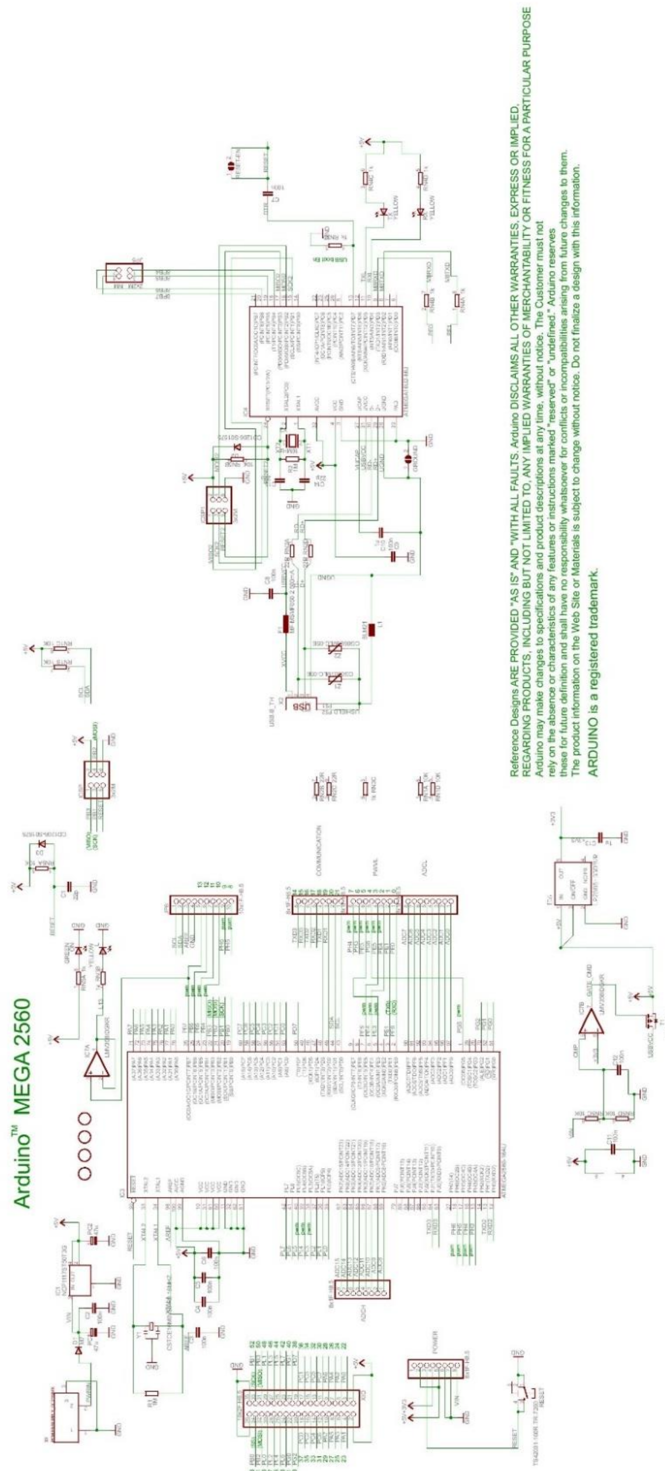
Arduino™ MEGA 2560
Reference Designs ARE PROVIDED "AS IS" AND "WITH ALL FAULTS. Arduino DISCLAIMS ALL OTHER WARRANTIES, EXPRESS OR IMPLIED,
REGARDING PRODUCTS, INCLUDING BUT NOT LIMITED TO, ANY IMPLIED WARRANTIES OF MERCHANTABILITY OR FITNESS FOR A PARTICULAR PURPOSE
Arduino may make changes to specifications and product descriptions at any time, without notice. The Customer must not
rely on the absence or characteristics of any features or instructions marked "reserved" or "undefined." Arduino reserves
these for future definition and shall have no responsibility whatsoever for conflicts or incompatibilities arising from future changes to them.
The product information on the Web Site or Materials is subject to change without notice. Do not finalize a design with this information.
ARDUINO is a registered trademark.

1. Pin Configurations

Figure 1-1. TQFP-pinout ATmega640/1280/2560

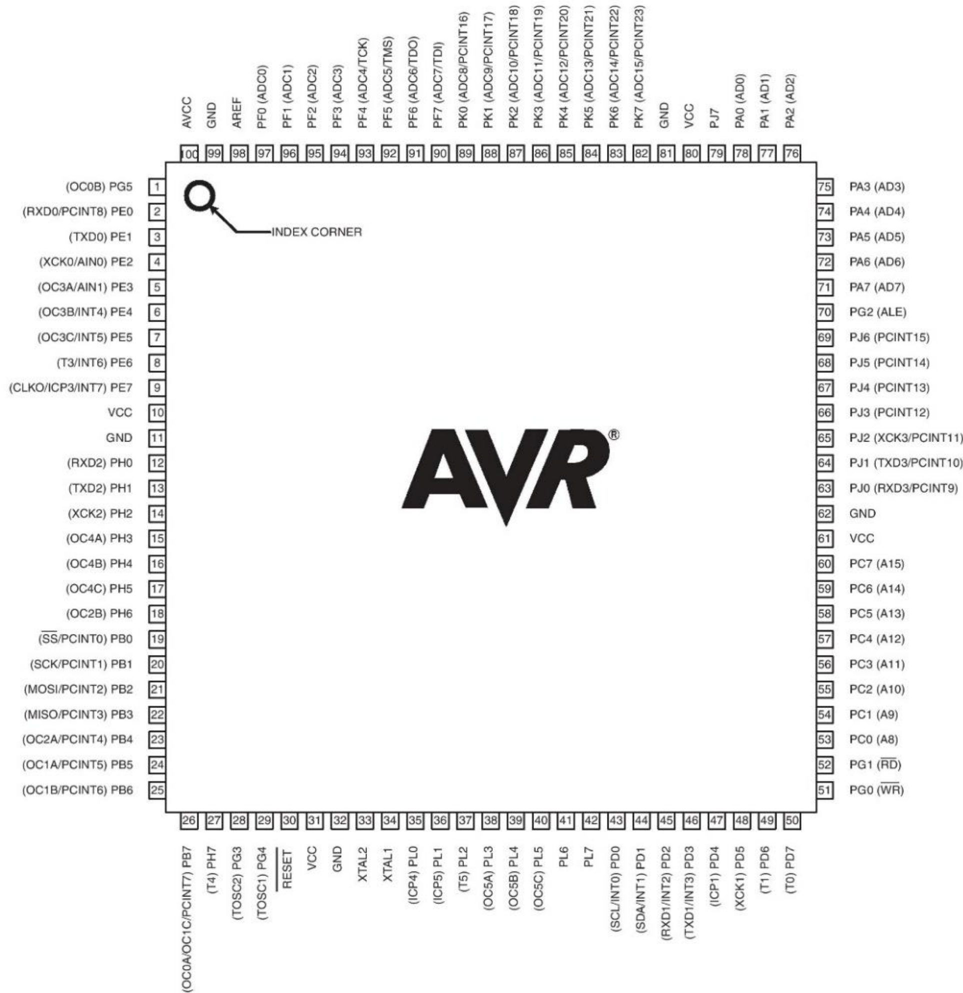

Figure 1-2. CBGA-pinout ATmega640/1280/2560

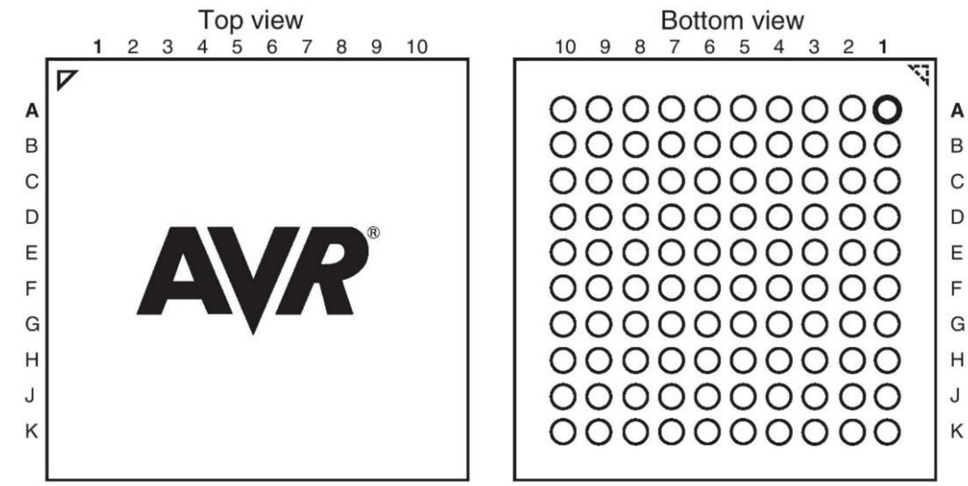

Table 1-1. CBGA-pinout ATmega640/1280/2560

	1	2	3	4	5	6	7	8	9	10
A	GND	AREF	PF0	PF2	PF5	PK0	PK3	PK6	GND	VCC
B	AVCC	PG5	PF1	PF3	PF6	PK1	PK4	PK7	PA0	PA2
C	PE2	PE0	PE1	PF4	PF7	PK2	PK5	PJ7	PA1	PA3
D	PE3	PE4	PE5	PE6	PH2	PA4	PA5	PA6	PA7	PG2
E	PE7	PH0	PH1	PH3	PH5	PJ6	PJ5	PJ4	PJ3	PJ2
F	VCC	PH4	PH6	PB0	PL4	PD1	PJ1	PJ0	PC7	GND
G	GND	PB1	PB2	PB5	PL2	PD0	PD5	PC5	PC6	VCC
H	PB3	PB4	RESET	PL1	PL3	PL7	PD4	PC4	PC3	PC2
J	PH7	PG3	PB6	PL0	XTAL2	PL6	PD3	PC1	PC0	PG1
K	PB7	PG4	VCC	GND	XTAL1	PL5	PD2	PD6	PD7	PG0

Note: The functions for each pin is the same as for the 100 pin packages shown in Figure 1-1 on page 2.

Figure 1-3. Pinout ATmega1281/2561

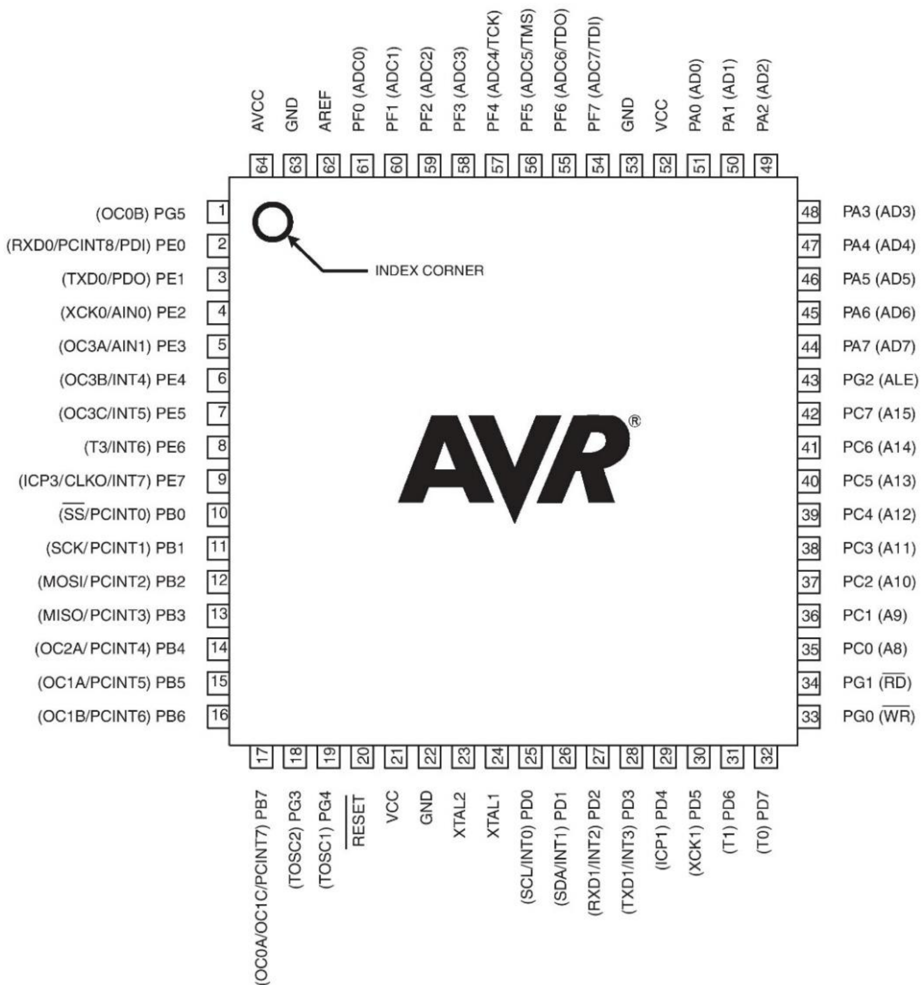

Note: The large center pad underneath the QFN/MLF package is made of metal and internally connected to GND. It should be soldered or glued to the board to ensure good mechanical stability. If the center pad is left unconnected, the package might loosen from the board.

2. Overview

The ATmega640/1280/1281/2560/2561 is a low-power CMOS 8-bit microcontroller based on the AVR enhanced RISC architecture. By executing powerful instructions in a single clock cycle, the ATmega640/1280/1281/2560/2561 achieves throughputs approaching 1 MIPS per MHz allowing the system designer to optimize power consumption versus processing speed.

2.1 Block Diagram

Figure 2-1. Block Diagram

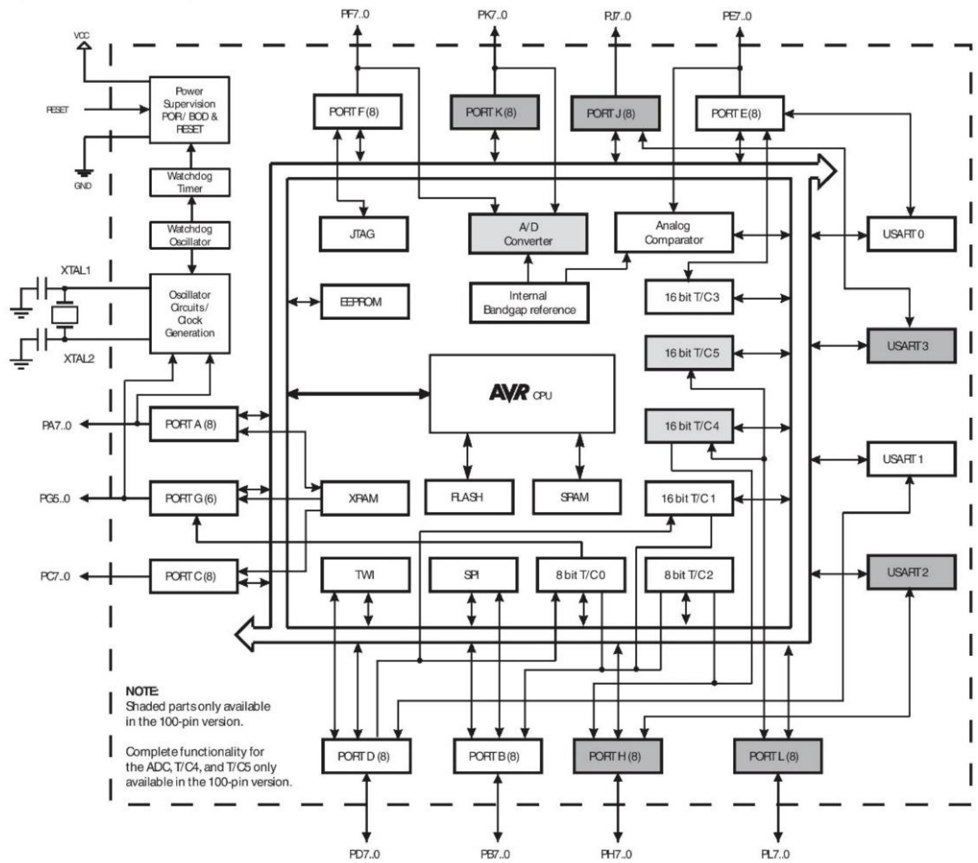

The Atmel® AVR® core combines a rich instruction set with 32 general purpose working registers. All the 32 registers are directly connected to the Arithmetic Logic Unit (ALU), allowing two independent registers to be accessed in one single instruction executed in one clock cycle. The resulting architecture is more code efficient while achieving throughputs up to ten times faster than conventional CISC microcontrollers.

The ATmega640/1280/1281/2560/2561 provides the following features: 64K/128K/256K bytes of In-System Programmable Flash with Read-While-Write capabilities, 4Kbytes EEPROM, 8Kbytes SRAM, 54/86 general purpose I/O lines, 32 general purpose working registers, Real Time Counter (RTC), six flexible Timer/Counters with compare modes and PWM, four USARTs, a byte oriented 2-wire Serial Interface, a 16-channel, 10-bit ADC with optional differential input stage with programmable gain, programmable Watchdog Timer with Internal Oscillator, an SPI serial port, IEEE® std. 1149.1 compliant JTAG test interface, also used for accessing the On-chip Debug system and programming and six software selectable power saving modes. The Idle mode stops the CPU while allowing the SRAM, Timer/Counters, SPI port, and interrupt system to continue functioning. The Power-down mode saves the register contents but freezes the Oscillator, disabling all other chip functions until the next interrupt or Hardware Reset. In Power-save mode, the asynchronous timer continues to run, allowing the user to maintain a timer base while the rest of the device is sleeping. The ADC Noise Reduction mode stops the CPU and all I/O modules except Asynchronous Timer and ADC, to minimize switching noise during ADC conversions. In Standby mode, the Crystal/Resonator Oscillator is running while the rest of the device is sleeping. This allows very fast start-up combined with low power consumption. In Extended Standby mode, both the main Oscillator and the Asynchronous Timer continue to run.

Atmel offers the QTouch® library for embedding capacitive touch buttons, sliders and wheels functionality into AVR microcontrollers. The patented charge-transfer signal acquisition offersrobust sensing and includes fully debounced reporting of touch keys and includes Adjacent Key Suppression® (AKS®) technology for unambiguous detection of key events. The easy-to-use QTouch Suite toolchain allows you to explore, develop and debug your own touch applications.

The device is manufactured using the Atmel high-density nonvolatile memory technology. The On-chip ISP Flash allows the program memory to be reprogrammed in-system through an SPI serial interface, by a conventional nonvolatile memory programmer, or by an On-chip Boot program running on the AVR core. The boot program can use any interface to download the application program in the application Flash memory. Software in the Boot Flash section will continue to run while the Application Flash section is updated, providing true Read-While-Write operation. By combining an 8-bit RISC CPU with In-System Self-Programmable Flash on a monolithic chip, the Atmel ATmega640/1280/1281/2560/2561 is a powerful microcontroller that provides a highly flexible and cost effective solution to many embedded control applications.

The ATmega640/1280/1281/2560/2561 AVR is supported with a full suite of program and system development tools including: C compilers, macro assemblers, program debugger/simulators, in-circuit emulators, and evaluation kits.

Appendix G: Optomax Digital Liquid Level Sensor

DATA SHEET

Liquid Level Switch

Optomax Digital
LLC200D3SH-LLPK1

SST
DESIGN • MANUFACTURE • CUSTOMISE • CONFIGURE

FEATURES

Optomax Digital liquid level switches are ideal for applications with restricted space that require a miniature, low power and low cost sensing solution.

The microcontroller based sensor is solid state, incorporating an infra-red LED and phototransistor which are optically coupled by the tip when the sensor is in air. When the sensing tip is immersed in liquid, the infra-red light escapes making the output change state.

Housing/ Mounting	Output Type / Logic	Supply Voltage	Output Current	Temp
M12x1	PUSH PULL 1 / 0 HIGH IN AIR	4.5 - 15.4 V VOLTAGE	UP TO 100mA CURRENT	-25°C to +80°C TEMPERATURE

TECHNICAL SPECIFICATIONS

Supply voltage (Vs)	$4.5V_{DC}$ to $15.4V_{DC}$
Supply current (Is)	2.5mA max. (Vs = $15.4V_{DC}$)
Output sink and source current (Iout)	100mA
Operating temperatures	-25°C to +80°C
Storage temperatures	-30°C to +85°C
Housing material	Polysulfone[1]
Sensor termination	24AWG, 250mm PTFE wires, 8mm tinned
Mounting thread[2]	M12x1x8g with hex nut[3]
Operating pressure	7bar / 101psi maximum[4]
Tightening torque	1.5Nm / 13.26 in-lb maximum

OUTPUT VALUES

Output Voltage[5] (Vout):	**Iout = 100mA**
Output High	Vout = Vs - 1V max
Output Low	Vout = 0V + 0.5V max

Other sensor options available on request, email: technical@sstsensing.com

Need help? Ask the expert
Tel: +44 (0)1236 459 020
and ask for "Technical"

NOTES

1) Before use check that the fluid in which you wish to use these devices is compatible with Polysulfone.
2) Sensor is mounted externally.
3) Hex nut and O-ring sold separately; email: technical@sstsensing.com for details.
4) When correctly sealed.
5) Voltages applicable to output value stated.

OUTLINE DRAWING

All dimensions shown in mm. Tolerances = ±1mm.

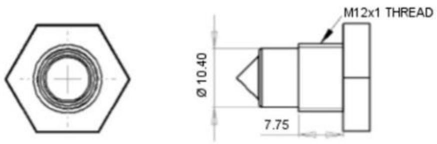

ELECTRICAL INTERFACE

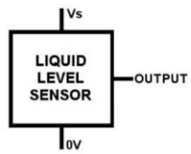

Wire	Designation
Red	Vs
Green	Output
Blue	0V

CIRCUIT DIAGRAM

Digital Output High in Air

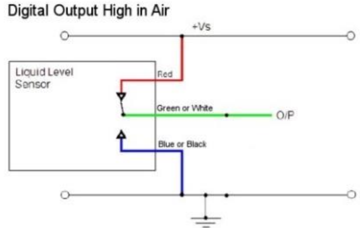

CAUTION: Take care when connecting loads.
The minimum load impedance should not exceed Vs/max output current.
NOTE: Shorting the output to Vs or 0V will result in irreparable damage to the sensor.

ORDER INFORMATION

Specify the part number listed below when ordering.

L L C 2 0 0 D 3 ☐ S H - L L P K 1

Housing Material	Housing Type	Operating Temp.	Output Logic
C Polysulfone	**2** M12x1	**0** -25 °C to +80°C	**Blank** Output High in air

CAUTION

Do not exceed maximum ratings and ensure sensor(s) are operated in accordance with their requirements.

Carefully follow all wiring instructions. Incorrect wiring can cause permanent damage to the device.

SST Sensing Ltd recommend using alcohol based cleaning agents. Do NOT use chlorinated solvents such as tricholerthane as these are likely to attack the sensor material.

Failure to comply with these instructions may result in product damage.

INFORMATION

As customer applications are outside of SST Sensing Ltd.'s control, the information provided is given without legal responsibility.

Customers should test under their own conditions to ensure that the equipment is suitable for their intended application. Before use, check that the fluid in which you wish to use these devices is compatible with Polysulfone.

For technical assistance or advice, please email:
technical@sstsensing.com

General Note: SST Sensing Ltd. reserves the right to make changes to product specifications without notice or liability.
All information is subject to SST Sensing Ltd.'s own data and considered accurate at time of going to print.

DS-0141 REV 1

5 HAGMILL CRESCENT, SHAWHEAD INDUSTRIAL ESTATE, COATBRIDGE, UK ML5 4NS
www.sstsensing.com | e: sales@sstsensing.com | t: +44 (0)1236 459020 | f: +44 (0)1236 459026

RoHS

Appendix H: Omega Pressure Transducer

HIGH SPEED USB OUTPUT PRESSURE TRANSDUCER
CONNECT DIRECTLY TO YOUR COMPUTER

High Speed 1000 Updates/per Second

Gage and Absolute Pressures
10 inH$_2$O to 5000 psi (25 mb to 345 bar)
Vacuum and Compound Ranges
10 inH$_2$O to 15 psi
Barometric and Differential Pressure Ranges

Fast Delivery!

PX409-USBH Series

NIST CE
Standard

PX409-015GUSBH shown actual size.

2 m (6') integral USB cable connects directly to your PC.

- 1000 Readings/Second
- Micro-Machined Silicon Sensor
- 316L SS Wetted Parts
- High ±0.08% BSL Accuracy
- Excellent Long Term Stability
- USB 2.0 and Below Compatible
- Standard USB Connector Termination
- Shock and Vibration Rated
- Ruggedized with Secondary Containment

The PX409 High Speed USBH Series connects directly to your computer. Free PC software enables you to chart, log, display, and output data for analysis. Also included are .NET APIs, and a command set for command-line access. The micro-machined silicon design is ideal for pressure or level applications in laboratory, test platforms, or bio/pharmaceutical applications as well as industrial applications that require a rugged, high accuracy transducer. The micro-machined silicon sensor provides a very stable transducer with exceptional high accuracy of ±0.08% and a broad compensated range of -29 to 85°C (-20 to 185°F). The modular construction allows for fast delivery of most configurations and fittings. Delivery is typically stock to 1 week!

FREE OMEGA® USBH Downloadable Software!

OMEGA is excited to announce the release of a major software update for USB Transducers! The fresh look and added features add even more value and flexibility to your transducer's performance.

Free OMEGA PC software takes the data from the transducer directly to the digital domain, turning your laptop or Windows® tablet (with USB connection) into a virtual meter, chart recorder, or data logger.

Also included are .NET APIs and a set for command-line access. Visit **ftp://ftp.omega.com/public/DASGroup/products/USBH/** to download your free copy.*

*Includes software to run TRH Central compatible devices.

SPECIFICATIONS

Accuracy: 0.08% BSL (linearity, hysteresis and repeatability combined)
Resolution: Up to 5.5 significant figures
Temperature Compensation (Over Compensated Range):
  Span: Range > 5 psi: ±0.5%
    Range ≤ 5 psi: ±1.0%
  Zero: Range > 5 psi: ±0.5%
    Range ≤ 5 psi: ±1.0%
Minimum Isolation:
  100 MΩ @ 50 Vdc case to sensor
  2 MΩ @ 50 Vdc case to output terminations
Pressure Cycles: 1 million, minimum
Long Term Stability (1-Year): ±0.1% full scale typical
A to D Conversion: 24-bit
Shock: 50 g, 11 mS half sine, vertical and horizontal axis
Vibration: 5-2000-5 Hz, 30 minute cycle, Curve L, Mil-Spec 810 figure 514-2-2, vertical and horizontal axis
Bandwidth: DC to 1000 updates per second typical (±3%)
Power Consumption: 0.35 W typical
CE Compliant: Meets industrial emissions and immunity EN61326
Environmental Protection: IP65

Metric threads and ranges available.

Secondary Containment
Gage/Vacuum/Compound Pressure:
  10 inH$_2$O to 5 psi: to 1000 psi
  15 to 1000 psi: to 3000 psi
  1500 to 5000 psi: to 10,000 psi
Absolute/Barometric Pressure:
  5 to 1000 psia: to 6000 psia
  1500 to 5000 psia: to 10,000 psia
Overpressure
Gage/Vacuum/Compound Pressure:
  10 inH$_2$O: 10 times span
  1 psi: 6 times span
  2.5 psi to 1000 psi: 4 times span
  1500 psi to 5000 psi: 7250 psi maximum
Absolute/Barometric Pressure:
  5 psia: 6 times span
  15 psia to 1000 psia: 4 times span
  1500 to 5000 psia: 7250 psia maximum
Wetted Parts: 316L stainless steel
Weight: 200 g (7 oz)
Operating Temperature Range: -40 to 85°C (-40 to 185°F)
Compensated Temperature:
  Ranges >5 psi: -29 to 85°C (-20 to 185°F)
  Ranges ≤5 psi: -17 to 85°C (0 to 185°F)

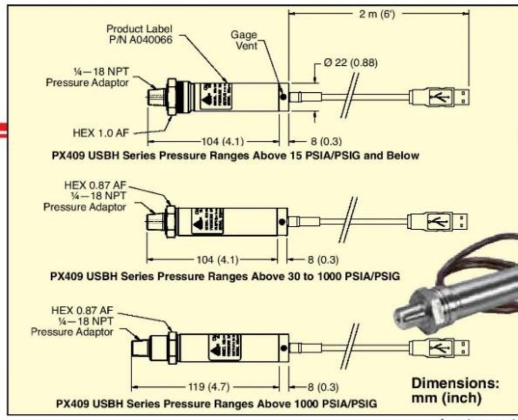

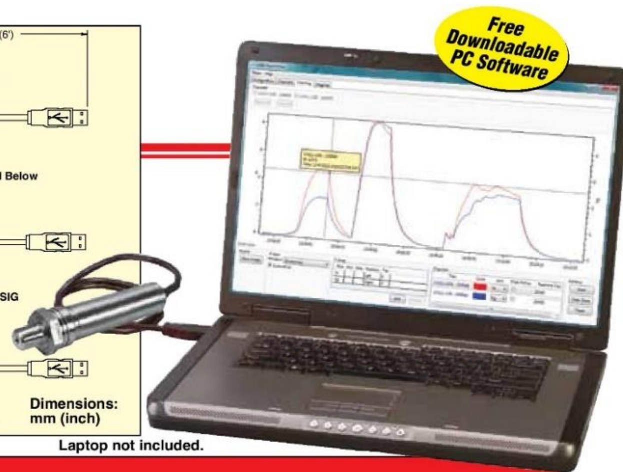

Laptop not included.

To Order

RANGE psi	RANGE bar	GAGE PRESSURE MODEL NO.	ABSOLUTE PRESSURE MODEL NO.
GAGE AND ABSOLUTE PRESSURE			
0 to 10 inH_2O	0 to 25 mb	**PX409-10WGUSBH**	—
0 to 1	0 to 69 mb	**PX409-001GUSBH**	—
0 to 2.5	0 to 172 mb	**PX409-2.5GUSBH**	—
0 to 5	0 to 345 mb	**PX409-005GUSBH**	**PX409-005AUSBH**
0 to 15	0 to 1	**PX409-015GUSBH**	**PX409-015AUSBH**
0 to 30	0 to 2.1	**PX409-030GUSBH**	**PX409-030AUSBH**
0 to 50	0 to 3.4	**PX409-050GUSBH**	**PX409-050AUSBH**
0 to 100	0 to 6.9	**PX409-100GUSBH**	**PX409-100AUSBH**
0 to 150	0 to 10.3	**PX409-150GUSBH**	**PX409-150AUSBH**
0 to 250	0 to 17.2	**PX409-250GUSBH**	**PX409-250AUSBH**
0 to 500	0 to 34.5	**PX409-500GUSBH**	**PX409-500AUSBH**
0 to 750	0 to 51.7	**PX409-750GUSBH**	**PX409-750AUSBH**
0 to 1000	0 to 69	**PX409-1.0KGUSBH**	**PX409-1.0KAUSBH**
0 to 1500	0 to 103	**PX409-1.5KGUSBH**	**PX409-1.5KAUSBH**
0 to 2500	0 to 172	**PX409-2.5KGUSBH**	**PX409-2.5KAUSBH**
0 to 3500	0 to 241	**PX409-3.5KGUSBH**	**PX409-3.5KAUSBH**
0 to 5000	0 to 345	**PX409-5.0KGUSBH**	**PX409-5.0KAUSBH**
VACUUM RANGES (NEGATIVE GAGE PRESSURE)			
0 to -10 inH_2O	0 to -25 mb	**PX409-10WVUSBH**	—
0 to -1 psi	0 to -69 mb	**PX409-001VUSBH**	—
0 to -2.5 psi	0 to -172 mb	**PX409-2.5VUSBH**	—
0 to -5 psi	0 to -345 mb	**PX409-005VUSBH**	—
0 to -15 psi	0 to -1	**PX409-015VUSBH**	—
COMPOUND GAGE RANGES			
± 10 inH_2O	± 25 mb	**PX409-10WCGUSBH**	—
± 1 psi	± 69 mb	**PX409-001CGUSBH**	—
± 2.5 psi	± 172 mb	**PX409-2.5CGUSBH**	—
± 5 psi	± 345 mb	**PX409-005CGUSBH**	—
± 15 psi	± 1	**PX409-015CGUSBH**	—
BAROMETRIC RANGES (ABSOLUTE PRESSURE)			
0 to 32 inHg	0 to 1100 mb	—	**PX409-32BUSBH**
16 to 32 inHg	550 to 1100 mb	—	**PX409-16BUSBH**
26 to 32 inHg	880 to 1100 mb	—	**PX409-26BUSBH**

Comes complete with 5-point NIST traceable calibration certificate, cable with USB connector, and free downloadable PC software.
***Ordering Examples: PX409-100GUSBH,** 2 m (6') cable with USB termination, 100 psig range, USB output.*
***PX409-16BUSBH,** 2 m (6') cable with USB termination, 16 to 32 inHg absolute barometric range, USB output.*

HIGH SPEED USB DIFFERENTIAL PRESSURE TRANSDUCERS

SPECIFICATIONS DIFFERENTIAL MODELS

Ranges: Unidirectional 10 inH_2O to 1000 psi

Line/Static Pressure: 500 psi maximum applied to both sides simultaneously

High Side Containment Pressure (Differential)

Wet/Dry and Wet/Wet:

10 inH_2O to 5 psi: to 1000 psi
15 to 1000 psi: to 3000 psi

Overpressure (Differential)

Wet/Dry and Wet/Wet:

10 inH_2O: 3.6 psi
1 psi: to 6 psi
2.5 psi to 750 psi: 4 times span
1000 psi: to 3000 psi

Weight: 227 g (8 oz)

Line Pressure: 500 psi maximum

Fitting: ¼-18 NPT male

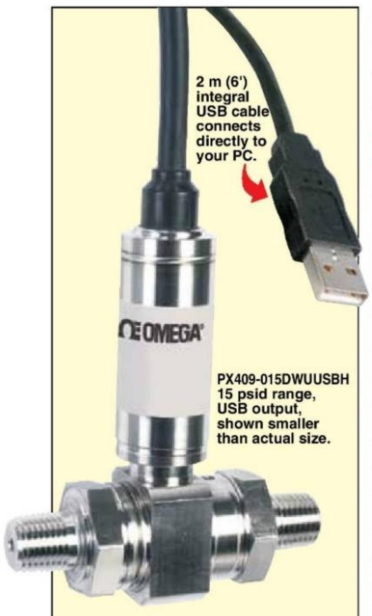

See PX409 for dimensions.

To Order

RANGE psi	RANGE bar	MODEL NO.
WET/DRY DIFFERENTIAL PRESSURE MODELS		
0 to 10 inH_2O	0 to 25.00 mb	PX409-10WDDUUSBH
0 to 1	0 to 69.00 mb	PX409-001DDUUSBH
0 to 2.5	0 to 172.0 mb	PX409-2.5DDUUSBH
0 to 5	0 to 345.0 mb	PX409-005DDUUSBH
0 to 15	0 to 1.000	PX409-015DDUUSBH
0 to 30	0 to 2.100	PX409-030DDUUSBH
0 to 50	0 to 3.400	PX409-050DDUUSBH
0 to 100	0 to 6.900	PX409-100DDUUSBH
0 to 150	0 to 10.30	PX409-150DDUUSBH
0 to 250	0 to 17.20	PX409-250DDUUSBH
0 to 500	0 to 34.50	PX409-500DDUUSBH
0 to 750	0 to 51.70	PX409-750DDUUSBH
0 to 1000	0 to 69.00	PX409-1.0KDDUUSBH
WET/WET DIFFERENTIAL PRESSURE MODELS		
0 to 10 inH_2O	0 to 25.00 mb	PX409-10WDWUUSBH
0 to 1	0 to 69.00 mb	PX409-001DWUUSBH
0 to 2.5	0 to 172.0 mb	PX409-2.5DWUUSBH
0 to 5	0 to 345.0 mb	PX409-005DWUUSBH
0 to 15	0 to 1.000	PX409-015DWUUSBH
0 to 30	0 to 2.100	PX409-030DWUUSBH
0 to 50	0 to 3.400	PX409-050DWUUSBH
0 to 100	0 to 6.900	PX409-100DWUUSBH
0 to 150	0 to 10.30	PX409-150DWUUSBH
0 to 250	0 to 17.20	PX409-250DWUUSBH
0 to 500	0 to 34.50	PX409-500DWUUSBH
0 to 750	0 to 51.70	PX409-750DWUUSBH
0 to 1000	0 to 69.00	PX409-1.0KDWUUSBH

Comes complete with 5-point NIST traceable calibration certificate, cable with USB connector, and free downloadable PC software.

Ordering Examples: PX409-100DDUUSBH, *Wet/Dry 0 to 100 psi differential high speed USB output transducer.*

PX409-2.5DWUUSBH, *Wet/Wet 0 to 2.5 psi differential high speed USB output transducer.*

OMEGA USBH MAJOR SOFTWARE UPDATE

OMEGA is excited to announce the release of a major software update for USB Transducers! The fresh look and added features add even more value and flexibility to your transducer's performance. Free OMEGA PC software takes the data from the transducer directly to the digital domain, turning your laptop or Windows® tablet (with USB connection) into a virtual meter, chart recorder, or data logger. Also included are .NET APIs and a set for command-line access.
Visit **ftp://ftp.omega.com/public/DASGroup/products/USBH/** to download your free copy.*
* Includes software to run TRH Central compatible devices.

Charting Window – The addition of a charting window allows you to see your data graphed in real time. The Y axis is configurable to allow simultaneous graphing of multiple engineering units. You can output the image of your data to a png file.

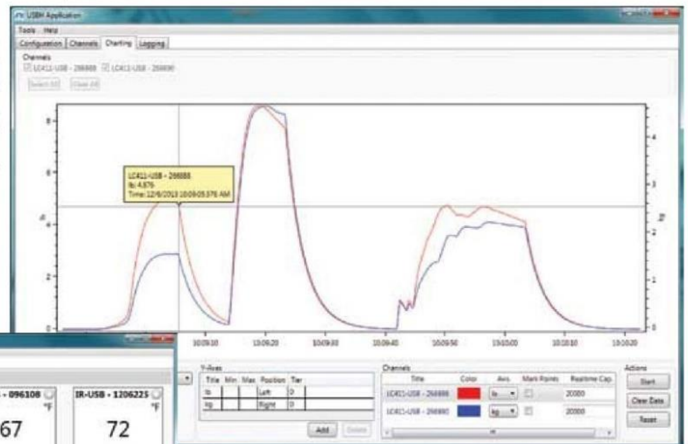

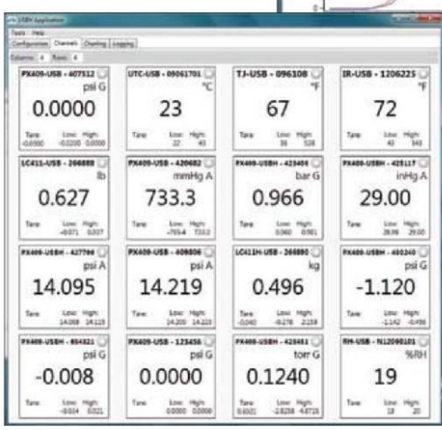

Channels Window – Display data from all of your sensors simultaneously. Each channel has configurable user alarms, three data filters, tare, resettable low/high indication, and sample rates ranging from 30 minutes to 1000 Hz.

Logging Window – A new xls filetype output option presents preformatted data for readability. In addition, Live Statistics are displayed, including the sensor information, the start/stop time, the number of samples taken, the current reading, and the High/Low readings. With the logging window, you can capture your data for later analysis.

PX409-USBH-425117

Units	psi
Count	10
Last	14.2349
Low	14.2349
High	14.2353

Support for Omega Pressure, Force, Temperature, and Humidity USB Transducers
One software package supports:
PX409-*-USB, PX409-*-USBH, LC411-*-USBH, TJ-USB, IR-USB, RH-USB and UTC-USB transducers.

Appendix I: Flow Chart for Modified Code